

Figure 5.38. Comparison of FDTD derived values of magnetic field strength by BEMC and measured values by SPEAG from AT&T antenna.

6 FDTD Calculation and Measurements of SAR in Kuster Head and Shoulders Homogeneous Model

6.1 Orientation with Tip of Nose in Contact with Radome and 9 mm Below Center of Four Patch Array

FDTD calculations were made of the peak and 1-gram average of the SARs in the Kuster homogeneous head model (described in section 3.2) exposed to the AT&T RU antenna. The results were compared to the measurements made by SPEAG described in Appendix A. The electrical properties of the head tissue corresponded to a relative permittivity of 41.0 and a conductivity of 1.69 S/m, which SPEAG specifies for modeling homogeneous head tissue in the PCS band based on their measurements at 1.8 GHz. The head was exposed with the face toward the antenna with the nose in direct contact with the radome at 9-mm below the geometric center of the 4-patch array. Graphical SAR data files and plots calculated throughout the entire head model were scaled for an input power of 79.62 mW to the antenna which corresponds to a far-field effective radiated power of 2.54 watts from the antenna with no models present.

Table 6.1 summarizes the calculated results of both the peak and average SARs calculated for each 1-mm thick slice in the xy plane as well as for the entire exposed head model. The first column of the table lists the first 17 characters of the name of the file containing the SAR data for the slices numbered from 11 to 344, corresponding to the distance in mm from the ftdt mesh origin in the z direction. The second and third columns of the table give the x and y coordinates in mm of the cell from the FDTD mesh origin within the slice experiencing the highest SAR. The fourth column gives the maximum SAR, the fifth column gives the SAR as averaged over the slice and the last column gives the number of cells within the slice. It may be noted from the table that the maximum SAR of 0.194 W/kg for the entire head model is in the 148th slice (file mansar1.xy148.sar) at x=81 mm and y=109 mm and the average SAR for the 19114 cells for that slice is 0.007947 W/kg. It can also be seen at the bottom of the table that the SAR as averaged over the 7444294 cells of the entire head is 0.004295W/kg.

The safe exposure standards in the United States for the public or uncontrolled environment including the FCC MPLs are based on limiting the maximum SAR as averaged over any gram of tissue in the shape of a cube to 1.6 W/kg and the SAR as averaged over the whole body to 0.08 W/kg. Thus the FDTD calculated SAR distribution data must be converted some way to reflect the average over any gram of tissue in the shape of a cube. So far there is no standardization on how this averaging process should be done to account for the irregular shape of tissue

boundaries such as encountered at the ears, nose, mouth, etc. If the averaging routine maintains the 1-gram cube entirely within the tissue boundaries so that a flat face of the cube cannot emerge outside of the tissue boundaries, the averaging process may miss regions of high SAR which commonly occur at the surface or at locations where there are sharp curves of the tissue surface. This will result in a lower average SAR than would be the case if the surfaces of the cube were allowed to extend beyond the tissue boundaries in order not to miss any tissue with high SAR near an irregular boundary. The latter could include a large amount of air in the averaging volume, requiring the cube to become larger to encompass the required gram of tissue thereby allowing more surface tissue with the higher SARs to weight the averaging process. In order to insure that the averaging process covers the "worst case" scenario, the FDTD averaging routine used in this analysis considered a cube of space centered at each FDTD cell within the tissue. The cube was then allowed to expand until a gram of tissue was contained within its boundaries. When 1 gram of tissue (to within 1% accuracy) was contained in the cube the SAR was averaged over the entire cube and the average value was assigned to the cell at the center of the cube. It should be realized that this could lead to pessimistically higher values of SAR at distances from the tissue surface that are shorter than the dimension of the averaging cube. The routine could be made to be less pessimistic by imposing an additional condition that the face of the averaging cube not be extended into the air anymore than necessary to enclose all of the tissue below the outermost point of the tissue boundary. It could become rather complicated to get some general agreement among the dosimetry experts on the best way to do this.

Table 6.2 illustrates the results of the 1-gram averaging of the fdfd output data. The format is essentially the same as used in Table 6.1, except the results can now be related to the FCC MPL. It may be noted from the table that the highest 1-g average SAR of 0.1319 W/kg occurs in the slice at $z=144$ mm, $x=81$ mm and $y=112$ mm. This is more than 12 times below the maximum permitted level of 1.6 W/kg. The SAR as averaged over the entire head consisting of 7,444,294 fdfd cells was calculated to be 0.004319 W/kg. However, the whole head average of 0.004295 W/kg as calculated by 1-mm fdfd cubes given in Table 6.1 is more accurate since there is considerable overlapping of the 1 gram cubes in determining the whole head average given in Table 6.2. Assuming an average head tissue density the same as water, the total mass of the phantom head tissue is $7,444,294/1,000,000 = 7.444$ kg. Therefore the total absorbed power is $0.004295 \times 7.444 = 0.031973$ W = 31.973mW which is 40.2% of the antenna input power. Though this calculation doesn't indicate what the whole-body averaged SAR would be, the whole body could not absorb any more than the full 79.62-mW input power to the antenna which for a 70 Kg man would correspond to a whole-body average SAR of 0.001377 W/kg. Thus we may conclude that the whole-body averaged SAR for an adult man with a head similar to that of the Kuster phantom head would be somewhere between 0.001377 and 0.004295 W/kg or from 18 to 58 times less than that allowed by the FCC MPL of 0.08 W/kg.

Table 6.1. Slice and Whole Head Model Peak and average SAR (averaged over slice) for Kuster Head and Shoulders Model Exposed to AT&T RU Antenna with Nose in Contact with Radome 9 mm Below Middle of Patch Array and (slice file number is distance in mm from FDTD space rectangular coordinates origin in z direction).

Name of Slice Data File	Peak SAR x and y coordinates		Peak SAR (W/kg)	Avg. SAR (W/kg)	Voxels in tissue
mansar1.xy11.sar	124	121	0.6038E-02	0.3086E-02	52
mansar1.xy12.sar	146	260	0.1036E+00	0.5861E-02	33632
mansar1.xy13.sar	147	260	0.7903E-01	0.5933E-02	33346
mansar1.xy14.sar	149	261	0.8060E-01	0.5890E-02	33090
mansar1.xy15.sar	145	252	0.6733E-01	0.5643E-02	32786
mansar1.xy16.sar	151	260	0.6439E-01	0.5275E-02	32492
mansar1.xy17.sar	150	256	0.4927E-01	0.4824E-02	32150
mansar1.xy18.sar	148	249	0.3758E-01	0.4378E-02	31818
mansar1.xy19.sar	130	168	0.3740E-01	0.3981E-02	31464
mansar1.xy20.sar	130	174	0.4980E-01	0.3647E-02	31096
mansar1.xy21.sar	131	171	0.6096E-01	0.3391E-02	30710
mansar1.xy22.sar	132	178	0.5679E-01	0.3205E-02	30352
mansar1.xy23.sar	133	169	0.5400E-01	0.3092E-02	29996
mansar1.xy24.sar	134	169	0.6729E-01	0.3036E-02	29646
mansar1.xy25.sar	134	173	0.6564E-01	0.3000E-02	29282
mansar1.xy26.sar	136	173	0.7206E-01	0.3006E-02	28940
mansar1.xy27.sar	136	173	0.8821E-01	0.3037E-02	28596
mansar1.xy28.sar	137	176	0.8358E-01	0.3061E-02	28262
mansar1.xy29.sar	138	178	0.9041E-01	0.3119E-02	27952
mansar1.xy30.sar	138	173	0.1018E+00	0.3176E-02	27624
mansar1.xy31.sar	138	173	0.6471E-01	0.3210E-02	27310
mansar1.xy32.sar	139	180	0.6914E-01	0.3252E-02	27000
mansar1.xy33.sar	139	177	0.8268E-01	0.3289E-02	26678
mansar1.xy34.sar	139	174	0.9320E-01	0.3305E-02	26348
mansar1.xy35.sar	140	179	0.7920E-01	0.3281E-02	26013
mansar1.xy36.sar	140	178	0.8538E-01	0.3262E-02	25669
mansar1.xy37.sar	140	177	0.9378E-01	0.3236E-02	25256
mansar1.xy38.sar	140	176	0.1113E+00	0.3215E-02	24854
mansar1.xy39.sar	140	174	0.1203E+00	0.3198E-02	24478
mansar1.xy40.sar	141	182	0.1134E+00	0.3203E-02	24094
mansar1.xy41.sar	141	179	0.9123E-01	0.3234E-02	23752
mansar1.xy42.sar	140	178	0.1020E+00	0.3288E-02	23406
mansar1.xy43.sar	141	178	0.9686E-01	0.3367E-02	23082
mansar1.xy44.sar	141	181	0.1022E+00	0.3463E-02	22732
mansar1.xy45.sar	141	172	0.1007E+00	0.3555E-02	22406
mansar1.xy46.sar	141	180	0.1351E+00	0.3664E-02	22080
mansar1.xy47.sar	143	184	0.1041E+00	0.3736E-02	21748
mansar1.xy48.sar	144	186	0.9324E-01	0.3802E-02	21410
mansar1.xy49.sar	141	177	0.8796E-01	0.3855E-02	21102
mansar1.xy50.sar	142	182	0.1234E+00	0.3902E-02	20778
mansar1.xy51.sar	141	179	0.1372E+00	0.3932E-02	20478
mansar1.xy52.sar	141	179	0.1015E+00	0.3956E-02	20158
mansar1.xy53.sar	141	179	0.1024E+00	0.3968E-02	19878
mansar1.xy54.sar	141	176	0.8431E-01	0.3980E-02	19610
mansar1.xy55.sar	141	175	0.8542E-01	0.4003E-02	19326
mansar1.xy56.sar	141	178	0.7796E-01	0.4044E-02	19028
mansar1.xy57.sar	143	184	0.9735E-01	0.4080E-02	18714
mansar1.xy58.sar	140	175	0.9000E-01	0.4122E-02	18404
mansar1.xy59.sar	141	176	0.8421E-01	0.4177E-02	18106

Name of Slice Data File	Peak SAR x and y coordinates	Peak SAR (W/kg)	Avg. SAR (W/kg)	Voxels in tissue
mansar1.xy60.sar	140 170	0.9652E-01	0.4242E-02	17800
mansar1.xy61.sar	141 180	0.8784E-01	0.4278E-02	17550
mansar1.xy62.sar	140 173	0.8657E-01	0.4323E-02	17248
mansar1.xy63.sar	140 175	0.8456E-01	0.4365E-02	17038
mansar1.xy64.sar	140 176	0.7617E-01	0.4403E-02	16772
mansar1.xy65.sar	139 172	0.6996E-01	0.4454E-02	16498
mansar1.xy66.sar	138 164	0.7103E-01	0.4489E-02	16238
mansar1.xy67.sar	141 181	0.7424E-01	0.4513E-02	16000
mansar1.xy68.sar	143 184	0.8908E-01	0.4529E-02	15752
mansar1.xy69.sar	139 177	0.7469E-01	0.4541E-02	15516
mansar1.xy70.sar	140 178	0.6286E-01	0.4547E-02	15286
mansar1.xy71.sar	138 170	0.6737E-01	0.4547E-02	15060
mansar1.xy72.sar	141 182	0.6598E-01	0.4547E-02	14844
mansar1.xy73.sar	139 178	0.7061E-01	0.4547E-02	14638
mansar1.xy74.sar	136 169	0.6747E-01	0.4529E-02	14480
mansar1.xy75.sar	135 162	0.6236E-01	0.4531E-02	14262
mansar1.xy76.sar	134 155	0.6435E-01	0.4525E-02	14072
mansar1.xy77.sar	134 158	0.5964E-01	0.4520E-02	13874
mansar1.xy78.sar	135 169	0.6549E-01	0.4513E-02	13686
mansar1.xy79.sar	134 162	0.6271E-01	0.4512E-02	13518
mansar1.xy80.sar	134 164	0.6214E-01	0.4512E-02	13360
mansar1.xy81.sar	134 165	0.5956E-01	0.4513E-02	13194
mansar1.xy82.sar	134 166	0.5939E-01	0.4512E-02	13066
mansar1.xy83.sar	132 154	0.6425E-01	0.4533E-02	12916
mansar1.xy84.sar	132 158	0.6146E-01	0.4541E-02	12794
mansar1.xy85.sar	132 160	0.6063E-01	0.4553E-02	12670
mansar1.xy86.sar	132 161	0.5917E-01	0.4574E-02	12548
mansar1.xy87.sar	133 169	0.6612E-01	0.4591E-02	12442
mansar1.xy88.sar	131 153	0.6080E-01	0.4584E-02	12398
mansar1.xy89.sar	131 160	0.6186E-01	0.4590E-02	12340
mansar1.xy90.sar	131 162	0.5894E-01	0.4623E-02	12232
mansar1.xy91.sar	132 169	0.6414E-01	0.4645E-02	12166
mansar1.xy92.sar	130 157	0.7198E-01	0.4677E-02	12082
mansar1.xy93.sar	130 159	0.6579E-01	0.4684E-02	12050
mansar1.xy94.sar	130 161	0.6643E-01	0.4690E-02	12002
mansar1.xy95.sar	131 166	0.6392E-01	0.4709E-02	11938
mansar1.xy96.sar	129 157	0.7386E-01	0.4729E-02	11890
mansar1.xy97.sar	129 159	0.6651E-01	0.4743E-02	11850
mansar1.xy98.sar	130 165	0.6504E-01	0.4743E-02	11816
mansar1.xy99.sar	129 162	0.6928E-01	0.4746E-02	11784
mansar1.xy100.sar	128 158	0.7466E-01	0.4756E-02	11746
mansar1.xy101.sar	128 159	0.6633E-01	0.4742E-02	11734
mansar1.xy102.sar	128 162	0.7157E-01	0.4722E-02	11724
mansar1.xy103.sar	128 164	0.7074E-01	0.4714E-02	11713
mansar1.xy104.sar	127 159	0.7268E-01	0.4699E-02	11712
mansar1.xy105.sar	127 162	0.7262E-01	0.4683E-02	11708
mansar1.xy106.sar	126 156	0.7303E-01	0.4668E-02	11706
mansar1.xy107.sar	126 162	0.7132E-01	0.4650E-02	11730
mansar1.xy108.sar	126 165	0.7150E-01	0.4626E-02	11746
mansar1.xy109.sar	125 165	0.8062E-01	0.4609E-02	11774
mansar1.xy110.sar	125 167	0.7908E-01	0.4592E-02	11824
mansar1.xy111.sar	122 157	0.9215E-01	0.4617E-02	11854
mansar1.xy112.sar	122 165	0.8395E-01	0.4754E-02	12002
mansar1.xy113.sar	122 168	0.7533E-01	0.5128E-02	12306
mansar1.xy114.sar	122 171	0.5917E-01	0.5653E-02	12688

Name of Slice Data File	Peak SAR x and y coordinates	Peak SAR (W/kg)	Avg. SAR (W/kg)	Voxels in tissue
mansar1.xy115.sar	126 178	0.5639E-01	0.6236E-02	13390
mansar1.xy116.sar	80 151	0.5204E-01	0.6783E-02	13892
mansar1.xy117.sar	74 146	0.5256E-01	0.7145E-02	14290
mansar1.xy118.sar	74 145	0.5830E-01	0.7462E-02	14670
mansar1.xy119.sar	75 141	0.6135E-01	0.7724E-02	14984
mansar1.xy120.sar	72 164	0.6810E-01	0.7961E-02	15298
mansar1.xy121.sar	72 140	0.6971E-01	0.8233E-02	15594
mansar1.xy122.sar	73 136	0.7985E-01	0.8513E-02	15904
mansar1.xy123.sar	88 121	0.8125E-01	0.8803E-02	16146
mansar1.xy124.sar	80 126	0.8882E-01	0.9087E-02	16396
mansar1.xy125.sar	78 127	0.1030E+00	0.9330E-02	16616
mansar1.xy126.sar	78 178	0.1180E+00	0.9535E-02	16834
mansar1.xy127.sar	81 121	0.1069E+00	0.9706E-02	17044
mansar1.xy128.sar	78 123	0.1156E+00	0.9856E-02	17240
mansar1.xy129.sar	78 182	0.1168E+00	0.9990E-02	17416
mansar1.xy130.sar	80 120	0.1394E+00	0.1013E-01	17554
mansar1.xy131.sar	78 121	0.1459E+00	0.1026E-01	17668
mansar1.xy132.sar	81 117	0.1381E+00	0.1033E-01	17816
mansar1.xy133.sar	78 120	0.1459E+00	0.1037E-01	17940
mansar1.xy134.sar	81 116	0.1580E+00	0.1039E-01	18014
mansar1.xy135.sar	77 121	0.1571E+00	0.1036E-01	18104
mansar1.xy136.sar	83 113	0.1514E+00	0.1028E-01	18178
mansar1.xy137.sar	80 115	0.1520E+00	0.1014E-01	18230
mansar1.xy138.sar	78 117	0.1552E+00	0.9993E-02	18292
mansar1.xy139.sar	80 114	0.1663E+00	0.9815E-02	18308
mansar1.xy140.sar	81 113	0.1911E+00	0.9619E-02	18362
mansar1.xy141.sar	79 114	0.1732E+00	0.9400E-02	18418
mansar1.xy142.sar	82 111	0.1870E+00	0.9166E-02	18496
mansar1.xy143.sar	84 109	0.1796E+00	0.8966E-02	18554
mansar1.xy144.sar	82 110	0.1687E+00	0.8752E-02	18670
mansar1.xy145.sar	80 111	0.1712E+00	0.8543E-02	18772
mansar1.xy146.sar	80 194	0.1644E+00	0.8337E-02	18900
mansar1.xy147.sar	80 110	0.1711E+00	0.8143E-02	19008
mansar1.xy148.sar	81 109	0.1936E+00	0.7947E-02	19114
mansar1.xy149.sar	81 196	0.1790E+00	0.7736E-02	19246
mansar1.xy150.sar	79 110	0.1846E+00	0.7538E-02	19348
mansar1.xy151.sar	79 195	0.1650E+00	0.7328E-02	19466
mansar1.xy152.sar	81 107	0.1686E+00	0.7154E-02	19542
mansar1.xy153.sar	78 110	0.1698E+00	0.6991E-02	19640
mansar1.xy154.sar	80 107	0.1707E+00	0.6834E-02	19728
mansar1.xy155.sar	80 198	0.1532E+00	0.6662E-02	19848
mansar1.xy156.sar	78 196	0.1437E+00	0.6510E-02	19948
mansar1.xy157.sar	79 107	0.1606E+00	0.6342E-02	20070
mansar1.xy158.sar	81 106	0.1508E+00	0.6177E-02	20202
mansar1.xy159.sar	82 105	0.1433E+00	0.6006E-02	20354
mansar1.xy160.sar	83 104	0.1269E+00	0.5839E-02	20532
mansar1.xy161.sar	80 106	0.1382E+00	0.5666E-02	20688
mansar1.xy162.sar	78 107	0.1402E+00	0.5494E-02	20846
mansar1.xy163.sar	78 198	0.1184E+00	0.5316E-02	21014
mansar1.xy164.sar	82 201	0.1073E+00	0.5149E-02	21140
mansar1.xy165.sar	83 103	0.9839E-01	0.4979E-02	21278
mansar1.xy166.sar	83 202	0.9898E-01	0.4807E-02	21416
mansar1.xy167.sar	79 106	0.1015E+00	0.4651E-02	21526
mansar1.xy168.sar	81 104	0.9416E-01	0.4501E-02	21622
mansar1.xy169.sar	80 105	0.1103E+00	0.4342E-02	21752

Name of Slice Data File	Peak SAR x and y coordinates	Peak SAR (W/kg)	Avg. SAR (W/kg)	Voxels in tissue
mansar1.xy170.sar	80 200	0.1004E+00	0.4188E-02	21874
mansar1.xy171.sar	79 106	0.9015E-01	0.4035E-02	21974
mansar1.xy172.sar	83 203	0.8824E-01	0.3885E-02	22128
mansar1.xy173.sar	84 204	0.8147E-01	0.3751E-02	22250
mansar1.xy174.sar	80 104	0.8924E-01	0.3630E-02	22348
mansar1.xy175.sar	82 203	0.9093E-01	0.3518E-02	22478
mansar1.xy176.sar	81 202	0.8516E-01	0.3407E-02	22614
mansar1.xy177.sar	80 103	0.7780E-01	0.3308E-02	22734
mansar1.xy178.sar	82 204	0.8198E-01	0.3218E-02	22896
mansar1.xy179.sar	84 206	0.8229E-01	0.3138E-02	23052
mansar1.xy180.sar	79 201	0.7664E-01	0.3075E-02	23180
mansar1.xy181.sar	85 208	0.6571E-01	0.3014E-02	23344
mansar1.xy182.sar	82 206	0.7437E-01	0.2967E-02	23514
mansar1.xy183.sar	79 203	0.6476E-01	0.2938E-02	23664
mansar1.xy184.sar	80 205	0.6455E-01	0.2921E-02	23822
mansar1.xy185.sar	79 204	0.6215E-01	0.2920E-02	23984
mansar1.xy186.sar	81 207	0.6328E-01	0.2947E-02	24186
mansar1.xy187.sar	80 206	0.6241E-01	0.2982E-02	24428
mansar1.xy188.sar	82 209	0.5937E-01	0.3047E-02	24658
mansar1.xy189.sar	82 209	0.5861E-01	0.3143E-02	24918
mansar1.xy190.sar	59 151	0.5620E-01	0.3185E-02	25100
mansar1.xy191.sar	60 151	0.5929E-01	0.3216E-02	25236
mansar1.xy192.sar	60 151	0.6171E-01	0.3241E-02	25422
mansar1.xy193.sar	61 151	0.6318E-01	0.3265E-02	25534
mansar1.xy194.sar	61 152	0.6413E-01	0.3281E-02	25692
mansar1.xy195.sar	62 152	0.6471E-01	0.3290E-02	25808
mansar1.xy196.sar	62 152	0.6507E-01	0.3301E-02	25944
mansar1.xy197.sar	63 152	0.6528E-01	0.3310E-02	26062
mansar1.xy198.sar	63 152	0.6574E-01	0.3322E-02	26194
mansar1.xy199.sar	63 152	0.6645E-01	0.3334E-02	26294
mansar1.xy200.sar	63 152	0.6767E-01	0.3342E-02	26438
mansar1.xy201.sar	63 153	0.6976E-01	0.3356E-02	26526
mansar1.xy202.sar	62 153	0.7327E-01	0.3356E-02	26628
mansar1.xy203.sar	56 157	0.8303E-01	0.3374E-02	26750
mansar1.xy204.sar	57 157	0.1060E+00	0.3390E-02	26816
mansar1.xy205.sar	54 154	0.8976E-01	0.3363E-02	26930
mansar1.xy206.sar	60 153	0.9407E-01	0.3361E-02	27006
mansar1.xy207.sar	56 153	0.1095E+00	0.3352E-02	27078
mansar1.xy208.sar	60 153	0.1035E+00	0.3330E-02	27160
mansar1.xy209.sar	58 156	0.1122E+00	0.3308E-02	27202
mansar1.xy210.sar	58 153	0.1306E+00	0.3271E-02	27260
mansar1.xy211.sar	62 153	0.1111E+00	0.3220E-02	27310
mansar1.xy212.sar	59 153	0.1203E+00	0.3205E-02	27350
mansar1.xy213.sar	60 155	0.1184E+00	0.3149E-02	27404
mansar1.xy214.sar	60 154	0.1194E+00	0.3107E-02	27442
mansar1.xy215.sar	64 153	0.1159E+00	0.3071E-02	27496
mansar1.xy216.sar	62 156	0.1222E+00	0.3035E-02	27550
mansar1.xy217.sar	62 153	0.1419E+00	0.3009E-02	27602
mansar1.xy218.sar	63 155	0.1404E+00	0.2967E-02	27652
mansar1.xy219.sar	63 154	0.1486E+00	0.2942E-02	27702
mansar1.xy220.sar	68 153	0.1136E+00	0.2913E-02	27764
mansar1.xy221.sar	68 153	0.1140E+00	0.2900E-02	27824
mansar1.xy222.sar	65 156	0.1153E+00	0.2889E-02	27888
mansar1.xy223.sar	65 153	0.1329E+00	0.2891E-02	27930
mansar1.xy224.sar	66 155	0.1199E+00	0.2877E-02	28016

Name of Slice Data File	Peak SAR x and y coordinates	Peak SAR (W/kg)	Avg. SAR (W/kg)	Voxels in tissue
mansar1.xy225.sar	67 156	0.1351E+00	0.2872E-02	28094
mansar1.xy226.sar	67 153	0.1479E+00	0.2879E-02	28162
mansar1.xy227.sar	68 155	0.1376E+00	0.2878E-02	28244
mansar1.xy228.sar	69 157	0.1340E+00	0.2889E-02	28340
mansar1.xy229.sar	69 153	0.1734E+00	0.2914E-02	28448
mansar1.xy230.sar	70 158	0.1423E+00	0.2912E-02	28538
mansar1.xy231.sar	70 157	0.1534E+00	0.2934E-02	28652
mansar1.xy232.sar	70 155	0.1572E+00	0.2973E-02	28736
mansar1.xy233.sar	70 155	0.1154E+00	0.2993E-02	28878
mansar1.xy234.sar	70 158	0.1181E+00	0.3026E-02	28988
mansar1.xy235.sar	70 158	0.1150E+00	0.3068E-02	29122
mansar1.xy236.sar	83 93	0.1041E+00	0.3118E-02	29262
mansar1.xy237.sar	82 94	0.1017E+00	0.3173E-02	29406
mansar1.xy238.sar	82 93	0.1090E+00	0.3236E-02	29540
mansar1.xy239.sar	82 93	0.1087E+00	0.3312E-02	29702
mansar1.xy240.sar	78 99	0.1190E+00	0.3387E-02	29864
mansar1.xy241.sar	78 98	0.1282E+00	0.3476E-02	30012
mansar1.xy242.sar	78 97	0.1250E+00	0.3579E-02	30184
mansar1.xy243.sar	77 98	0.1174E+00	0.3684E-02	30324
mansar1.xy244.sar	76 100	0.1233E+00	0.3795E-02	30510
mansar1.xy245.sar	79 95	0.1359E+00	0.3883E-02	30644
mansar1.xy246.sar	78 96	0.1209E+00	0.3937E-02	30808
mansar1.xy247.sar	81 94	0.1175E+00	0.3982E-02	30912
mansar1.xy248.sar	82 94	0.1130E+00	0.4011E-02	30994
mansar1.xy249.sar	78 96	0.1423E+00	0.4042E-02	31060
mansar1.xy250.sar	75 99	0.1386E+00	0.4070E-02	31112
mansar1.xy251.sar	75 99	0.1152E+00	0.4086E-02	31172
mansar1.xy252.sar	80 95	0.1199E+00	0.4098E-02	31220
mansar1.xy253.sar	78 97	0.1490E+00	0.4107E-02	31252
mansar1.xy254.sar	75 100	0.1455E+00	0.4086E-02	31278
mansar1.xy255.sar	71 106	0.1315E+00	0.4043E-02	31310
mansar1.xy256.sar	77 99	0.1472E+00	0.3991E-02	31328
mansar1.xy257.sar	75 101	0.1390E+00	0.3946E-02	31340
mansar1.xy258.sar	72 107	0.1364E+00	0.3895E-02	31344
mansar1.xy259.sar	76 101	0.1521E+00	0.3816E-02	31348
mansar1.xy260.sar	73 106	0.1544E+00	0.3762E-02	31364
mansar1.xy261.sar	74 105	0.1443E+00	0.3711E-02	31374
mansar1.xy262.sar	80 97	0.1571E+00	0.3661E-02	31370
mansar1.xy263.sar	79 98	0.1419E+00	0.3625E-02	31372
mansar1.xy264.sar	72 110	0.1243E+00	0.3593E-02	31372
mansar1.xy265.sar	74 106	0.1269E+00	0.3595E-02	31372
mansar1.xy266.sar	79 98	0.1425E+00	0.3636E-02	31349
mansar1.xy267.sar	79 207	0.1304E+00	0.3668E-02	31324
mansar1.xy268.sar	78 101	0.1260E+00	0.3712E-02	31302
mansar1.xy269.sar	78 100	0.1471E+00	0.3765E-02	31276
mansar1.xy270.sar	80 98	0.1600E+00	0.3834E-02	31244
mansar1.xy271.sar	79 206	0.1483E+00	0.3892E-02	31212
mansar1.xy272.sar	74 108	0.1377E+00	0.3952E-02	31187
mansar1.xy273.sar	74 197	0.1297E+00	0.4011E-02	31157
mansar1.xy274.sar	75 106	0.1172E+00	0.4075E-02	31120
mansar1.xy275.sar	78 101	0.1400E+00	0.4132E-02	31088
mansar1.xy276.sar	79 100	0.1447E+00	0.4182E-02	31048
mansar1.xy277.sar	81 98	0.1428E+00	0.4242E-02	31000
mansar1.xy278.sar	80 206	0.1381E+00	0.4285E-02	30930
mansar1.xy279.sar	74 196	0.1168E+00	0.4311E-02	30884

Name of Slice Data File	Peak SAR x and y coordinates	Peak SAR (W/kg)	Avg. SAR (W/kg)	Voxels in tissue
mansar1.xy280.sar	78 102	0.1323E+00	0.4340E-02	30806
mansar1.xy281.sar	78 203	0.1345E+00	0.4359E-02	30728
mansar1.xy282.sar	79 204	0.1291E+00	0.4363E-02	30664
mansar1.xy283.sar	81 206	0.1203E+00	0.4363E-02	30580
mansar1.xy284.sar	79 102	0.1282E+00	0.4351E-02	30468
mansar1.xy285.sar	79 203	0.1257E+00	0.4335E-02	30378
mansar1.xy286.sar	82 206	0.1150E+00	0.4303E-02	30292
mansar1.xy287.sar	78 106	0.1101E+00	0.4273E-02	30170
mansar1.xy288.sar	78 200	0.1128E+00	0.4229E-02	30054
mansar1.xy289.sar	78 108	0.1059E+00	0.4183E-02	29946
mansar1.xy290.sar	81 103	0.1100E+00	0.4143E-02	29786
mansar1.xy291.sar	81 202	0.1066E+00	0.4083E-02	29648
mansar1.xy292.sar	80 106	0.1102E+00	0.4037E-02	29490
mansar1.xy293.sar	80 199	0.1053E+00	0.3974E-02	29316
mansar1.xy294.sar	86 205	0.9437E-01	0.3929E-02	29148
mansar1.xy295.sar	82 106	0.9106E-01	0.3859E-02	28950
mansar1.xy296.sar	81 109	0.8290E-01	0.3815E-02	28756
mansar1.xy297.sar	83 107	0.7638E-01	0.3768E-02	28530
mansar1.xy298.sar	85 106	0.8401E-01	0.3715E-02	28282
mansar1.xy299.sar	88 104	0.7776E-01	0.3667E-02	28078
mansar1.xy300.sar	88 201	0.6659E-01	0.3602E-02	27840
mansar1.xy301.sar	87 199	0.7061E-01	0.3585E-02	27650
mansar1.xy302.sar	88 199	0.6395E-01	0.3543E-02	27346
mansar1.xy303.sar	89 199	0.6357E-01	0.3510E-02	27056
mansar1.xy304.sar	90 199	0.6231E-01	0.3486E-02	26710
mansar1.xy305.sar	91 199	0.5671E-01	0.3460E-02	26366
mansar1.xy306.sar	93 106	0.5039E-01	0.3440E-02	26008
mansar1.xy307.sar	93 108	0.5121E-01	0.3428E-02	25634
mansar1.xy308.sar	93 110	0.4983E-01	0.3404E-02	25254
mansar1.xy309.sar	93 112	0.4560E-01	0.3385E-02	24840
mansar1.xy310.sar	93 115	0.4463E-01	0.3373E-02	24428
mansar1.xy311.sar	111 214	0.4474E-01	0.3362E-02	24006
mansar1.xy312.sar	99 199	0.4866E-01	0.3355E-02	23596
mansar1.xy313.sar	96 114	0.3739E-01	0.3361E-02	23182
mansar1.xy314.sar	100 109	0.3613E-01	0.3362E-02	22718
mansar1.xy315.sar	116 214	0.3452E-01	0.3367E-02	22268
mansar1.xy316.sar	118 214	0.3591E-01	0.3387E-02	21842
mansar1.xy317.sar	108 200	0.3131E-01	0.3414E-02	21362
mansar1.xy318.sar	121 214	0.3386E-01	0.3436E-02	20854
mansar1.xy319.sar	112 102	0.3330E-01	0.3462E-02	20358
mansar1.xy320.sar	114 205	0.3511E-01	0.3478E-02	19812
mansar1.xy321.sar	106 118	0.2761E-01	0.3500E-02	19306
mansar1.xy322.sar	108 115	0.2778E-01	0.3535E-02	18796
mansar1.xy323.sar	107 120	0.2512E-01	0.3597E-02	18254
mansar1.xy324.sar	108 123	0.2556E-01	0.3646E-02	17696
mansar1.xy325.sar	108 132	0.2276E-01	0.3690E-02	17092
mansar1.xy326.sar	117 109	0.2249E-01	0.3734E-02	16494
mansar1.xy327.sar	117 112	0.2165E-01	0.3816E-02	15922
mansar1.xy328.sar	122 108	0.2059E-01	0.3888E-02	15262
mansar1.xy329.sar	122 111	0.2071E-01	0.3968E-02	14614
mansar1.xy330.sar	121 116	0.1965E-01	0.4047E-02	13936
mansar1.xy331.sar	120 122	0.1893E-01	0.4136E-02	13232
mansar1.xy332.sar	121 125	0.1866E-01	0.4247E-02	12560
mansar1.xy333.sar	122 132	0.1694E-01	0.4360E-02	11840
mansar1.xy334.sar	126 123	0.1641E-01	0.4493E-02	11140

Name of Slice Data File	Peak SAR x and y coordinates		Peak SAR (W/kg)	Avg. SAR (W/kg)	Voxels in tissue
mansar1.xy335.sar	130	121	0.1580E-01	0.4645E-02	10348
mansar1.xy336.sar	132	123	0.1548E-01	0.4802E-02	9482
mansar1.xy337.sar	135	124	0.1533E-01	0.4968E-02	8586
mansar1.xy338.sar	137	128	0.1471E-01	0.5140E-02	7662
mansar1.xy339.sar	140	128	0.1361E-01	0.5314E-02	6710
mansar1.xy340.sar	146	126	0.1341E-01	0.5551E-02	5828
mansar1.xy341.sar	149	133	0.1293E-01	0.5783E-02	4770
mansar1.xy342.sar	155	132	0.1238E-01	0.6002E-02	3632
mansar1.xy343.sar	173	138	0.1363E-01	0.6275E-02	2554
mansar1.xy344.sar	171	140	0.8473E-02	0.5555E-02	710

Location and values for peak and average SAR for total volume of exposed tissue

mansar1.xy148.sar	81	109	0.1936E+00	0.4295E-02	7444294
-------------------	----	-----	------------	------------	---------

Table 6.2. Slice and Whole Head Model Peak and average (averaged over slice) 1 Gram Average SAR for Kuster Head and Shoulders Model Exposed to AT&T RU Antenna with Nose in Contact with Radome 9 mm Below Middle of Patch Array and (slice file number is distance in mm from FDTD space rectangular coordinates origin in z direction).

Name of Slice Data File	Peak SAR x and y coordinates	Peak SAR (W/kg)	Avg. SAR (W/kg)	Voxels in tissue
mansar1.xy11.lgsa	125 191	0.2355E-01	0.1906E-01	52
mansar1.xy12.lgsa	146 260	0.4668E-01	0.5950E-02	33632
mansar1.xy13.lgsa	147 260	0.4616E-01	0.5808E-02	33346
mansar1.xy14.lgsa	147 259	0.4586E-01	0.5488E-02	33090
mansar1.xy15.lgsa	148 257	0.4469E-01	0.5305E-02	32786
mansar1.xy16.lgsa	146 252	0.4436E-01	0.5057E-02	32492
mansar1.xy17.lgsa	147 251	0.4292E-01	0.4784E-02	32150
mansar1.xy18.lgsa	150 255	0.3867E-01	0.4487E-02	31818
mansar1.xy19.lgsa	150 252	0.3385E-01	0.4186E-02	31464
mansar1.xy20.lgsa	136 176	0.3493E-01	0.3888E-02	31096
mansar1.xy21.lgsa	136 176	0.3774E-01	0.3624E-02	30710
mansar1.xy22.lgsa	136 175	0.4082E-01	0.3418E-02	30352
mansar1.xy23.lgsa	135 175	0.4413E-01	0.3268E-02	29996
mansar1.xy24.lgsa	136 175	0.4698E-01	0.3160E-02	29646
mansar1.xy25.lgsa	137 176	0.4909E-01	0.3083E-02	29282
mansar1.xy26.lgsa	135 175	0.5095E-01	0.3051E-02	28940
mansar1.xy27.lgsa	136 175	0.5266E-01	0.3039E-02	28596
mansar1.xy28.lgsa	137 176	0.5342E-01	0.3040E-02	28262
mansar1.xy29.lgsa	137 175	0.5493E-01	0.3071E-02	27952
mansar1.xy30.lgsa	138 176	0.5492E-01	0.3102E-02	27624
mansar1.xy31.lgsa	139 176	0.5434E-01	0.3135E-02	27310
mansar1.xy32.lgsa	139 176	0.5473E-01	0.3175E-02	27000
mansar1.xy33.lgsa	139 176	0.5550E-01	0.3206E-02	26678
mansar1.xy34.lgsa	139 176	0.5811E-01	0.3213E-02	26348
mansar1.xy35.lgsa	140 177	0.5715E-01	0.3206E-02	26013
mansar1.xy36.lgsa	140 178	0.5984E-01	0.3206E-02	25669
mansar1.xy37.lgsa	140 178	0.6200E-01	0.3197E-02	25256
mansar1.xy38.lgsa	140 177	0.6326E-01	0.3181E-02	24854
mansar1.xy39.lgsa	141 179	0.6432E-01	0.3181E-02	24478
mansar1.xy40.lgsa	141 178	0.6634E-01	0.3189E-02	24094
mansar1.xy41.lgsa	141 179	0.6853E-01	0.3232E-02	23752
mansar1.xy42.lgsa	141 179	0.7050E-01	0.3281E-02	23406
mansar1.xy43.lgsa	141 179	0.7204E-01	0.3354E-02	23082
mansar1.xy44.lgsa	141 178	0.7291E-01	0.3411E-02	22732
mansar1.xy45.lgsa	141 177	0.7290E-01	0.3485E-02	22406
mansar1.xy46.lgsa	141 177	0.7338E-01	0.3554E-02	22080
mansar1.xy47.lgsa	142 180	0.7263E-01	0.3608E-02	21748
mansar1.xy48.lgsa	142 180	0.7293E-01	0.3673E-02	21410
mansar1.xy49.lgsa	142 179	0.7306E-01	0.3741E-02	21102
mansar1.xy50.lgsa	142 179	0.7268E-01	0.3782E-02	20778
mansar1.xy51.lgsa	142 179	0.7192E-01	0.3817E-02	20478
mansar1.xy52.lgsa	142 179	0.7065E-01	0.3852E-02	20158
mansar1.xy53.lgsa	142 180	0.6960E-01	0.3891E-02	19878
mansar1.xy54.lgsa	142 180	0.6873E-01	0.3960E-02	19610
mansar1.xy55.lgsa	142 180	0.6790E-01	0.3986E-02	19326
mansar1.xy56.lgsa	142 180	0.6689E-01	0.4010E-02	19028
mansar1.xy57.lgsa	142 179	0.6573E-01	0.4037E-02	18714
mansar1.xy58.lgsa	142 179	0.6457E-01	0.4049E-02	18404

Name of Slice Data File	Peak SAR x and y coordinates	Peak SAR (W/kg)	Avg. SAR (W/kg)	Voxels in tissue
mansar1.xy59.lgsa	142 179	0.6333E-01	0.4090E-02	18106
mansar1.xy60.lgsa	141 178	0.6286E-01	0.4108E-02	17800
mansar1.xy61.lgsa	141 179	0.6258E-01	0.4211E-02	17550
mansar1.xy62.lgsa	141 179	0.6157E-01	0.4243E-02	17248
mansar1.xy63.lgsa	141 179	0.6042E-01	0.4340E-02	17038
mansar1.xy64.lgsa	141 180	0.5939E-01	0.4358E-02	16772
mansar1.xy65.lgsa	141 180	0.5796E-01	0.4361E-02	16498
mansar1.xy66.lgsa	140 178	0.5662E-01	0.4421E-02	16238
mansar1.xy67.lgsa	140 178	0.5592E-01	0.4422E-02	16000
mansar1.xy68.lgsa	140 178	0.5477E-01	0.4459E-02	15752
mansar1.xy69.lgsa	140 178	0.5347E-01	0.4477E-02	15516
mansar1.xy70.lgsa	140 179	0.5267E-01	0.4495E-02	15286
mansar1.xy71.lgsa	139 177	0.5196E-01	0.4492E-02	15060
mansar1.xy72.lgsa	139 177	0.5072E-01	0.4482E-02	14844
mansar1.xy73.lgsa	139 177	0.4954E-01	0.4467E-02	14638
mansar1.xy74.lgsa	139 178	0.4873E-01	0.4491E-02	14480
mansar1.xy75.lgsa	139 178	0.4758E-01	0.4480E-02	14262
mansar1.xy76.lgsa	139 177	0.4655E-01	0.4459E-02	14072
mansar1.xy77.lgsa	138 175	0.4570E-01	0.4475E-02	13874
mansar1.xy78.lgsa	135 168	0.4534E-01	0.4467E-02	13686
mansar1.xy79.lgsa	135 169	0.4507E-01	0.4458E-02	13518
mansar1.xy80.lgsa	134 165	0.4492E-01	0.4482E-02	13360
mansar1.xy81.lgsa	134 166	0.4490E-01	0.4473E-02	13194
mansar1.xy82.lgsa	134 167	0.4480E-01	0.4482E-02	13066
mansar1.xy83.lgsa	133 164	0.4502E-01	0.4463E-02	12916
mansar1.xy84.lgsa	133 165	0.4506E-01	0.4498E-02	12794
mansar1.xy85.lgsa	133 166	0.4500E-01	0.4504E-02	12670
mansar1.xy86.lgsa	133 167	0.4495E-01	0.4503E-02	12548
mansar1.xy87.lgsa	132 164	0.4556E-01	0.4509E-02	12442
mansar1.xy88.lgsa	132 165	0.4590E-01	0.4544E-02	12398
mansar1.xy89.lgsa	132 166	0.4604E-01	0.4570E-02	12340
mansar1.xy90.lgsa	131 163	0.4636E-01	0.4583E-02	12232
mansar1.xy91.lgsa	131 163	0.4647E-01	0.4576E-02	12166
mansar1.xy92.lgsa	131 164	0.4686E-01	0.4576E-02	12082
mansar1.xy93.lgsa	131 165	0.4712E-01	0.4604E-02	12050
mansar1.xy94.lgsa	130 162	0.4733E-01	0.4631E-02	12002
mansar1.xy95.lgsa	130 163	0.4790E-01	0.4642E-02	11938
mansar1.xy96.lgsa	130 164	0.4827E-01	0.4633E-02	11890
mansar1.xy97.lgsa	130 165	0.4842E-01	0.4675E-02	11850
mansar1.xy98.lgsa	130 166	0.4831E-01	0.4674E-02	11816
mansar1.xy99.lgsa	129 163	0.4849E-01	0.4662E-02	11784
mansar1.xy100.lgs	129 165	0.4900E-01	0.4667E-02	11746
mansar1.xy101.lgs	129 166	0.4903E-01	0.4683E-02	11734
mansar1.xy102.lgs	129 166	0.4851E-01	0.4659E-02	11724
mansar1.xy103.lgs	128 165	0.4914E-01	0.4628E-02	11713
mansar1.xy104.lgs	128 166	0.4857E-01	0.4640E-02	11712
mansar1.xy105.lgs	127 164	0.4806E-01	0.4598E-02	11708
mansar1.xy106.lgs	127 166	0.4785E-01	0.4559E-02	11706
mansar1.xy107.lgs	126 164	0.4682E-01	0.4559E-02	11730
mansar1.xy108.lgs	125 161	0.4626E-01	0.4555E-02	11746
mansar1.xy109.lgs	127 165	0.4510E-01	0.4557E-02	11774
mansar1.xy110.lgs	126 165	0.4424E-01	0.4551E-02	11824
mansar1.xy111.lgs	123 158	0.4280E-01	0.4558E-02	11854
mansar1.xy112.lgs	122 159	0.4088E-01	0.4777E-02	12002
mansar1.xy113.lgs	122 159	0.3902E-01	0.5284E-02	12306

Name of Slice Data File	Peak SAR x and y coordinates	Peak SAR (W/kg)	Avg. SAR (W/kg)	Voxels in tissue
mansar1.xy114.lgs	121 159	0.3750E-01	0.5735E-02	12688
mansar1.xy115.lgs	121 159	0.3590E-01	0.6358E-02	13390
mansar1.xy116.lgs	76 146	0.4666E-01	0.6860E-02	13892
mansar1.xy117.lgs	74 145	0.4995E-01	0.7235E-02	14290
mansar1.xy118.lgs	74 142	0.5324E-01	0.7589E-02	14670
mansar1.xy119.lgs	75 139	0.5631E-01	0.7888E-02	14984
mansar1.xy120.lgs	74 139	0.5927E-01	0.8156E-02	15298
mansar1.xy121.lgs	74 137	0.6357E-01	0.8413E-02	15594
mansar1.xy122.lgs	79 131	0.6637E-01	0.8728E-02	15904
mansar1.xy123.lgs	79 130	0.6928E-01	0.8952E-02	16146
mansar1.xy124.lgs	82 125	0.7491E-01	0.9227E-02	16396
mansar1.xy125.lgs	82 123	0.8096E-01	0.9459E-02	16616
mansar1.xy126.lgs	81 123	0.8526E-01	0.9678E-02	16834
mansar1.xy127.lgs	81 122	0.8949E-01	0.9893E-02	17044
mansar1.xy128.lgs	80 122	0.9343E-01	0.1006E-01	17240
mansar1.xy129.lgs	79 122	0.9725E-01	0.1019E-01	17416
mansar1.xy130.lgs	82 119	0.1021E+00	0.1027E-01	17554
mansar1.xy131.lgs	82 118	0.1062E+00	0.1034E-01	17668
mansar1.xy132.lgs	82 118	0.1086E+00	0.1041E-01	17816
mansar1.xy133.lgs	81 118	0.1126E+00	0.1044E-01	17940
mansar1.xy134.lgs	81 118	0.1147E+00	0.1040E-01	18014
mansar1.xy135.lgs	81 117	0.1185E+00	0.1038E-01	18104
mansar1.xy136.lgs	81 116	0.1217E+00	0.1032E-01	18178
mansar1.xy137.lgs	81 116	0.1227E+00	0.1021E-01	18230
mansar1.xy138.lgs	81 115	0.1263E+00	0.1008E-01	18292
mansar1.xy139.lgs	81 115	0.1263E+00	0.9921E-02	18308
mansar1.xy140.lgs	81 114	0.1289E+00	0.9744E-02	18362
mansar1.xy141.lgs	81 114	0.1288E+00	0.9549E-02	18418
mansar1.xy142.lgs	81 113	0.1307E+00	0.9334E-02	18496
mansar1.xy143.lgs	81 113	0.1304E+00	0.9068E-02	18554
mansar1.xy144.lgs	81 112	0.1319E+00	0.8892E-02	18670
mansar1.xy145.lgs	81 112	0.1311E+00	0.8707E-02	18772
mansar1.xy146.lgs	80 112	0.1313E+00	0.8530E-02	18900
mansar1.xy147.lgs	81 111	0.1301E+00	0.8316E-02	19008
mansar1.xy148.lgs	80 111	0.1307E+00	0.8129E-02	19114
mansar1.xy149.lgs	80 111	0.1284E+00	0.7928E-02	19246
mansar1.xy150.lgs	81 109	0.1279E+00	0.7744E-02	19348
mansar1.xy151.lgs	80 110	0.1264E+00	0.7575E-02	19466
mansar1.xy152.lgs	81 108	0.1248E+00	0.7358E-02	19542
mansar1.xy153.lgs	80 109	0.1229E+00	0.7160E-02	19640
mansar1.xy154.lgs	81 108	0.1198E+00	0.6973E-02	19728
mansar1.xy155.lgs	80 108	0.1194E+00	0.6788E-02	19848
mansar1.xy156.lgs	80 108	0.1159E+00	0.6625E-02	19948
mansar1.xy157.lgs	80 108	0.1122E+00	0.6445E-02	20070
mansar1.xy158.lgs	79 108	0.1101E+00	0.6279E-02	20202
mansar1.xy159.lgs	79 108	0.1056E+00	0.6116E-02	20354
mansar1.xy160.lgs	80 107	0.1015E+00	0.5969E-02	20532
mansar1.xy161.lgs	80 107	0.9570E-01	0.5793E-02	20688
mansar1.xy162.lgs	81 107	0.9218E-01	0.5634E-02	20846
mansar1.xy163.lgs	79 107	0.8950E-01	0.5471E-02	21014
mansar1.xy164.lgs	79 107	0.8586E-01	0.5287E-02	21140
mansar1.xy165.lgs	79 107	0.8207E-01	0.5133E-02	21278
mansar1.xy166.lgs	82 105	0.7875E-01	0.4950E-02	21416
mansar1.xy167.lgs	82 105	0.7557E-01	0.4755E-02	21526
mansar1.xy168.lgs	80 201	0.7309E-01	0.4590E-02	21622

Name of Slice Data File	Peak SAR x and y coordinates	Peak SAR (W/kg)	Avg. SAR (W/kg)	Voxels in tissue
mansar1.xy169.lgs	80 201	0.7065E-01	0.4431E-02	21752
mansar1.xy170.lgs	82 203	0.6983E-01	0.4289E-02	21874
mansar1.xy171.lgs	82 203	0.6798E-01	0.4144E-02	21974
mansar1.xy172.lgs	82 203	0.6598E-01	0.4021E-02	22128
mansar1.xy173.lgs	82 203	0.6404E-01	0.3872E-02	22250
mansar1.xy174.lgs	82 203	0.6202E-01	0.3723E-02	22348
mansar1.xy175.lgs	81 203	0.6111E-01	0.3599E-02	22478
mansar1.xy176.lgs	81 203	0.5912E-01	0.3496E-02	22614
mansar1.xy177.lgs	82 204	0.5739E-01	0.3397E-02	22734
mansar1.xy178.lgs	83 206	0.5621E-01	0.3303E-02	22896
mansar1.xy179.lgs	83 206	0.5507E-01	0.3221E-02	23052
mansar1.xy180.lgs	82 206	0.5368E-01	0.3161E-02	23180
mansar1.xy181.lgs	82 206	0.5213E-01	0.3090E-02	23344
mansar1.xy182.lgs	82 207	0.5130E-01	0.3050E-02	23514
mansar1.xy183.lgs	82 207	0.5019E-01	0.3016E-02	23664
mansar1.xy184.lgs	82 208	0.4935E-01	0.3001E-02	23822
mansar1.xy185.lgs	82 208	0.4815E-01	0.3000E-02	23984
mansar1.xy186.lgs	82 209	0.4742E-01	0.3027E-02	24186
mansar1.xy187.lgs	83 209	0.4661E-01	0.3080E-02	24428
mansar1.xy188.lgs	82 209	0.4586E-01	0.3147E-02	24658
mansar1.xy189.lgs	82 210	0.4560E-01	0.3218E-02	24918
mansar1.xy190.lgs	82 210	0.4495E-01	0.3249E-02	25100
mansar1.xy191.lgs	83 210	0.4426E-01	0.3264E-02	25236
mansar1.xy192.lgs	61 153	0.4450E-01	0.3277E-02	25422
mansar1.xy193.lgs	61 153	0.4623E-01	0.3289E-02	25534
mansar1.xy194.lgs	61 153	0.4727E-01	0.3311E-02	25692
mansar1.xy195.lgs	62 153	0.4827E-01	0.3322E-02	25808
mansar1.xy196.lgs	62 153	0.4926E-01	0.3347E-02	25944
mansar1.xy197.lgs	62 153	0.5030E-01	0.3353E-02	26062
mansar1.xy198.lgs	63 154	0.5168E-01	0.3366E-02	26194
mansar1.xy199.lgs	62 154	0.5339E-01	0.3387E-02	26294
mansar1.xy200.lgs	62 154	0.5564E-01	0.3403E-02	26438
mansar1.xy201.lgs	62 154	0.5805E-01	0.3402E-02	26526
mansar1.xy202.lgs	62 154	0.6088E-01	0.3386E-02	26628
mansar1.xy203.lgs	62 154	0.6420E-01	0.3402E-02	26750
mansar1.xy204.lgs	62 154	0.6748E-01	0.3397E-02	26816
mansar1.xy205.lgs	62 155	0.7116E-01	0.3391E-02	26930
mansar1.xy206.lgs	62 155	0.7496E-01	0.3409E-02	27006
mansar1.xy207.lgs	62 155	0.7830E-01	0.3386E-02	27078
mansar1.xy208.lgs	62 155	0.8131E-01	0.3363E-02	27160
mansar1.xy209.lgs	62 155	0.8385E-01	0.3329E-02	27202
mansar1.xy210.lgs	63 155	0.8625E-01	0.3291E-02	27260
mansar1.xy211.lgs	63 155	0.8831E-01	0.3253E-02	27310
mansar1.xy212.lgs	63 155	0.9015E-01	0.3227E-02	27350
mansar1.xy213.lgs	63 155	0.9182E-01	0.3169E-02	27404
mansar1.xy214.lgs	63 155	0.9299E-01	0.3137E-02	27442
mansar1.xy215.lgs	64 155	0.9384E-01	0.3110E-02	27496
mansar1.xy216.lgs	65 155	0.9399E-01	0.3075E-02	27550
mansar1.xy217.lgs	65 155	0.9411E-01	0.3047E-02	27602
mansar1.xy218.lgs	65 155	0.9422E-01	0.3008E-02	27652
mansar1.xy219.lgs	67 155	0.9443E-01	0.2984E-02	27702
mansar1.xy220.lgs	66 155	0.9507E-01	0.2959E-02	27764
mansar1.xy221.lgs	67 155	0.9555E-01	0.2943E-02	27824
mansar1.xy222.lgs	67 155	0.9604E-01	0.2919E-02	27888
mansar1.xy223.lgs	67 155	0.9596E-01	0.2899E-02	27930

Name of Slice Data File	Peak SAR x and y coordinates	Peak SAR (W/kg)	Avg. SAR (W/kg)	Voxels in tissue
mansar1.xy224.lgs	67 155	0.9635E-01	0.2886E-02	28016
mansar1.xy225.lgs	69 155	0.9706E-01	0.2887E-02	28094
mansar1.xy226.lgs	69 155	0.9810E-01	0.2889E-02	28162
mansar1.xy227.lgs	69 155	0.9851E-01	0.2891E-02	28244
mansar1.xy228.lgs	68 155	0.9894E-01	0.2914E-02	28340
mansar1.xy229.lgs	69 155	0.9917E-01	0.2931E-02	28448
mansar1.xy230.lgs	70 155	0.9646E-01	0.2930E-02	28538
mansar1.xy231.lgs	70 155	0.9445E-01	0.2977E-02	28652
mansar1.xy232.lgs	70 156	0.9130E-01	0.2996E-02	28736
mansar1.xy233.lgs	71 156	0.8767E-01	0.3042E-02	28878
mansar1.xy234.lgs	71 156	0.8320E-01	0.3077E-02	28988
mansar1.xy235.lgs	83 95	0.7920E-01	0.3132E-02	29122
mansar1.xy236.lgs	82 96	0.8089E-01	0.3179E-02	29262
mansar1.xy237.lgs	81 96	0.8256E-01	0.3246E-02	29406
mansar1.xy238.lgs	81 97	0.8468E-01	0.3302E-02	29540
mansar1.xy239.lgs	79 97	0.8719E-01	0.3373E-02	29702
mansar1.xy240.lgs	79 97	0.8917E-01	0.3450E-02	29864
mansar1.xy241.lgs	80 96	0.9092E-01	0.3534E-02	30012
mansar1.xy242.lgs	79 97	0.9287E-01	0.3646E-02	30184
mansar1.xy243.lgs	79 97	0.9412E-01	0.3723E-02	30324
mansar1.xy244.lgs	79 97	0.9512E-01	0.3833E-02	30510
mansar1.xy245.lgs	79 96	0.9647E-01	0.3923E-02	30644
mansar1.xy246.lgs	78 97	0.9753E-01	0.4015E-02	30808
mansar1.xy247.lgs	78 97	0.9758E-01	0.4071E-02	30912
mansar1.xy248.lgs	77 98	0.9801E-01	0.4104E-02	30994
mansar1.xy249.lgs	77 98	0.9831E-01	0.4134E-02	31060
mansar1.xy250.lgs	76 99	0.9759E-01	0.4135E-02	31112
mansar1.xy251.lgs	77 99	0.9700E-01	0.4130E-02	31172
mansar1.xy252.lgs	77 99	0.9724E-01	0.4125E-02	31220
mansar1.xy253.lgs	76 100	0.9748E-01	0.4109E-02	31252
mansar1.xy254.lgs	76 100	0.9811E-01	0.4072E-02	31278
mansar1.xy255.lgs	76 101	0.9773E-01	0.4046E-02	31310
mansar1.xy256.lgs	77 100	0.9810E-01	0.4016E-02	31328
mansar1.xy257.lgs	75 102	0.9917E-01	0.3971E-02	31340
mansar1.xy258.lgs	76 102	0.9936E-01	0.3912E-02	31344
mansar1.xy259.lgs	76 102	0.9955E-01	0.3841E-02	31348
mansar1.xy260.lgs	76 103	0.9840E-01	0.3793E-02	31364
mansar1.xy261.lgs	76 103	0.9819E-01	0.3739E-02	31374
mansar1.xy262.lgs	77 102	0.9769E-01	0.3708E-02	31370
mansar1.xy263.lgs	77 103	0.9644E-01	0.3694E-02	31372
mansar1.xy264.lgs	78 101	0.9647E-01	0.3685E-02	31372
mansar1.xy265.lgs	79 99	0.9691E-01	0.3699E-02	31372
mansar1.xy266.lgs	79 99	0.9763E-01	0.3713E-02	31349
mansar1.xy267.lgs	79 100	0.9653E-01	0.3707E-02	31324
mansar1.xy268.lgs	78 102	0.9678E-01	0.3737E-02	31302
mansar1.xy269.lgs	79 100	0.9784E-01	0.3781E-02	31276
mansar1.xy270.lgs	79 101	0.9753E-01	0.3823E-02	31244
mansar1.xy271.lgs	79 101	0.9854E-01	0.3862E-02	31212
mansar1.xy272.lgs	79 101	0.9905E-01	0.3928E-02	31187
mansar1.xy273.lgs	79 101	0.9950E-01	0.3985E-02	31157
mansar1.xy274.lgs	79 101	0.9980E-01	0.4060E-02	31120
mansar1.xy275.lgs	79 101	0.9939E-01	0.4122E-02	31088
mansar1.xy276.lgs	79 102	0.9826E-01	0.4173E-02	31048
mansar1.xy277.lgs	79 102	0.9730E-01	0.4225E-02	31000
mansar1.xy278.lgs	79 102	0.9604E-01	0.4253E-02	30930

Name of Slice Data File	Peak SAR x and y coordinates	Peak SAR (W/kg)	Avg. SAR (W/kg)	Voxels in tissue
mansar1.xy279.lgs	79 103	0.9451E-01	0.4298E-02	30884
mansar1.xy280.lgs	79 102	0.9345E-01	0.4335E-02	30806
mansar1.xy281.lgs	78 105	0.9208E-01	0.4347E-02	30728
mansar1.xy282.lgs	79 103	0.9058E-01	0.4357E-02	30664
mansar1.xy283.lgs	79 104	0.8893E-01	0.4359E-02	30580
mansar1.xy284.lgs	78 106	0.8714E-01	0.4365E-02	30468
mansar1.xy285.lgs	79 105	0.8530E-01	0.4338E-02	30378
mansar1.xy286.lgs	79 105	0.8375E-01	0.4319E-02	30292
mansar1.xy287.lgs	78 107	0.8168E-01	0.4305E-02	30170
mansar1.xy288.lgs	79 106	0.7950E-01	0.4258E-02	30054
mansar1.xy289.lgs	79 107	0.7732E-01	0.4223E-02	29946
mansar1.xy290.lgs	79 107	0.7549E-01	0.4187E-02	29786
mansar1.xy291.lgs	79 108	0.7308E-01	0.4129E-02	29648
mansar1.xy292.lgs	80 107	0.7077E-01	0.4082E-02	29490
mansar1.xy293.lgs	79 109	0.6872E-01	0.4022E-02	29316
mansar1.xy294.lgs	80 109	0.6590E-01	0.3974E-02	29148
mansar1.xy295.lgs	81 108	0.6375E-01	0.3908E-02	28950
mansar1.xy296.lgs	81 109	0.6141E-01	0.3864E-02	28756
mansar1.xy297.lgs	82 109	0.5863E-01	0.3804E-02	28530
mansar1.xy298.lgs	82 110	0.5629E-01	0.3744E-02	28282
mansar1.xy299.lgs	83 110	0.5353E-01	0.3694E-02	28078
mansar1.xy300.lgs	83 112	0.5119E-01	0.3644E-02	27840
mansar1.xy301.lgs	84 112	0.4853E-01	0.3624E-02	27650
mansar1.xy302.lgs	85 112	0.4619E-01	0.3561E-02	27346
mansar1.xy303.lgs	86 112	0.4389E-01	0.3532E-02	27056
mansar1.xy304.lgs	87 112	0.4150E-01	0.3506E-02	26710
mansar1.xy305.lgs	88 112	0.3939E-01	0.3478E-02	26366
mansar1.xy306.lgs	88 114	0.3724E-01	0.3455E-02	26008
mansar1.xy307.lgs	89 114	0.3555E-01	0.3425E-02	25634
mansar1.xy308.lgs	91 113	0.3344E-01	0.3397E-02	25254
mansar1.xy309.lgs	91 115	0.3174E-01	0.3372E-02	24840
mansar1.xy310.lgs	94 111	0.3047E-01	0.3359E-02	24428
mansar1.xy311.lgs	94 113	0.2928E-01	0.3345E-02	24006
mansar1.xy312.lgs	95 113	0.2810E-01	0.3337E-02	23596
mansar1.xy313.lgs	97 112	0.2666E-01	0.3339E-02	23182
mansar1.xy314.lgs	98 112	0.2555E-01	0.3339E-02	22718
mansar1.xy315.lgs	99 113	0.2424E-01	0.3354E-02	22268
mansar1.xy316.lgs	102 197	0.2340E-01	0.3375E-02	21842
mansar1.xy317.lgs	104 198	0.2266E-01	0.3387E-02	21362
mansar1.xy318.lgs	105 197	0.2164E-01	0.3401E-02	20854
mansar1.xy319.lgs	104 114	0.2080E-01	0.3421E-02	20358
mansar1.xy320.lgs	109 200	0.2006E-01	0.3442E-02	19812
mansar1.xy321.lgs	109 198	0.1937E-01	0.3476E-02	19306
mansar1.xy322.lgs	109 197	0.1899E-01	0.3514E-02	18796
mansar1.xy323.lgs	112 199	0.1789E-01	0.3561E-02	18254
mansar1.xy324.lgs	113 198	0.1712E-01	0.3597E-02	17696
mansar1.xy325.lgs	113 195	0.1619E-01	0.3644E-02	17092
mansar1.xy326.lgs	116 197	0.1553E-01	0.3704E-02	16494
mansar1.xy327.lgs	118 197	0.1487E-01	0.3779E-02	15922
mansar1.xy328.lgs	119 196	0.1434E-01	0.3842E-02	15262
mansar1.xy329.lgs	119 114	0.1372E-01	0.3910E-02	14614
mansar1.xy330.lgs	117 122	0.1317E-01	0.3982E-02	13936
mansar1.xy331.lgs	119 122	0.1270E-01	0.4072E-02	13232
mansar1.xy332.lgs	120 125	0.1202E-01	0.4174E-02	12560
mansar1.xy333.lgs	123 123	0.1149E-01	0.4276E-02	11840

Name of Slice Data File	Peak SAR x and y coordinates		Peak SAR (W/kg)	Avg. SAR (W/kg)	Voxels in tissue
mansar1.xy334.lgs	124	125	0.1109E-01	0.4396E-02	11140
mansar1.xy335.lgs	127	124	0.1051E-01	0.4526E-02	10348
mansar1.xy336.lgs	129	126	0.9884E-02	0.4662E-02	9482
mansar1.xy337.lgs	133	124	0.9465E-02	0.4804E-02	8586
mansar1.xy338.lgs	135	128	0.9091E-02	0.4948E-02	7662
mansar1.xy339.lgs	139	125	0.8742E-02	0.5087E-02	6710
mansar1.xy340.lgs	141	129	0.8414E-02	0.5192E-02	5828
mansar1.xy341.lgs	147	127	0.8032E-02	0.5286E-02	4770
mansar1.xy342.lgs	151	131	0.7640E-02	0.5359E-02	3632
mansar1.xy343.lgs	157	131	0.7252E-02	0.5449E-02	2554
mansar1.xy344.lgs	164	172	0.6800E-02	0.5610E-02	710

**Location and values for peak and average 1 gram average SAR for
total volume of exposed tissue**

mansar1.xy144.lgs	81	112	0.1319E+00	0.4319E-02	744429
-------------------	----	-----	------------	------------	--------

Figure 3.4 illustrates the orientation of the Kuster head model with respect to the antenna in the sagittal or xz plane at $y = 154$ mm from the origin of the rectangular coordinate system at the lower-front-left corner of the fdtd mesh. The horizontal black lines, A through K denotes the horizontal xy planes where the SAR data was plotted and printed. However, SAR data were calculated for all of the 333, 1-mm thick horizontal xy slices as well as for the vertical slices denoted by L through N in the sagittal xz plane of the simulated head tissue illustrated in Figure 3.5.

Figure 6.1 illustrates the FDTD derived SAR distribution in xz planes through the head corresponding to the vertical slices K (through the center of the left row of antenna patches), L (through the center of the array of patches) and M (through the right row of patches) defined in Figure 3.5. The SAR distributions as averaged over each 1 mm cubical cell or voxel, calculated by the FDTD program are depicted as a color graphs with each color representing a 6 dB range of SAR values. The maximum SAR corresponding to the 0-dB reference is shown below each graph. Note that the SAR in the center of the head model drops to levels lower than -30 decibels with respect to the maximum of 0.172 W/kg at or near the facial surface of the model.

Figures 6.2 and 6.3 respectively illustrate the SAR distribution in the horizontal xy planes at slices labeled as A through E and F through K as denoted in Figure 3.4. As for the previous figure each color representing the SAR distribution as averaged over each 1-mm cubical cell corresponds to a 6-dB range of SAR values. The maximum SAR corresponding to 0 dB is listed below each graph in the figure. The peak SAR for the entire head model, 0.194 W/kg occurs at the location of the black plus sign in the scan through the slice denoted as E in Figure 6.2.

Figures 6.4 and 6.5 illustrate the respective color plots of the SAR distribution in the xy planes denoted by A through E and F through K as identified in Figure 3.4. The legend for these plots is set for the color red to represent all SARs at or greater than the value 1.6 W/kg allowed by the FCC MPL. The maximum value of the SAR for each plot is shown in the text below the plots. The maximum 1-gram average for the entire head model, 0.132 W/kg occurs at the location of the black plus sign in slice D of Figure 6.4.

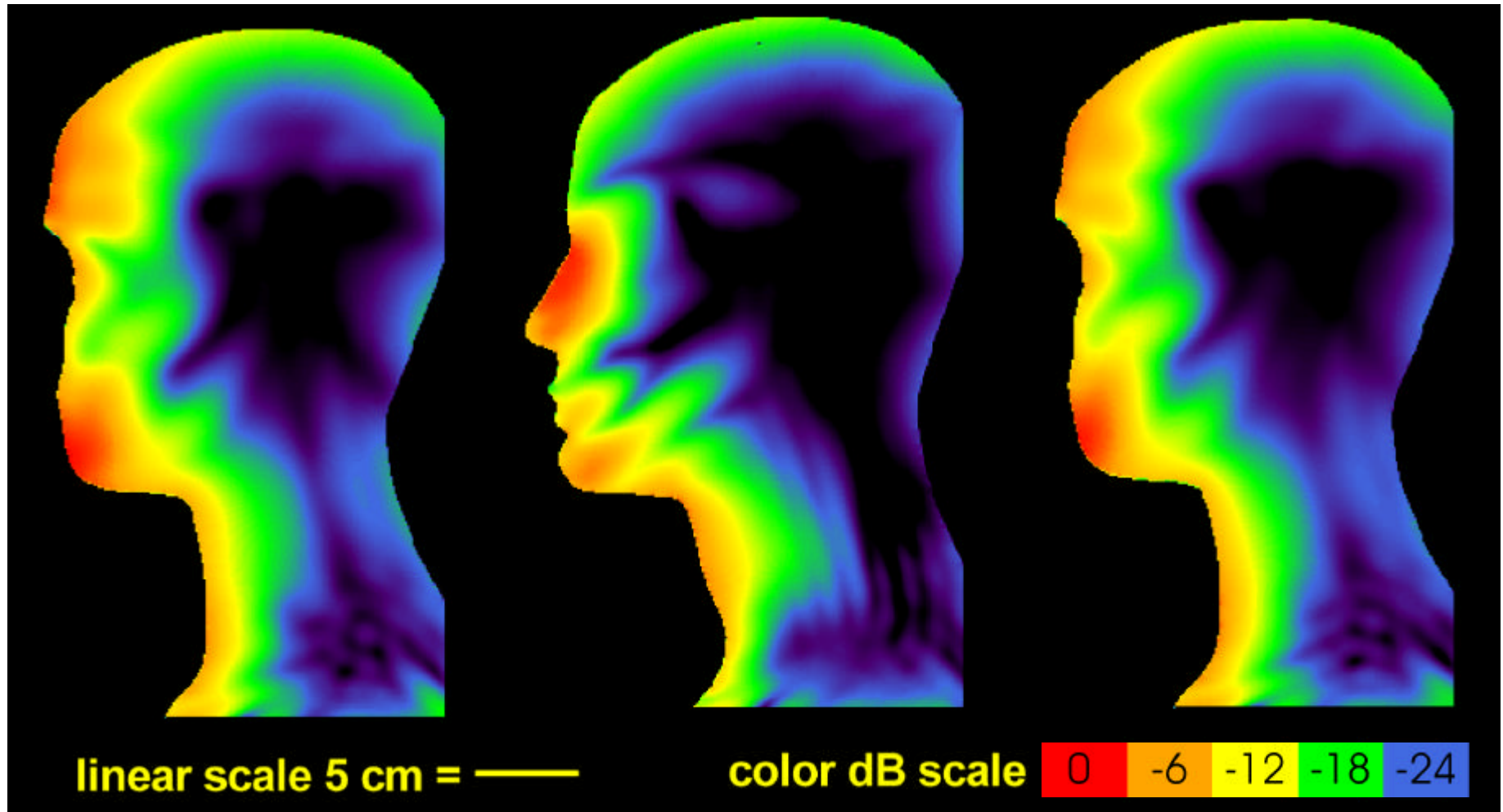
It is difficult to make an accurate plot by plot comparison of the FDTD derived SAR and the corresponding measurements made by SPEAG as discussed in Appendix A because (a) the latter were based on a medium with a 8 % higher conductivity of 1.83 S/m rather than the desired target value of 1.69 S/m, which as explained in the appendix was the lowest achievable with the water/sugar composition at 1.92 GHz and (b) the 2-dimensional plots of the measured SARs for the latter were done in planes parallel to the ground plane rather than in the two orthogonal planes perpendicular to the ground plane as obtained from the

calculations. Restrictions on computer memory prohibited detailed calculations to be made in all planes using a single computer run so to save time the two orientations that produced the most informative color plots given in the preceding figures were chosen. To avoid a long computer run to obtain data for 2-dimensional plots in the yz-planes parallel to the antenna ground plane, a program was written to sort some of the calculated data from the xy planes to make a plot of the maximum calculated SAR occurring in planes parallel to the antenna ground plane for comparison with the measured maxima in those planes.

Figure 6.6 illustrates a comparison between the FDTD maximum derived values of peak (blue curve) and 1 gram average SAR (green curve) in each yz plane slice of the Kuster head model and the measured values by SPEAG (red deltas for peak) and SARTest (orange delta for peak and orange diamond for 1-gram average) versus distance x from the ground plane. The SPEAG measurements are discussed in page 29 to 32 and in Sub-Appendix H of Appendix A and the SARTest measurements are tabulated in Table 1 of Appendix C. The peak value of 0.17 W/kg measured by SARTest is close but lower than the calculated value of 0.194 W/kg. The 1-gram average of 0.09 W/kg obtained by SARTest is somewhat lower than the maximum calculated 1-gram average SAR of 0.13 W/kg. However when SARTest measured the SARs for an exposed inhomogeneous model with a layer of skin the obtained respective peak and 1-gram average values of 0.2 and 0.17 W/kg as indicated in Table 2 of Appendix C. Appendix C provides all details on the methodology used for making the measurements. The SPEAG measured peak values fall well below the calculated peak values. This may be due in part to the fact that the calculations are based on a net power of 79.62 mW delivered to the antenna while the measurements are based on an incident power of 80.0 mW to the antenna which can result in a lower net power because of the amount of reflected power from the surface of the model. The calculations must be based on "worst case" conditions where lacking any information on how well the antenna remains tuned when close to the exposed subject, it is assumed that all of the available power is delivered to the antenna. As stated in page 24 of Appendix A, due to the irregular shape of the model the measurements could not be made at all locations within the simulated tissue especially close to boundaries. There appears to be a more likely reason that the measured maximum SARs fall below the calculated maximum SARs at the cross-sectional planes further from the source. As seen from the color graphs at these locations the SARs tend to be higher at the boundaries of the planes due to defracted energy or surface wave propagation around the surface of the model a region that is not accessible by the measurement probe. The measurements indicated that the highest SAR of 0.0637 W/kg (14 dB below the FCC MPL) occurred in the lower left side of the face in front of the patch with the highest radiation. The highest radiation from the FDTD model of the antenna came from the lower right patch which produced the maximum SAR of 0.194 W/kg (9 dB below the FCC MPL) at the right side of the face. It should be noted, however the FCC MPL is based on the maximum 1 gram average SAR which was found to be 0.132 W/kg (10.8 dB below the MPL) by the calculations and 0.09 W/kg (0.17

W/kg or 9.7 dB below the MPL in the skin clad phantom head) by the SARTest measurements. SPEAG indicated that the maximum 1-gram average measurement could not be made in the phantom because of the irregular boundaries of the simulated tissue.

SPEAG made measurements of the peak SAR along a line perpendicular to the antenna through the nose of the model as a function of distance from the ground plane shown in Figure 3.9 of Appendix A. Data from the FDTD calculations showing peak and 1 gram average SAR along the same line were plotted with the measured data as shown in Figure 6.7. For this case the measured peak values followed nearly the same pattern but with a maximum value (0.081 W/kg) higher than the calculated peak value (0.0535 W/kg) and the 1-gram average value (0.0448 W/kg).

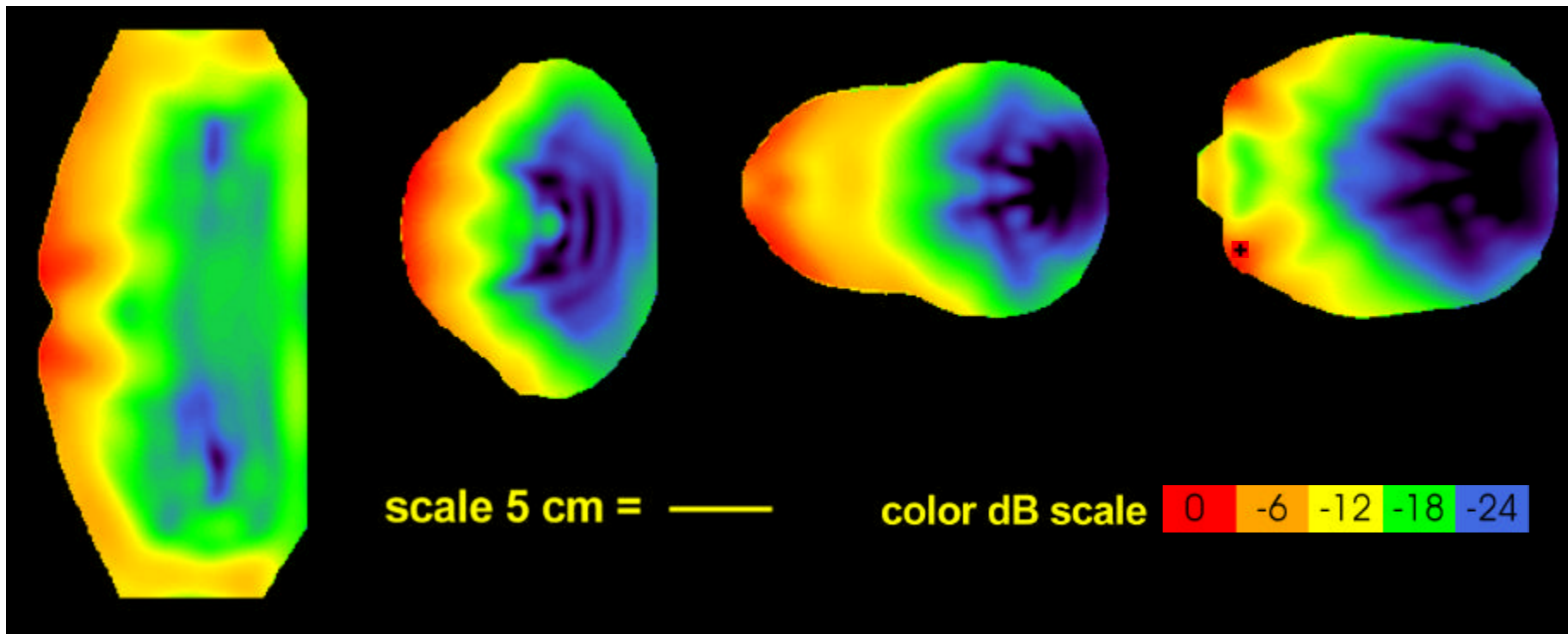


scan K, slice 118
0 dB = 0.152 W/kg

scan L, slice 154
0 dB = 0.172 W/kg

scan M, slice 191
0 dB = 0.163 W/kg

Figure 6.1. FDTD derived x-z plane SAR distributions in Kuster model head exposed to AT&T RU antenna.



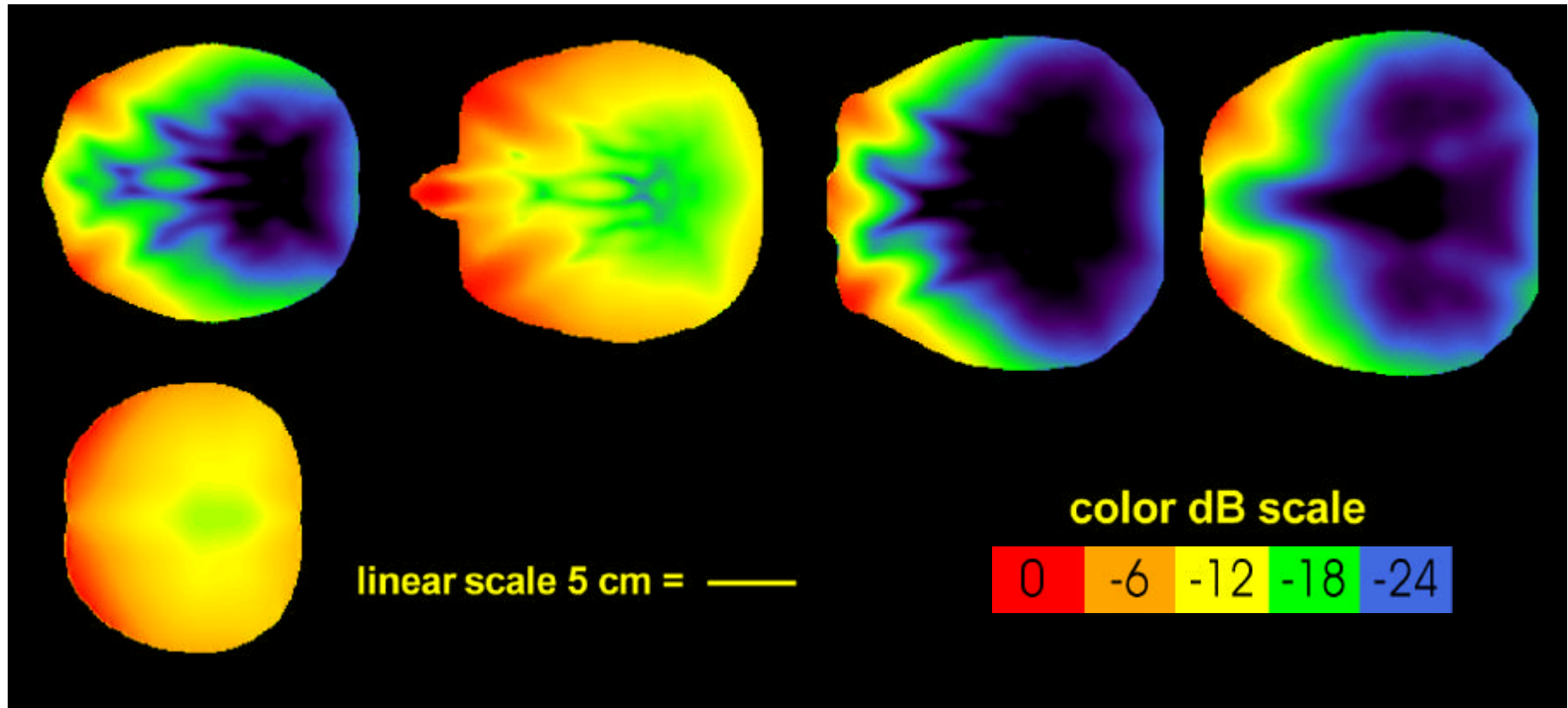
scan A, slice 20
0 dB = 0.0507 W/kg
W/kg

scan B, slice 70
0 dB = 0.064 W/kg

scan C, slice 126
0 dB = 0.120 W/kg

scan E, slice 148
0 dB = 0.194

Figure 6.2. FDTD derived x-y plane SAR distributions in Kuster model head exposed to AT&T RU antenna (black plus sign in scan E indicates location of maximum SAR for whole head).



scan F, slice 175
278
0 dB = 0.0926 W/kg
W/k

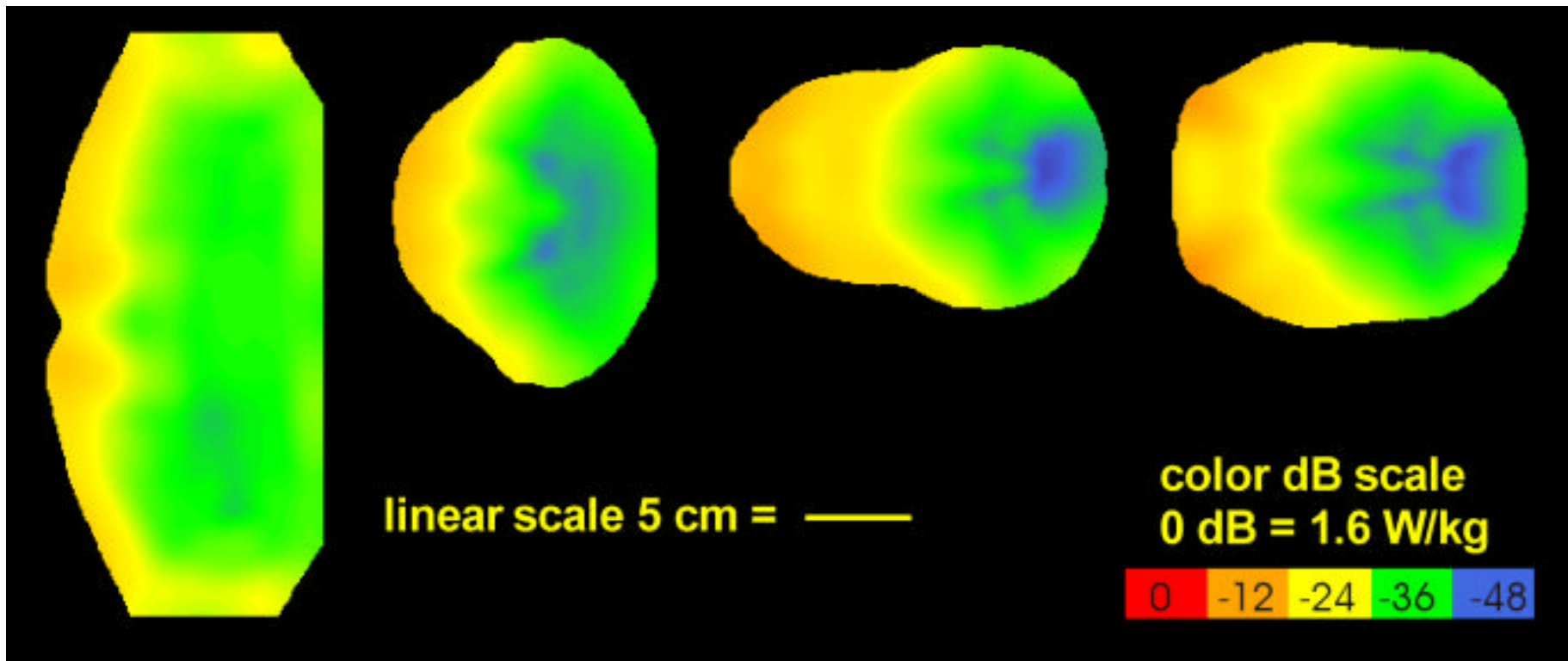
scan G, slice 193
0 dB = 0.0643 W/kg

scan I, slice 240
0 dB = 0.121 W/kg

scan J, slice
0 dB = 0.141

scan K, slice 325
0 dB = 0.0229 W/kg

Figure 6.3. FDTD derived x-y plane SAR distributions in Kuster model head exposed to AT&T RU antenna.



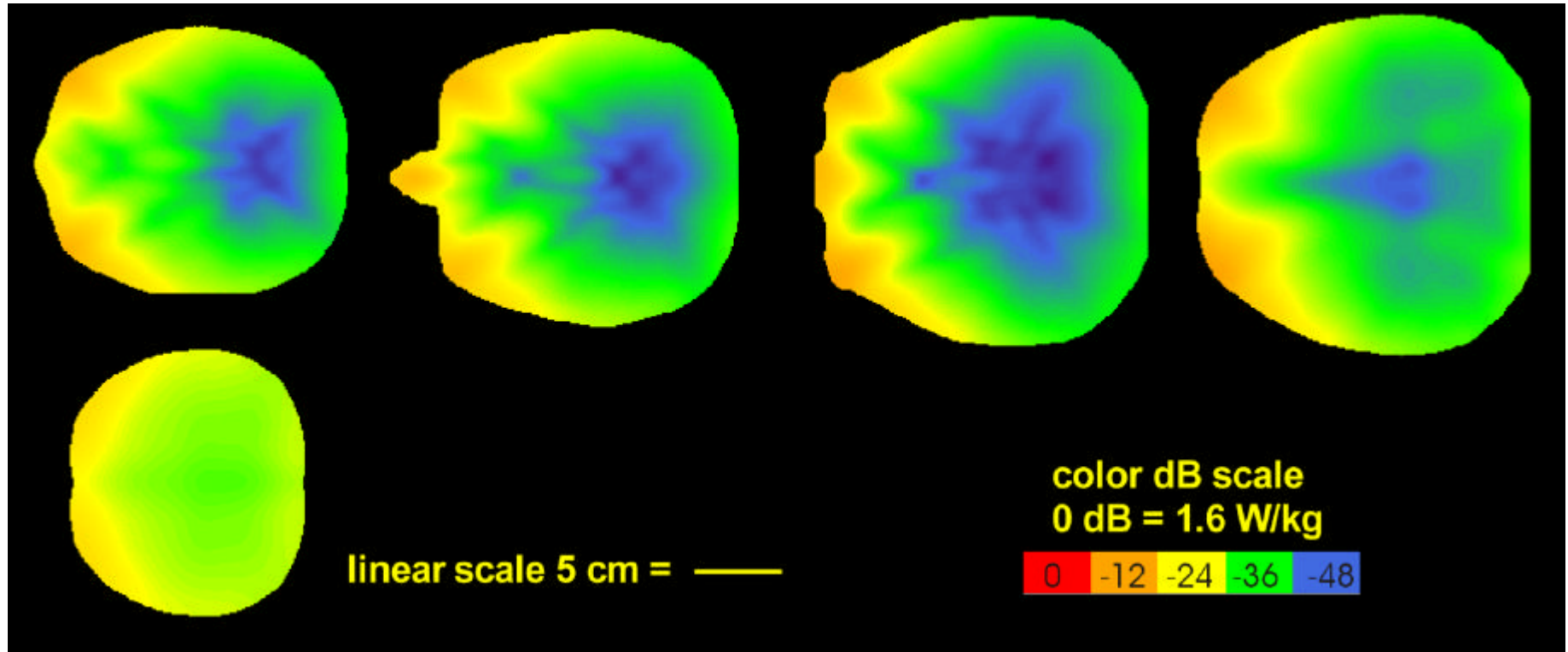
scan A, slice 20
Max = 0.0356

scan B, slice 70
Max = 0.0536

scan C, slice 126
Max = 0.0868

scan D, slice 144
Max = 0.134

Figure 6.4. FDTD derived x-y plane 1 gram average SAR (W/kg) distributions in Kuster model head exposed to AT&T RU antenna compared to maximum allowed by ANSI/IEEE standard.



scan F, slice 175
278
Max = 0.0622

scan G, slice 193
Max = 0.0471

scan I, slice 240
Max = 0.0908

scan J, slice
Max = 0.0978

scan K, slice 325
Max = 0.0165

Figure 6.5. FDTD derived x-y plane 1 gram average SAR (W/kg) distributions in Kuster model head exposed to AT&T RU antenna compared to ANSI/IEEE standard.

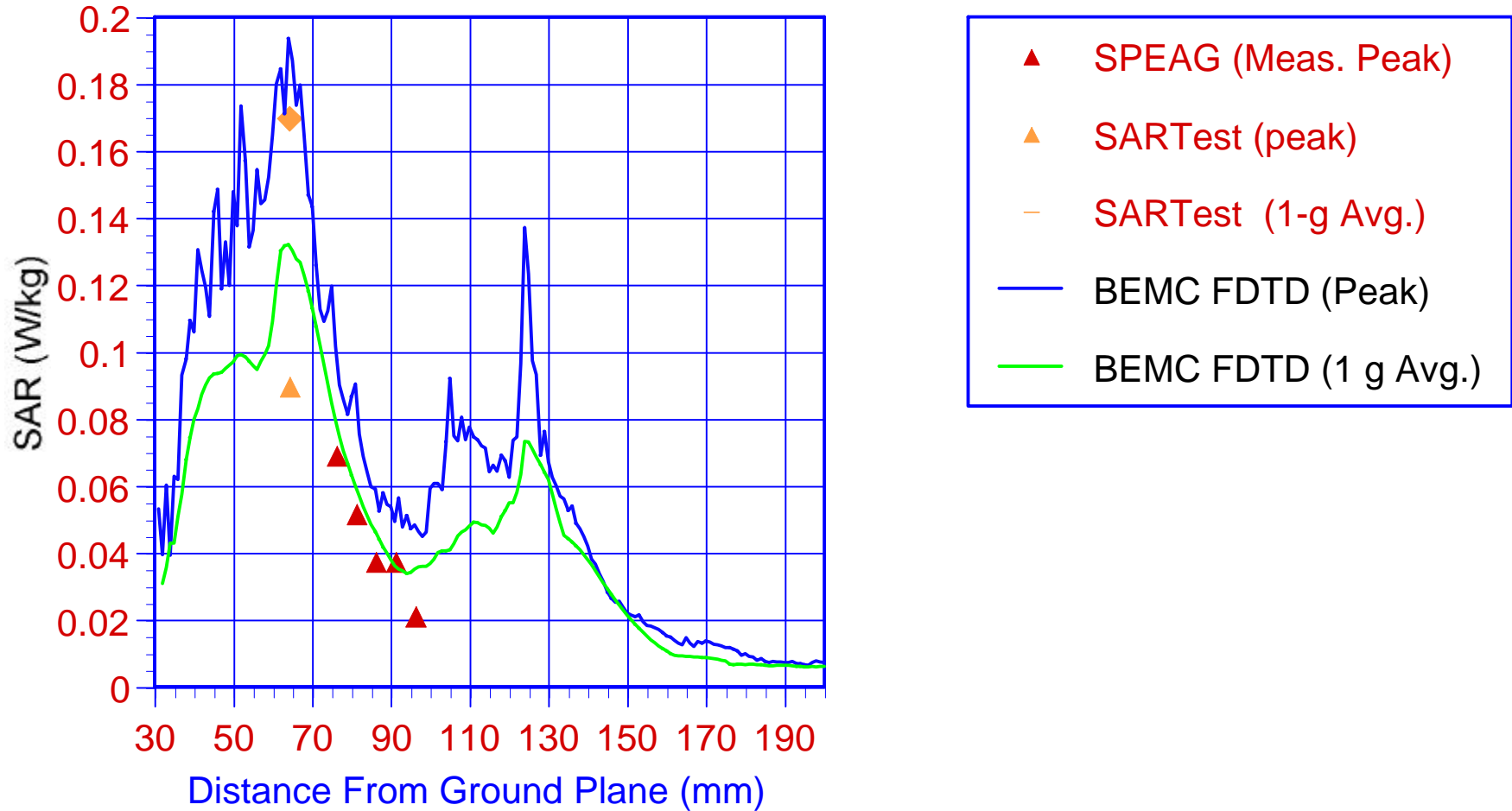


Figure 6.6. Comparison of FDTD maximum derived values of peak and 1 gram average SAR by BEMC in each yz plane slice of the Kuster head model as a function of and measured values by SPEAG and SARTest versus distance x from ground plane with face of Kuster phantom head model exposed to AT&T RU antenna with tip of nose in contact with radome (31 cm from ground plane) and 9 mm below center of patch array (SARTest peak SAR of 0,09 W/kg was highest measured at accessible locations but unreported value obtained from extrapolation to phantom boundary of 0.26 W/kg was used to obtain 1-gram average of 0.17 W/kg).

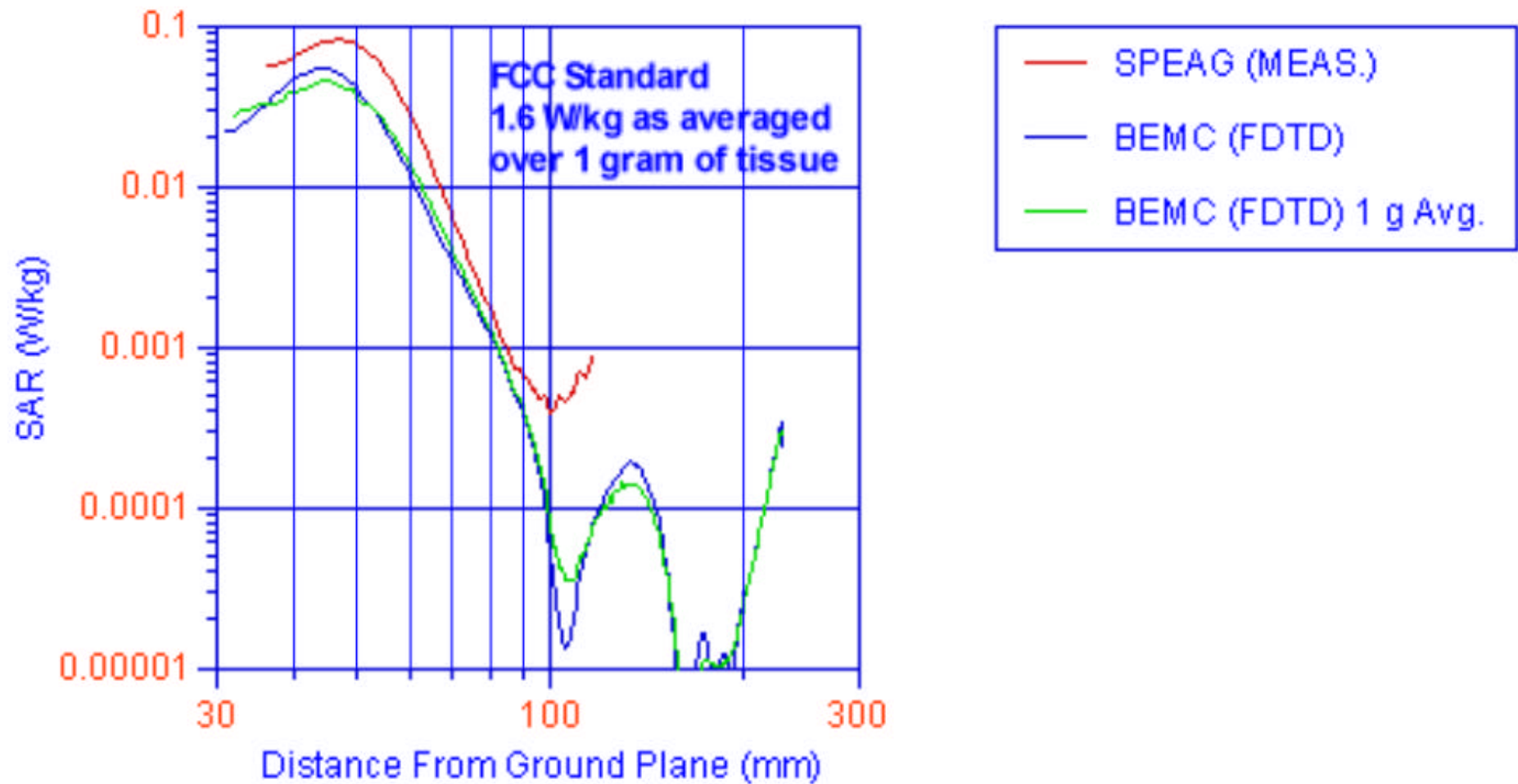


Figure 6.7. Comparison of FDTD derived values of SAR by BEMC and measured values by SPEAG with face of Kuster phantom head model exposed to AT&T RU antenna with tip of nose in contact with radome (31 cm from ground plane) and 9 mm below center of patch array (values plotted along line through tip of nose and perpendicular to ground plane).

6.2 Orientation with Tip of Nose in Contact with Radome and Centered over Lower Right Patch

The near field calculations and measurements indicated that the fields were highest in front of the patch radiators in the antenna array. In fact the calculated fields were found to be the highest in front of the lower right patch. In order to evaluate the worst case conditions FDTD calculations were made of the peak and 1-gram average of the SARs in the Kuster homogeneous head model when exposed to the AT&T RU antenna with the tip of the nose in contact with the radome and centered over the lower right patch as illustrated in Figures 3.6 and 3.7. The results were compared to the measurements made by SPEAG described in Appendix A. The highest fields for the antenna used to perform the measurements occurred in front of the lower left patch so the measurements were done with the nose of the model oriented over that patch.

Table 6.3 summarizes the calculated results of both the peak and average SARs calculated for each 1-mm thick slice in the xy plane as well as for the entire exposed head model. The format of the table is the same as previously discussed for Table 6.1. It may be noted from the table that the maximum SAR of 3.49 W/kg for the entire head model is in the 63rd slice (file mansar1.yz63.sar) at y=225 mm and z=115 mm and the average SAR for the 886 cells of that slice is 0.583 W/kg. It can also be seen at the bottom of the table that the SAR as averaged over the 5611108 cells of the entire head model is 0.00665 W/kg.

Table 6.4 illustrates the results of the 1-gram averaging of the fdttd output data. The format is the same as discussed for Table 6.2. It may be noted from the table that the highest 1-g average SAR of 1.53 W/kg occurs in the slice at x=60 mm at the position y=226 mm and z=117 mm. This is only 0.223 dB below the FCC MPL of 1.6 W/kg. However, it must be noted that with the intended 2 watt e.i.r.p. operation of the antenna, the SAR would actually be 1.6 dB below the FCC MPL if exposure continued at this level as averaged over any 30-minute period. Furthermore it is unlikely that a subject would hold his or her nose against the radome for such an extended period. Even for exposures in this position for up to a minute, the time averaged SAR would be no greater than -16 dB below the FCC MPL. Assuming an average head tissue density the same as water, the total mass of the phantom head tissue is $5611108/1,000,000 = 5.61$ kg. Using the average SAR of 0.00665 from Table 6.3 the total absorbed power is $0.00665 \times 5.61 = 0.0373$ W = 37.3 mW which is 46.85 % of the antenna input power. For the worst case of all of the 79.62 mW of radiated power absorbed by a 70-Kg man the whole-body average SAR would be 0.001377 W/kg. Thus we may conclude that under these exposure conditions the whole-body averaged SAR for an adult man with a head similar to that of the Kuster phantom head would be somewhere between 0.001377 and 0.00665 W/kg or from 12 to 58 times less than that allowed by the FCC MPL of 0.08 W/kg.

Table 6.3 Slice and Whole Head Model Peak and average SAR (averaged over slice) for Kuster Head and Shoulders Model Exposed to AT&T RU Antenna with Nose in Contact with Radome and centered over lower left patch (slice file number is distance in mm from FDTD space rectangular coordinates origin in x direction).

Name of Slice Data File	Peak SAR y and z coordinates	Peak SAR (W/kg)	Avg. SAR (W/kg)	Voxels in tissue
kuster3.yz49.sar	225 126	0.9698E+00	0.6452E+00	36
kuster3.yz50.sar	225 128	0.1709E+01	0.8013E+00	70
kuster3.yz51.sar	227 130	0.2083E+01	0.9135E+00	110
kuster3.yz52.sar	228 133	0.1687E+01	0.9645E+00	134
kuster3.yz53.sar	227 133	0.2761E+01	0.1041E+01	164
kuster3.yz54.sar	224 133	0.2211E+01	0.1065E+01	200
kuster3.yz55.sar	227 136	0.2355E+01	0.1068E+01	238
kuster3.yz56.sar	229 136	0.2094E+01	0.1057E+01	278
kuster3.yz57.sar	226 118	0.3082E+01	0.1062E+01	312
kuster3.yz58.sar	226 118	0.2384E+01	0.1014E+01	356
kuster3.yz59.sar	225 117	0.3117E+01	0.1000E+01	390
kuster3.yz60.sar	225 118	0.2685E+01	0.8896E+00	472
kuster3.yz61.sar	226 116	0.2934E+01	0.7885E+00	562
kuster3.yz62.sar	225 117	0.2616E+01	0.6989E+00	678
kuster3.yz63.sar	225 115	0.3485E+01	0.5830E+00	886
kuster3.yz64.sar	226 114	0.2930E+01	0.4717E+00	1368
kuster3.yz65.sar	226 114	0.1705E+01	0.3807E+00	1830
kuster3.yz66.sar	226 122	0.1308E+01	0.2907E+00	2492
kuster3.yz67.sar	226 124	0.1218E+01	0.2281E+00	3214
kuster3.yz68.sar	226 125	0.1139E+01	0.1822E+00	4038
kuster3.yz69.sar	226 126	0.1057E+01	0.1484E+00	4992
kuster3.yz70.sar	226 126	0.9770E+00	0.1242E+00	5910
kuster3.yz71.sar	226 126	0.8943E+00	0.1072E+00	6874
kuster3.yz72.sar	226 126	0.8118E+00	0.9066E-01	7822
kuster3.yz73.sar	226 127	0.7335E+00	0.7745E-01	8706
kuster3.yz74.sar	226 127	0.6587E+00	0.6696E-01	9592
kuster3.yz75.sar	226 127	0.5882E+00	0.5823E-01	10542
kuster3.yz76.sar	226 127	0.5229E+00	0.5085E-01	11814
kuster3.yz77.sar	226 127	0.4631E+00	0.4603E-01	13084
kuster3.yz78.sar	226 128	0.4096E+00	0.4143E-01	14116
kuster3.yz79.sar	226 128	0.3621E+00	0.3737E-01	15686
kuster3.yz80.sar	226 128	0.3195E+00	0.3393E-01	16408
kuster3.yz81.sar	226 128	0.2815E+00	0.3154E-01	17276
kuster3.yz82.sar	226 128	0.2476E+00	0.2952E-01	18136
kuster3.yz83.sar	226 128	0.2175E+00	0.2734E-01	18814
kuster3.yz84.sar	226 128	0.1906E+00	0.2527E-01	19366
kuster3.yz85.sar	226 128	0.1667E+00	0.2339E-01	19950
kuster3.yz86.sar	226 128	0.1455E+00	0.2173E-01	20386
kuster3.yz87.sar	226 129	0.1267E+00	0.2023E-01	20738
kuster3.yz88.sar	226 129	0.1101E+00	0.1884E-01	21072
kuster3.yz89.sar	226 129	0.9557E-01	0.1757E-01	21398
kuster3.yz90.sar	226 129	0.8287E-01	0.1642E-01	21720
kuster3.yz91.sar	226 129	0.7185E-01	0.1536E-01	21992
kuster3.yz92.sar	165 159	0.7209E-01	0.1442E-01	22286
kuster3.yz93.sar	185 240	0.7560E-01	0.1356E-01	22578
kuster3.yz94.sar	182 239	0.8330E-01	0.1289E-01	23200
kuster3.yz95.sar	184 240	0.6241E-01	0.1211E-01	23456
kuster3.yz96.sar	181 241	0.7021E-01	0.1145E-01	23744
kuster3.yz97.sar	181 242	0.7207E-01	0.1088E-01	24068

Name of Slice Data File	Peak SAR y and z coordinates	Peak SAR (W/kg)	Avg. SAR (W/kg)	Voxels in tissue
kuster3.yz98.sar	167 231	0.8040E-01	0.1032E-01	24349
kuster3.yz99.sar	168 233	0.7429E-01	0.9833E-02	24639
kuster3.yz100.sar	169 235	0.7135E-01	0.9403E-02	24908
kuster3.yz101.sar	166 233	0.8173E-01	0.9001E-02	25195
kuster3.yz102.sar	178 243	0.7824E-01	0.8622E-02	25456
kuster3.yz103.sar	169 238	0.7071E-01	0.8303E-02	25717
kuster3.yz104.sar	166 236	0.8258E-01	0.8016E-02	25980
kuster3.yz105.sar	174 243	0.8057E-01	0.7742E-02	26190
kuster3.yz106.sar	167 239	0.7896E-01	0.7524E-02	26419
kuster3.yz107.sar	165 238	0.7773E-01	0.7351E-02	26659
kuster3.yz108.sar	186 252	0.8372E-01	0.7182E-02	26869
kuster3.yz109.sar	172 245	0.9009E-01	0.7192E-02	27330
kuster3.yz110.sar	168 244	0.7193E-01	0.6991E-02	27527
kuster3.yz111.sar	167 244	0.7859E-01	0.6852E-02	27777
kuster3.yz112.sar	165 243	0.8113E-01	0.6702E-02	27954
kuster3.yz113.sar	176 251	0.9073E-01	0.6556E-02	28163
kuster3.yz114.sar	168 247	0.8064E-01	0.6413E-02	28330
kuster3.yz115.sar	172 250	0.8276E-01	0.6283E-02	28536
kuster3.yz116.sar	169 249	0.8907E-01	0.6140E-02	28709
kuster3.yz117.sar	167 248	0.8711E-01	0.6003E-02	28885
kuster3.yz118.sar	166 248	0.8805E-01	0.5870E-02	29045
kuster3.yz119.sar	169 251	0.8615E-01	0.5732E-02	29233
kuster3.yz120.sar	167 250	0.9815E-01	0.5610E-02	29399
kuster3.yz121.sar	166 250	0.8573E-01	0.5524E-02	29590
kuster3.yz122.sar	165 250	0.8756E-01	0.5414E-02	29730
kuster3.yz123.sar	168 253	0.8393E-01	0.5346E-02	29935
kuster3.yz124.sar	153 239	0.8321E-01	0.5328E-02	30287
kuster3.yz125.sar	173 257	0.7464E-01	0.5202E-02	30477
kuster3.yz126.sar	168 255	0.7374E-01	0.5115E-02	30667
kuster3.yz127.sar	161 249	0.8288E-01	0.5021E-02	30886
kuster3.yz128.sar	167 255	0.7633E-01	0.4929E-02	31143
kuster3.yz129.sar	166 255	0.7452E-01	0.4852E-02	31407
kuster3.yz130.sar	159 249	0.7641E-01	0.4759E-02	31705
kuster3.yz131.sar	152 242	0.8295E-01	0.4678E-02	32035
kuster3.yz132.sar	158 249	0.7941E-01	0.4593E-02	32359
kuster3.yz133.sar	168 258	0.7648E-01	0.4532E-02	32710
kuster3.yz134.sar	166 257	0.7792E-01	0.4448E-02	33005
kuster3.yz135.sar	155 248	0.7520E-01	0.4384E-02	33294
kuster3.yz136.sar	166 258	0.7195E-01	0.4315E-02	33515
kuster3.yz137.sar	165 258	0.7483E-01	0.4251E-02	33744
kuster3.yz138.sar	168 260	0.7154E-01	0.4211E-02	33984
kuster3.yz139.sar	152 247	0.8512E-01	0.4204E-02	34355
kuster3.yz140.sar	151 247	0.7233E-01	0.4136E-02	34555
kuster3.yz141.sar	166 260	0.6954E-01	0.4059E-02	34738
kuster3.yz142.sar	165 260	0.7031E-01	0.4002E-02	34917
kuster3.yz143.sar	150 247	0.6507E-01	0.3939E-02	35081
kuster3.yz144.sar	166 261	0.6810E-01	0.3871E-02	35240
kuster3.yz145.sar	165 261	0.6960E-01	0.3801E-02	35417
kuster3.yz146.sar	167 262	0.6651E-01	0.3728E-02	35572
kuster3.yz147.sar	166 262	0.6592E-01	0.3651E-02	35708
kuster3.yz148.sar	170 264	0.6212E-01	0.3578E-02	35844
kuster3.yz149.sar	165 262	0.6610E-01	0.3521E-02	35988
kuster3.yz150.sar	155 255	0.5999E-01	0.3452E-02	36145
kuster3.yz151.sar	150 251	0.6259E-01	0.3378E-02	36283
kuster3.yz152.sar	157 257	0.6199E-01	0.3308E-02	36402

Name of Slice Data File	Peak SAR y and z coordinates	Peak SAR (W/kg)	Avg. SAR (W/kg)	Voxels in tissue
kuster3.yz153.sar	170 265	0.6198E-01	0.3251E-02	36523
kuster3.yz154.sar	145 245	0.6126E-01	0.3209E-02	36732
kuster3.yz155.sar	152 254	0.5801E-01	0.3137E-02	36847
kuster3.yz156.sar	166 264	0.5733E-01	0.3071E-02	36967
kuster3.yz157.sar	150 253	0.5723E-01	0.3004E-02	37066
kuster3.yz158.sar	151 254	0.5411E-01	0.2942E-02	37173
kuster3.yz159.sar	164 263	0.5585E-01	0.2882E-02	37273
kuster3.yz160.sar	162 262	0.5481E-01	0.2817E-02	37352
kuster3.yz161.sar	167 265	0.5532E-01	0.2756E-02	37435
kuster3.yz162.sar	150 254	0.5690E-01	0.2697E-02	37529
kuster3.yz163.sar	158 260	0.5388E-01	0.2639E-02	37595
kuster3.yz164.sar	155 258	0.5707E-01	0.2584E-02	37698
kuster3.yz165.sar	152 256	0.5412E-01	0.2530E-02	37773
kuster3.yz166.sar	159 261	0.5134E-01	0.2479E-02	37856
kuster3.yz167.sar	153 257	0.5416E-01	0.2425E-02	37925
kuster3.yz168.sar	170 267	0.5321E-01	0.2373E-02	37981
kuster3.yz169.sar	170 267	0.5127E-01	0.2332E-02	38076
kuster3.yz170.sar	165 265	0.4616E-01	0.2279E-02	38108
kuster3.yz171.sar	166 266	0.4276E-01	0.2235E-02	38151
kuster3.yz172.sar	165 265	0.5465E-01	0.2193E-02	38165
kuster3.yz173.sar	165 265	0.5330E-01	0.2148E-02	38190
kuster3.yz174.sar	162 263	0.5419E-01	0.2109E-02	38232
kuster3.yz175.sar	162 263	0.4902E-01	0.2066E-02	38244
kuster3.yz176.sar	155 259	0.4585E-01	0.2024E-02	38275
kuster3.yz177.sar	155 259	0.4815E-01	0.1986E-02	38309
kuster3.yz178.sar	158 261	0.4705E-01	0.1946E-02	38322
kuster3.yz179.sar	168 267	0.4345E-01	0.1912E-02	38354
kuster3.yz180.sar	167 266	0.5307E-01	0.1881E-02	38382
kuster3.yz181.sar	167 266	0.4713E-01	0.1849E-02	38385
kuster3.yz182.sar	165 266	0.3957E-01	0.1818E-02	38394
kuster3.yz183.sar	165 266	0.3900E-01	0.1791E-02	38422
kuster3.yz184.sar	165 266	0.3860E-01	0.1766E-02	38425
kuster3.yz185.sar	165 266	0.3819E-01	0.1742E-02	38431
kuster3.yz186.sar	165 266	0.3768E-01	0.1716E-02	38417
kuster3.yz187.sar	165 266	0.3694E-01	0.1691E-02	38419
kuster3.yz188.sar	178 270	0.3578E-01	0.1667E-02	38419
kuster3.yz189.sar	161 10	0.3696E-01	0.1644E-02	38390
kuster3.yz190.sar	158 261	0.3811E-01	0.1622E-02	38392
kuster3.yz191.sar	167 266	0.4019E-01	0.1600E-02	38372
kuster3.yz192.sar	165 265	0.4239E-01	0.1575E-02	38348
kuster3.yz193.sar	158 10	0.4249E-01	0.1551E-02	38292
kuster3.yz194.sar	150 255	0.3482E-01	0.1528E-02	38224
kuster3.yz195.sar	157 260	0.3551E-01	0.1503E-02	38167
kuster3.yz196.sar	168 266	0.3573E-01	0.1477E-02	38115
kuster3.yz197.sar	153 257	0.3745E-01	0.1453E-02	38040
kuster3.yz198.sar	158 10	0.4454E-01	0.1433E-02	37970
kuster3.yz199.sar	157 10	0.4289E-01	0.1413E-02	37917
kuster3.yz200.sar	165 264	0.3783E-01	0.1401E-02	37690
kuster3.yz201.sar	168 265	0.3556E-01	0.1381E-02	37607
kuster3.yz202.sar	156 258	0.3662E-01	0.1367E-02	37544
kuster3.yz203.sar	157 10	0.4379E-01	0.1354E-02	37459
kuster3.yz204.sar	156 10	0.4007E-01	0.1340E-02	37297
kuster3.yz205.sar	165 263	0.3521E-01	0.1332E-02	37204
kuster3.yz206.sar	156 257	0.3480E-01	0.1325E-02	37086
kuster3.yz207.sar	156 10	0.4695E-01	0.1318E-02	36982

Name of Slice Data File	Peak SAR y and z coordinates	Peak SAR (W/kg)	Avg. SAR (W/kg)	Voxels in tissue
kuster3.yz208.sar	155 10	0.4025E-01	0.1313E-02	36867
kuster3.yz209.sar	157 11	0.3797E-01	0.1309E-02	36700
kuster3.yz210.sar	168 263	0.3181E-01	0.1309E-02	36563
kuster3.yz211.sar	166 262	0.3218E-01	0.1306E-02	36420
kuster3.yz212.sar	164 260	0.3186E-01	0.1304E-02	36273
kuster3.yz213.sar	163 259	0.2848E-01	0.1302E-02	36115
kuster3.yz214.sar	176 265	0.2991E-01	0.1301E-02	35921
kuster3.yz215.sar	174 264	0.3320E-01	0.1307E-02	35566
kuster3.yz216.sar	168 261	0.3356E-01	0.1309E-02	35349
kuster3.yz217.sar	171 262	0.3333E-01	0.1317E-02	35144
kuster3.yz218.sar	159 12	0.3146E-01	0.1320E-02	34936
kuster3.yz219.sar	157 10	0.3194E-01	0.1326E-02	34691
kuster3.yz220.sar	161 255	0.2958E-01	0.1328E-02	34472
kuster3.yz221.sar	168 259	0.3229E-01	0.1335E-02	34206
kuster3.yz222.sar	169 259	0.2881E-01	0.1338E-02	33917
kuster3.yz223.sar	163 14	0.3029E-01	0.1335E-02	33651
kuster3.yz224.sar	159 10	0.2866E-01	0.1334E-02	33359
kuster3.yz225.sar	170 258	0.2744E-01	0.1331E-02	33052
kuster3.yz226.sar	160 10	0.2904E-01	0.1323E-02	32736
kuster3.yz227.sar	161 10	0.3160E-01	0.1320E-02	32368
kuster3.yz228.sar	179 260	0.2608E-01	0.1309E-02	31983
kuster3.yz229.sar	163 10	0.2535E-01	0.1309E-02	31556
kuster3.yz230.sar	163 10	0.3202E-01	0.1310E-02	30650
kuster3.yz231.sar	169 253	0.3050E-01	0.1307E-02	30129
kuster3.yz232.sar	185 259	0.2797E-01	0.1307E-02	29605
kuster3.yz233.sar	181 257	0.2751E-01	0.1315E-02	29036
kuster3.yz234.sar	165 10	0.2945E-01	0.1324E-02	28414
kuster3.yz235.sar	165 10	0.2862E-01	0.1338E-02	27783
kuster3.yz236.sar	173 251	0.2615E-01	0.1357E-02	27011
kuster3.yz237.sar	181 254	0.2516E-01	0.1379E-02	26189
kuster3.yz238.sar	187 255	0.2271E-01	0.1404E-02	24998
kuster3.yz239.sar	179 251	0.2553E-01	0.1426E-02	24003
kuster3.yz240.sar	183 252	0.2340E-01	0.1449E-02	23067
kuster3.yz241.sar	171 10	0.2014E-01	0.1465E-02	22154
kuster3.yz242.sar	185 251	0.2071E-01	0.1477E-02	21293
kuster3.yz243.sar	173 10	0.2268E-01	0.1485E-02	20442
kuster3.yz244.sar	175 10	0.2028E-01	0.1511E-02	19598
kuster3.yz245.sar	191 249	0.1952E-01	0.1478E-02	18008
kuster3.yz246.sar	187 247	0.1797E-01	0.1473E-02	17216
kuster3.yz247.sar	180 10	0.2114E-01	0.1474E-02	16441
kuster3.yz248.sar	182 10	0.1689E-01	0.1478E-02	15660
kuster3.yz249.sar	184 10	0.1667E-01	0.1481E-02	14860
kuster3.yz250.sar	186 10	0.1625E-01	0.1483E-02	14056
kuster3.yz251.sar	188 10	0.1646E-01	0.1490E-02	13294
kuster3.yz252.sar	190 10	0.1542E-01	0.1499E-02	12518
kuster3.yz253.sar	193 10	0.1398E-01	0.1513E-02	11764
kuster3.yz254.sar	195 10	0.1438E-01	0.1537E-02	10998
kuster3.yz255.sar	197 10	0.1500E-01	0.1569E-02	10214
kuster3.yz256.sar	200 10	0.1407E-01	0.1610E-02	9464
kuster3.yz257.sar	203 10	0.1271E-01	0.1666E-02	8714
kuster3.yz258.sar	207 10	0.9944E-02	0.1735E-02	7970
kuster3.yz259.sar	232 12	0.5783E-02	0.1782E-02	7232

Location and values for peak and average SAR for total volume of exposed tissue
kuster3.yz63.sar 225 115 0.3485E+01 0.6650E-02 5611108

Table 6.4. Slice and Whole Head Model Peak and average (averaged over slice) 1 Gram Average SAR for Kuster Head and Shoulders Model Exposed to AT&T RU Antenna with Nose in Contact with Radome and centered over lower right patch (slice file number is distance in mm from FDTD space rectangular coordinates origin in x direction).

Name of Slice Data File	Peak SAR y and z coordinates		Peak SAR (W/kg)	Avg. SAR (W/kg)	Voxels in tissue
kuster3.yz49.lgsa	228	129	0.1063E+01	0.9486E+00	36
kuster3.yz50.lgsa	228	131	0.1195E+01	0.9794E+00	70
kuster3.yz51.lgsa	228	134	0.1354E+01	0.1020E+01	110
kuster3.yz52.lgsa	228	134	0.1354E+01	0.1042E+01	134
kuster3.yz53.lgsa	229	135	0.1409E+01	0.1062E+01	164
kuster3.yz54.lgsa	227	134	0.1412E+01	0.1077E+01	200
kuster3.yz55.lgsa	229	135	0.1412E+01	0.1090E+01	238
kuster3.yz56.lgsa	229	135	0.1405E+01	0.1085E+01	278
kuster3.yz57.lgsa	228	135	0.1384E+01	0.1076E+01	312
kuster3.yz58.lgsa	226	118	0.1380E+01	0.1035E+01	356
kuster3.yz59.lgsa	227	118	0.1470E+01	0.9968E+00	390
kuster3.yz60.lgsa	226	117	0.1532E+01	0.8931E+00	472
kuster3.yz61.lgsa	225	118	0.1506E+01	0.7907E+00	562
kuster3.yz62.lgsa	226	118	0.1428E+01	0.6904E+00	678
kuster3.yz63.lgsa	227	120	0.1333E+01	0.5643E+00	886
kuster3.yz64.lgsa	227	120	0.1246E+01	0.4461E+00	1368
kuster3.yz65.lgsa	227	121	0.1160E+01	0.3557E+00	1830
kuster3.yz66.lgsa	227	121	0.1066E+01	0.2741E+00	2492
kuster3.yz67.lgsa	227	123	0.9773E+00	0.2171E+00	3214
kuster3.yz68.lgsa	227	126	0.9015E+00	0.1759E+00	4038
kuster3.yz69.lgsa	227	126	0.8311E+00	0.1432E+00	4992
kuster3.yz70.lgsa	227	127	0.7634E+00	0.1203E+00	5910
kuster3.yz71.lgsa	227	127	0.6970E+00	0.1024E+00	6874
kuster3.yz72.lgsa	227	128	0.6343E+00	0.8683E-01	7822
kuster3.yz73.lgsa	227	128	0.5631E+00	0.7478E-01	8706
kuster3.yz74.lgsa	227	128	0.5168E+00	0.6529E-01	9592
kuster3.yz75.lgsa	227	128	0.4560E+00	0.5665E-01	10542
kuster3.yz76.lgsa	228	129	0.4141E+00	0.4976E-01	11814
kuster3.yz77.lgsa	227	128	0.3631E+00	0.4442E-01	13084
kuster3.yz78.lgsa	228	129	0.3282E+00	0.4018E-01	14116
kuster3.yz79.lgsa	228	129	0.2910E+00	0.3639E-01	15686
kuster3.yz80.lgsa	228	129	0.2575E+00	0.3343E-01	16408
kuster3.yz81.lgsa	228	130	0.2275E+00	0.3103E-01	17276
kuster3.yz82.lgsa	227	129	0.1980E+00	0.2870E-01	18136
kuster3.yz83.lgsa	227	129	0.1745E+00	0.2663E-01	18814
kuster3.yz84.lgsa	227	129	0.1536E+00	0.2465E-01	19366
kuster3.yz85.lgsa	227	129	0.1349E+00	0.2292E-01	19950
kuster3.yz86.lgsa	227	129	0.1183E+00	0.2132E-01	20386
kuster3.yz87.lgsa	227	129	0.1036E+00	0.1986E-01	20738
kuster3.yz88.lgsa	227	129	0.9063E-01	0.1852E-01	21072
kuster3.yz89.lgsa	228	130	0.8033E-01	0.1728E-01	21398
kuster3.yz90.lgsa	228	130	0.7007E-01	0.1619E-01	21720
kuster3.yz91.lgsa	228	130	0.6108E-01	0.1514E-01	21992
kuster3.yz92.lgsa	228	130	0.5323E-01	0.1422E-01	22286
kuster3.yz93.lgsa	186	242	0.5195E-01	0.1333E-01	22578
kuster3.yz94.lgsa	185	243	0.5205E-01	0.1264E-01	23200
kuster3.yz95.lgsa	185	244	0.5213E-01	0.1193E-01	23456
kuster3.yz96.lgsa	185	244	0.5229E-01	0.1125E-01	23744
kuster3.yz97.lgsa	184	245	0.5219E-01	0.1069E-01	24068
kuster3.yz98.lgsa	186	246	0.5209E-01	0.1015E-01	24349

Name of Slice Data File	Peak SAR y and z coordinates		Peak SAR (W/kg)	Avg. SAR (W/kg)	Voxels in tissue
kuster3.yz99.lgsa	181	245	0.5189E-01	0.9649E-02	24639
kuster3.yz100.lgs	181	246	0.5231E-01	0.9220E-02	24908
kuster3.yz101.lgs	183	247	0.5251E-01	0.8852E-02	25195
kuster3.yz102.lgs	169	239	0.5284E-01	0.8473E-02	25456
kuster3.yz103.lgs	173	243	0.5375E-01	0.8174E-02	25717
kuster3.yz104.lgs	172	243	0.5453E-01	0.7887E-02	25980
kuster3.yz105.lgs	171	243	0.5491E-01	0.7622E-02	26190
kuster3.yz106.lgs	171	244	0.5525E-01	0.7408E-02	26419
kuster3.yz107.lgs	170	244	0.5546E-01	0.7195E-02	26659
kuster3.yz108.lgs	170	245	0.5565E-01	0.7019E-02	26869
kuster3.yz109.lgs	169	245	0.5575E-01	0.6989E-02	27330
kuster3.yz110.lgs	170	247	0.5579E-01	0.6840E-02	27527
kuster3.yz111.lgs	169	247	0.5583E-01	0.6688E-02	27777
kuster3.yz112.lgs	169	248	0.5612E-01	0.6525E-02	27954
kuster3.yz113.lgs	170	249	0.5630E-01	0.6394E-02	28163
kuster3.yz114.lgs	170	250	0.5636E-01	0.6244E-02	28330
kuster3.yz115.lgs	169	250	0.5641E-01	0.6119E-02	28536
kuster3.yz116.lgs	170	251	0.5637E-01	0.5980E-02	28709
kuster3.yz117.lgs	170	252	0.5665E-01	0.5850E-02	28885
kuster3.yz118.lgs	169	252	0.5693E-01	0.5724E-02	29045
kuster3.yz119.lgs	170	253	0.5682E-01	0.5620E-02	29233
kuster3.yz120.lgs	168	253	0.5693E-01	0.5497E-02	29399
kuster3.yz121.lgs	169	254	0.5651E-01	0.5394E-02	29590
kuster3.yz122.lgs	168	254	0.5603E-01	0.5269E-02	29730
kuster3.yz123.lgs	169	255	0.5541E-01	0.5180E-02	29935
kuster3.yz124.lgs	169	256	0.5513E-01	0.5176E-02	30287
kuster3.yz125.lgs	168	256	0.5459E-01	0.5061E-02	30477
kuster3.yz126.lgs	170	257	0.5407E-01	0.4981E-02	30667
kuster3.yz127.lgs	169	257	0.5376E-01	0.4876E-02	30886
kuster3.yz128.lgs	171	259	0.5348E-01	0.4796E-02	31143
kuster3.yz129.lgs	170	259	0.5302E-01	0.4697E-02	31407
kuster3.yz130.lgs	168	258	0.5260E-01	0.4624E-02	31705
kuster3.yz131.lgs	171	260	0.5204E-01	0.4563E-02	32035
kuster3.yz132.lgs	170	260	0.5221E-01	0.4459E-02	32359
kuster3.yz133.lgs	169	260	0.5210E-01	0.4408E-02	32710
kuster3.yz134.lgs	168	260	0.5170E-01	0.4344E-02	33005
kuster3.yz135.lgs	169	261	0.5113E-01	0.4270E-02	33294
kuster3.yz136.lgs	169	261	0.5045E-01	0.4196E-02	33515
kuster3.yz137.lgs	168	261	0.5005E-01	0.4127E-02	33744
kuster3.yz138.lgs	169	262	0.4962E-01	0.4083E-02	33984
kuster3.yz139.lgs	168	262	0.4923E-01	0.4095E-02	34355
kuster3.yz140.lgs	169	263	0.4880E-01	0.4016E-02	34555
kuster3.yz141.lgs	169	263	0.4776E-01	0.3947E-02	34738
kuster3.yz142.lgs	166	262	0.4743E-01	0.3893E-02	34917
kuster3.yz143.lgs	168	263	0.4654E-01	0.3827E-02	35081
kuster3.yz144.lgs	167	263	0.4621E-01	0.3742E-02	35240
kuster3.yz145.lgs	166	263	0.4593E-01	0.3683E-02	35417
kuster3.yz146.lgs	168	264	0.4533E-01	0.3609E-02	35572
kuster3.yz147.lgs	167	264	0.4512E-01	0.3546E-02	35708
kuster3.yz148.lgs	167	264	0.4463E-01	0.3475E-02	35844
kuster3.yz149.lgs	166	264	0.4419E-01	0.3414E-02	35988
kuster3.yz150.lgs	168	265	0.4342E-01	0.3352E-02	36145
kuster3.yz151.lgs	167	265	0.4317E-01	0.3280E-02	36283
kuster3.yz152.lgs	157	258	0.4261E-01	0.3208E-02	36402
kuster3.yz153.lgs	155	257	0.4214E-01	0.3139E-02	36523
kuster3.yz154.lgs	156	258	0.4202E-01	0.3107E-02	36732
kuster3.yz155.lgs	154	257	0.4137E-01	0.3033E-02	36847

Name of Slice Data File	Peak SAR y and z coordinates	Peak SAR (W/kg)	Avg. SAR (W/kg)	Voxels in tissue
kuster3.yz156.lgs	167 266	0.4107E-01	0.2976E-02	36967
kuster3.yz157.lgs	167 266	0.4056E-01	0.2917E-02	37066
kuster3.yz158.lgs	167 266	0.3996E-01	0.2852E-02	37173
kuster3.yz159.lgs	167 266	0.3951E-01	0.2790E-02	37273
kuster3.yz160.lgs	166 266	0.3948E-01	0.2725E-02	37352
kuster3.yz161.lgs	158 261	0.3924E-01	0.2666E-02	37435
kuster3.yz162.lgs	158 261	0.3883E-01	0.2609E-02	37529
kuster3.yz163.lgs	159 262	0.3844E-01	0.2546E-02	37595
kuster3.yz164.lgs	159 262	0.3794E-01	0.2499E-02	37698
kuster3.yz165.lgs	159 262	0.3742E-01	0.2447E-02	37773
kuster3.yz166.lgs	157 261	0.3680E-01	0.2401E-02	37856
kuster3.yz167.lgs	158 262	0.3646E-01	0.2353E-02	37925
kuster3.yz168.lgs	155 260	0.3627E-01	0.2306E-02	37981
kuster3.yz169.lgs	155 260	0.3579E-01	0.2263E-02	38076
kuster3.yz170.lgs	166 267	0.3564E-01	0.2213E-02	38108
kuster3.yz171.lgs	166 267	0.3525E-01	0.2168E-02	38151
kuster3.yz172.lgs	155 260	0.3449E-01	0.2122E-02	38165
kuster3.yz173.lgs	166 267	0.3437E-01	0.2087E-02	38190
kuster3.yz174.lgs	166 267	0.3392E-01	0.2046E-02	38232
kuster3.yz175.lgs	171 269	0.3376E-01	0.1997E-02	38244
kuster3.yz176.lgs	171 269	0.3338E-01	0.1955E-02	38275
kuster3.yz177.lgs	171 269	0.3284E-01	0.1923E-02	38309
kuster3.yz178.lgs	159 263	0.3240E-01	0.1886E-02	38322
kuster3.yz179.lgs	171 269	0.3200E-01	0.1857E-02	38354
kuster3.yz180.lgs	171 269	0.3158E-01	0.1827E-02	38382
kuster3.yz181.lgs	168 268	0.3195E-01	0.1799E-02	38385
kuster3.yz182.lgs	170 269	0.3136E-01	0.1768E-02	38394
kuster3.yz183.lgs	166 267	0.3085E-01	0.1741E-02	38422
kuster3.yz184.lgs	166 267	0.3048E-01	0.1716E-02	38425
kuster3.yz185.lgs	166 267	0.3027E-01	0.1694E-02	38431
kuster3.yz186.lgs	168 268	0.2980E-01	0.1668E-02	38417
kuster3.yz187.lgs	168 268	0.2943E-01	0.1649E-02	38419
kuster3.yz188.lgs	168 268	0.2916E-01	0.1626E-02	38419
kuster3.yz189.lgs	168 268	0.2880E-01	0.1603E-02	38390
kuster3.yz190.lgs	168 268	0.2834E-01	0.1584E-02	38392
kuster3.yz191.lgs	165 266	0.2778E-01	0.1560E-02	38372
kuster3.yz192.lgs	161 264	0.2748E-01	0.1541E-02	38348
kuster3.yz193.lgs	164 265	0.2665E-01	0.1518E-02	38292
kuster3.yz194.lgs	162 264	0.2636E-01	0.1496E-02	38224
kuster3.yz195.lgs	162 264	0.2613E-01	0.1482E-02	38167
kuster3.yz196.lgs	162 264	0.2584E-01	0.1458E-02	38115
kuster3.yz197.lgs	164 265	0.2566E-01	0.1435E-02	38040
kuster3.yz198.lgs	168 267	0.2497E-01	0.1415E-02	37970
kuster3.yz199.lgs	158 11	0.2521E-01	0.1401E-02	37917
kuster3.yz200.lgs	158 11	0.2553E-01	0.1374E-02	37690
kuster3.yz201.lgs	158 11	0.2604E-01	0.1360E-02	37607
kuster3.yz202.lgs	158 11	0.2661E-01	0.1352E-02	37544
kuster3.yz203.lgs	159 12	0.2712E-01	0.1338E-02	37459
kuster3.yz204.lgs	157 11	0.2804E-01	0.1332E-02	37297
kuster3.yz205.lgs	157 11	0.2790E-01	0.1325E-02	37204
kuster3.yz206.lgs	157 11	0.2744E-01	0.1315E-02	37086
kuster3.yz207.lgs	157 11	0.2723E-01	0.1314E-02	36982
kuster3.yz208.lgs	156 11	0.2738E-01	0.1308E-02	36867
kuster3.yz209.lgs	156 11	0.2696E-01	0.1304E-02	36700
kuster3.yz210.lgs	156 11	0.2626E-01	0.1304E-02	36563
kuster3.yz211.lgs	156 11	0.2564E-01	0.1310E-02	36420
kuster3.yz212.lgs	156 11	0.2544E-01	0.1313E-02	36273

Name of Slice Data File	Peak SAR y and z coordinates		Peak SAR (W/kg)	Avg. SAR (W/kg)	Voxels in tissue
kuster3.yz213.lgs	156	11	0.2516E-01	0.1315E-02	36115
kuster3.yz214.lgs	156	11	0.2485E-01	0.1320E-02	35921
kuster3.yz215.lgs	156	11	0.2454E-01	0.1311E-02	35566
kuster3.yz216.lgs	157	11	0.2339E-01	0.1314E-02	35349
kuster3.yz217.lgs	157	11	0.2287E-01	0.1320E-02	35144
kuster3.yz218.lgs	157	11	0.2283E-01	0.1325E-02	34936
kuster3.yz219.lgs	157	11	0.2239E-01	0.1328E-02	34691
kuster3.yz220.lgs	158	11	0.2171E-01	0.1335E-02	34472
kuster3.yz221.lgs	158	11	0.2178E-01	0.1339E-02	34206
kuster3.yz222.lgs	159	11	0.2120E-01	0.1340E-02	33917
kuster3.yz223.lgs	159	11	0.2119E-01	0.1338E-02	33651
kuster3.yz224.lgs	160	11	0.2063E-01	0.1334E-02	33359
kuster3.yz225.lgs	160	11	0.2056E-01	0.1336E-02	33052
kuster3.yz226.lgs	161	11	0.1973E-01	0.1336E-02	32736
kuster3.yz227.lgs	161	11	0.1973E-01	0.1333E-02	32368
kuster3.yz228.lgs	162	11	0.1926E-01	0.1333E-02	31983
kuster3.yz229.lgs	163	11	0.1829E-01	0.1331E-02	31556
kuster3.yz230.lgs	164	11	0.1752E-01	0.1312E-02	30650
kuster3.yz231.lgs	164	11	0.1750E-01	0.1316E-02	30129
kuster3.yz232.lgs	165	11	0.1663E-01	0.1322E-02	29605
kuster3.yz233.lgs	166	11	0.1587E-01	0.1328E-02	29036
kuster3.yz234.lgs	166	11	0.1587E-01	0.1337E-02	28414
kuster3.yz235.lgs	166	11	0.1566E-01	0.1351E-02	27783
kuster3.yz236.lgs	167	11	0.1494E-01	0.1365E-02	27011
kuster3.yz237.lgs	168	11	0.1429E-01	0.1382E-02	26189
kuster3.yz238.lgs	169	11	0.1350E-01	0.1404E-02	24998
kuster3.yz239.lgs	170	11	0.1281E-01	0.1428E-02	24003
kuster3.yz240.lgs	182	253	0.1207E-01	0.1451E-02	23067
kuster3.yz241.lgs	181	252	0.1174E-01	0.1472E-02	22154
kuster3.yz242.lgs	181	251	0.1121E-01	0.1478E-02	21293
kuster3.yz243.lgs	186	252	0.1082E-01	0.1480E-02	20442
kuster3.yz244.lgs	183	250	0.1049E-01	0.1484E-02	19598
kuster3.yz245.lgs	188	250	0.9804E-02	0.1464E-02	18008
kuster3.yz246.lgs	184	247	0.9236E-02	0.1468E-02	17216
kuster3.yz247.lgs	188	248	0.9032E-02	0.1471E-02	16441
kuster3.yz248.lgs	189	247	0.8509E-02	0.1476E-02	15660
kuster3.yz249.lgs	192	247	0.8033E-02	0.1481E-02	14860
kuster3.yz250.lgs	192	246	0.7841E-02	0.1484E-02	14056
kuster3.yz251.lgs	191	244	0.7207E-02	0.1493E-02	13294
kuster3.yz252.lgs	192	243	0.6682E-02	0.1508E-02	12518
kuster3.yz253.lgs	195	243	0.6258E-02	0.1522E-02	11764
kuster3.yz254.lgs	197	242	0.5690E-02	0.1537E-02	10998
kuster3.yz255.lgs	198	11	0.5717E-02	0.1547E-02	10214
kuster3.yz256.lgs	201	11	0.5614E-02	0.1515E-02	9464
kuster3.yz257.lgs	204	11	0.5638E-02	0.1474E-02	8714
kuster3.yz258.lgs	208	11	0.5417E-02	0.1484E-02	7970
kuster3.yz259.lgs	211	11	0.5246E-02	0.1476E-02	7232

Location and values for peak and average 1 gram average SAR for total volume of exposed tissue

kuster3.yz60.lgsa	226	117	0.1532E+01	0.6501E-02	5611108
--------------------------	------------	------------	-------------------	-------------------	----------------

Figure 3.6 illustrates the orientation of the Kuster head model with respect to the antenna in the sagittal or xz plane at $y = 228$ mm from the origin of the rectangular coordinate system at the lower-front-left corner of the fdtd mesh. The horizontal black lines, A through I denotes the horizontal xy planes where the SAR data was plotted and printed. However, SAR data were calculated for all of the 210, 1-mm thick horizontal xy slices as well as for the vertical slices denoted by J through U in the sagittal xz plane of the simulated head tissue illustrated in Figure 3.6.

Figure 6.8 illustrates the FDTD derived SAR distribution in xz planes through the head corresponding to the vertical slices V (through the center of the left row of antenna patches), W (through the center of the array of patches) and X (through the right row of patches) defined in Figure 3.7. The SAR distributions as averaged over each 1 mm cubical cell or voxel, calculated by the FDTD program are depicted as a color graphs with each color representing a 9 dB range of SAR values. The maximum SAR corresponding to the 0-dB reference is shown below each graph. Note that the SAR in the head drops to levels lower than -36 decibels with respect to the maximum of 3.18 W/kg at or near the facial surface of the model denoted by the black plus sign in scan W.

Figures 6.9, 6.10 and 6.11 respectively illustrate the SAR distribution in the horizontal xy planes at slices labeled as A through C, D through F, and G through I as denoted in Figure 3.6. In these figures each color representing the SAR distribution as averaged over each 1-mm cubical cell corresponds to a 6-dB range of SAR values. The maximum SAR corresponding to 0 dB is listed below each graph in the figure. The maximum SAR for all of these illustrated slices is 2.93 W/kg occurring at the location of the black plus sign in the scan through the slice denoted as E in Figure 6.10.

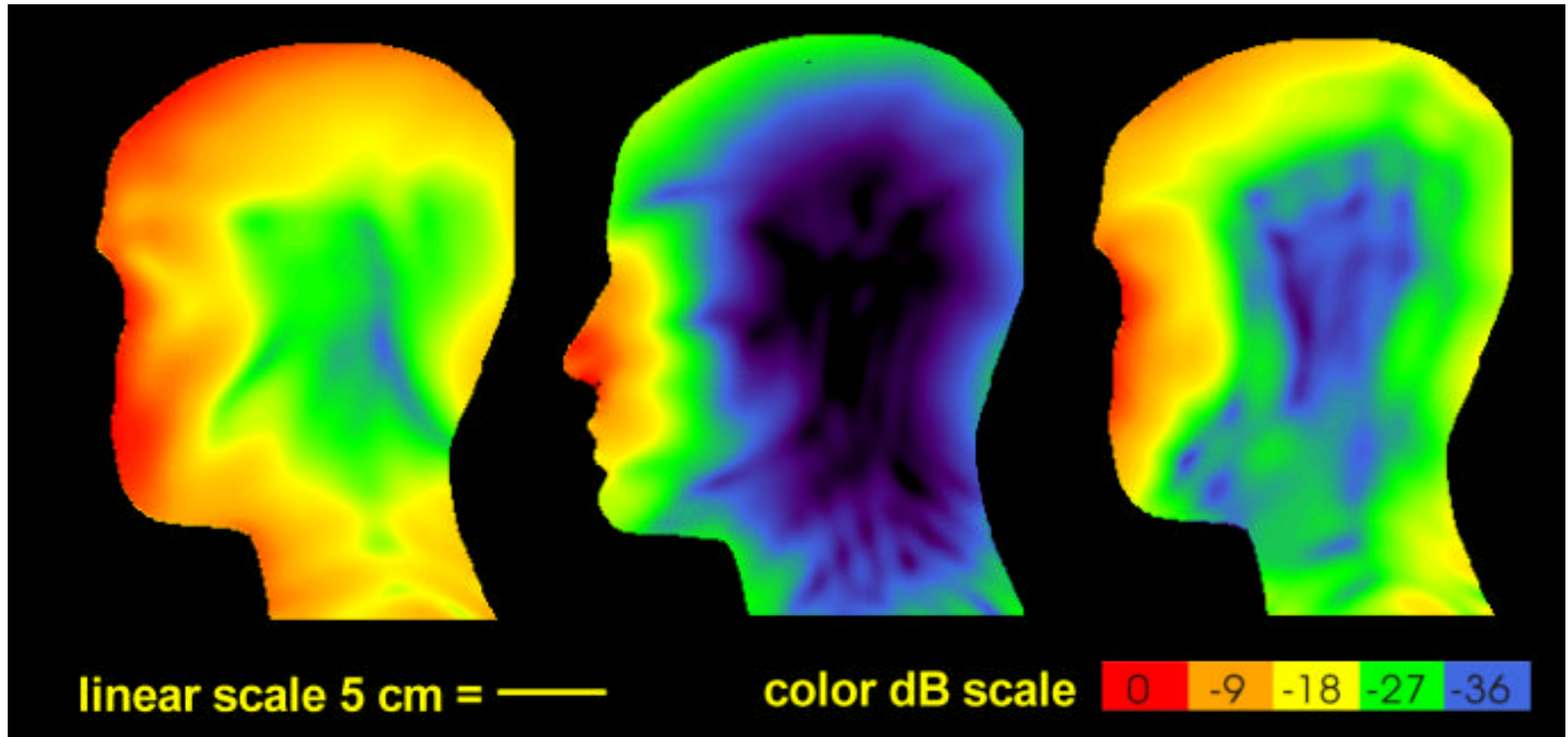
Figures 6.12, 6.13 and 6.14 illustrate the respective color plots of the SAR distribution in the vertical yz planes denoted by L through O, P through R, and S through U as identified in Figures 3.6 and 6.7. The legend for these plots is the same as used for the previous figures. The maximum value of the SAR for the entire head model is 3.49 W/kg occurring at the location of the black plus sign in scan through the slice denoted as K in Figure 6.12.

Figures 6.15, 6.16 and 6.17 illustrate the respective color plots of the 1-gram average SAR distribution in the yz planes denoted by K through O, P through R, and S through U as identified in Figures 3.6 and 3.7. The legend for these plots is set for the color red to represent all SARs at or greater than the value 1.6 W/kg allowed by the FCC MPL. The maximum value of the SAR for each plot is shown in the text below the plots. The maximum 1-gram average for the entire head model, 1.53 W/kg occurs at the location of the black plus sign in the slice denoted as K in Figure 6.15.

Figure 6.18 illustrates a comparison between the FDTD maximum derived values of peak and 1 gram average SAR in each yz plane slice of the Kuster head as a function of distance x from the ground plane and the SPEAG measured values at 76-mm and 81-mm, respectively given in the last two figures in SubAppendix H of Appendix A. The maximum measured SAR of 0.0545 W/kg (based on 80 mW input power to the antenna) in the yz plane at x=76-mm is very close to the calculated 1 gram average value of 0.0532 W/kg. However, the maximum measured SAR of 0.0307 W/kg in the yz plane at x=81-mm falls below the calculated 1-gram average value of 0.0522 W/kg. As explained in the discussion relating to Figures 6.6 and 6.7 in the Section 6.1 this probably results from the fact that the measurement probe cannot be placed at the tissue periphery where the highest SARs occur in the yz planes further from the source. The graph in Figure 6.18 clearly indicates a dual slope characteristic where the calculated SAR curve decays very rapidly with distance up to 76-mm from the ground plane followed by a much smaller rate of decay where the SAR at the surface exceeds that at the interior of the model. When the comparisons of the calculated and measured SARs are made along the same line through the model there is very good agreement in the results. This is illustrated by the comparison of FDTD calculations and the SPEAG measurement results obtained from Figure 3.10a of Appendix A. These results obtained along a line perpendicular to the antenna through the nose of the model as a function of distance from the ground plane are shown in Figure 6.19. For this case the rapid decay of the SAR with distance prevails to a distance of 155-mm from the source before the higher SAR at the back surface of the model begins to affect the SAR curve, causing it to increase with decreasing distance to the back surface of the model. For this case the agreement between the calculated values denoted by the blue curve and the measured values denoted by the red curve is so close that the curves lay virtually on the top of each other

6.3 Orientation with Side of Head in contact with Radome in various positions

SPEAG conducted measurements on another model called the Generic Twin Phantom exposed to the AT&T RU antenna with the side of the head in contact with the radome and oriented over center of the array and each patch. These results are discussed in Appendix A, pages 33 and 34 and Sub-Appendix I. The results, summarized in Table 3.2 of Appendix A show maximum 1 gram average SARs varying from 0.22 to 0.43 W/kg (-8.6 to -5.7 dB from the FCC MPL) with the maximum occurring exposures near the bottom right patch.

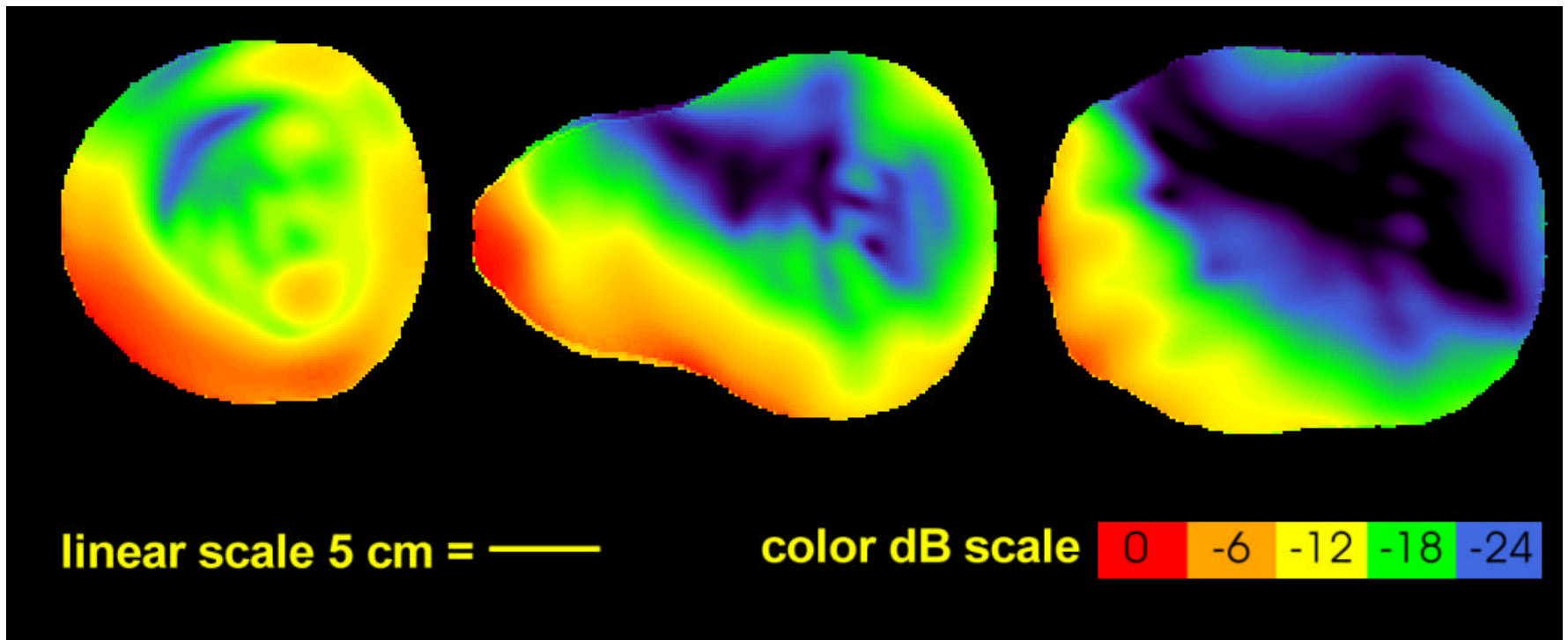


scan V, slice 190
0 dB = 0.0834 W/kg

scan W, slice 228
0 dB = 3.18 W/kg

scan X, slice 265
0 dB = 0.0967 W/kg

Figure 6.8. FDTD derived x-z plane SAR distributions (V-X) in Kuster model head exposed to AT&T RU Antenna with tip of nose in contact with radome and centered over lower right patch (black + denotes position nearest maximum SAR for entire model).

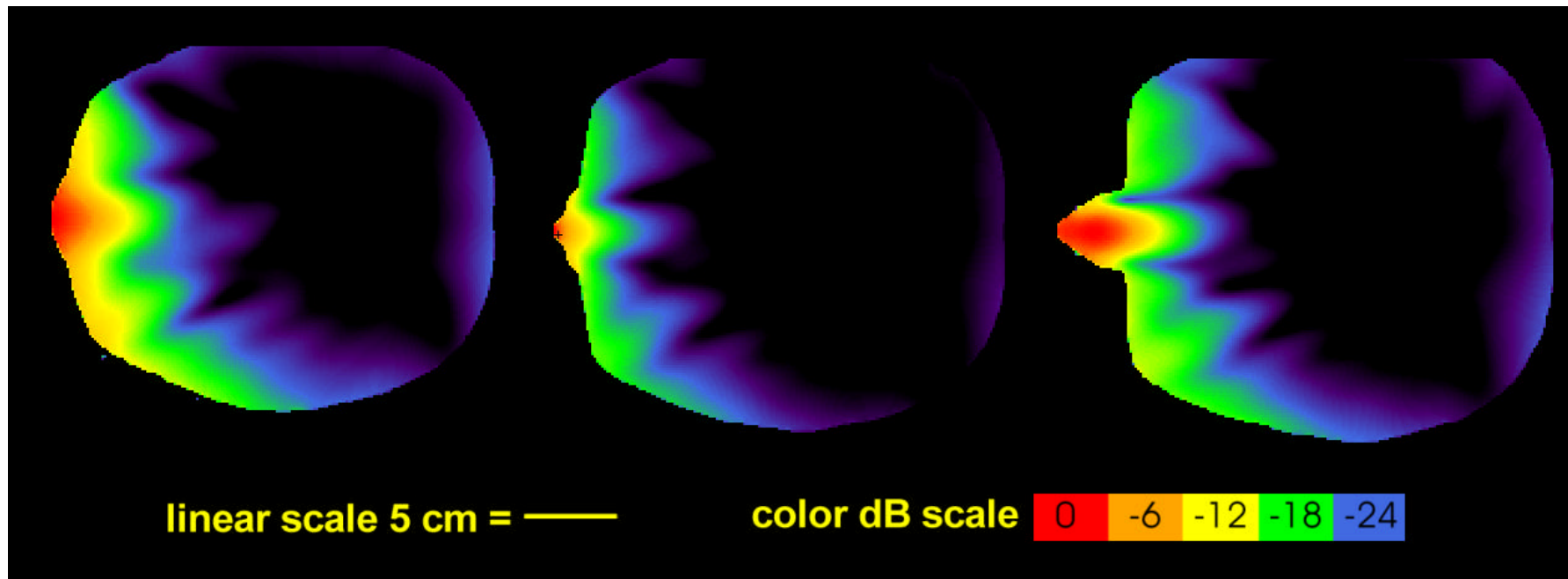


scan A, slice 25
0 dB = 0.0214 W/kg

scan B, slice 55
0 dB = 0.0333 W/kg

scan C, slice 75
0 dB = 0.0992 W/kg

Figure 6.9. FDTD derived x-y plane SAR distributions (A-C) in Kuster model head exposed to AT&T RU Antenna with tip of nose in contact with radome and centered over lower right patch.

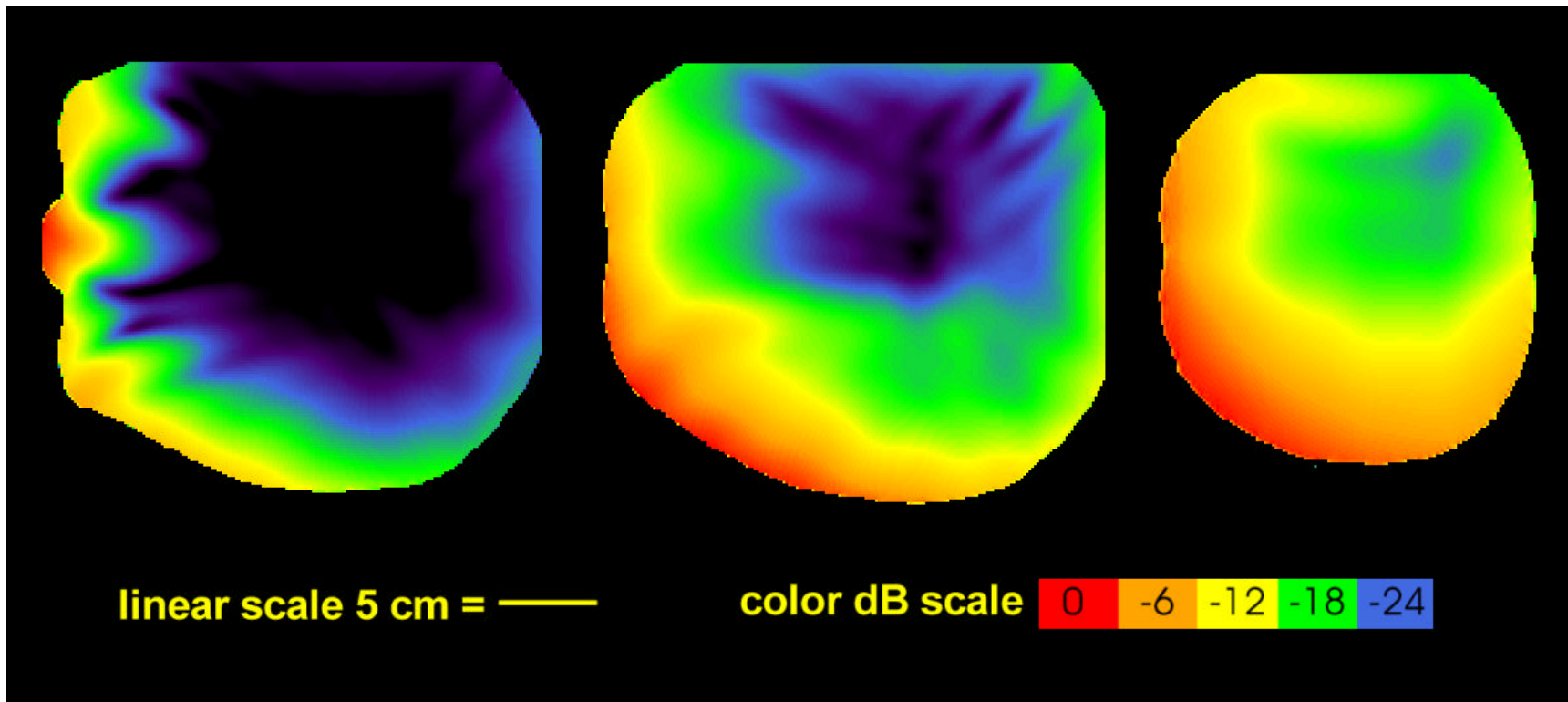


scan D, slice 105
0 dB = 0.623 W/kg

scan E, slice 115
0 dB = 2.93 W/kg

scan F, slice 126
0 dB = 1.37 W/kg

Figure 6.10. FDTD derived x-y plane SAR distributions (D-F) in Kuster model head exposed to AT&T RU Antenna with tip of nose in contact with radome and centered over lower right patch (black + denotes position nearest maximum SAR for entire model).

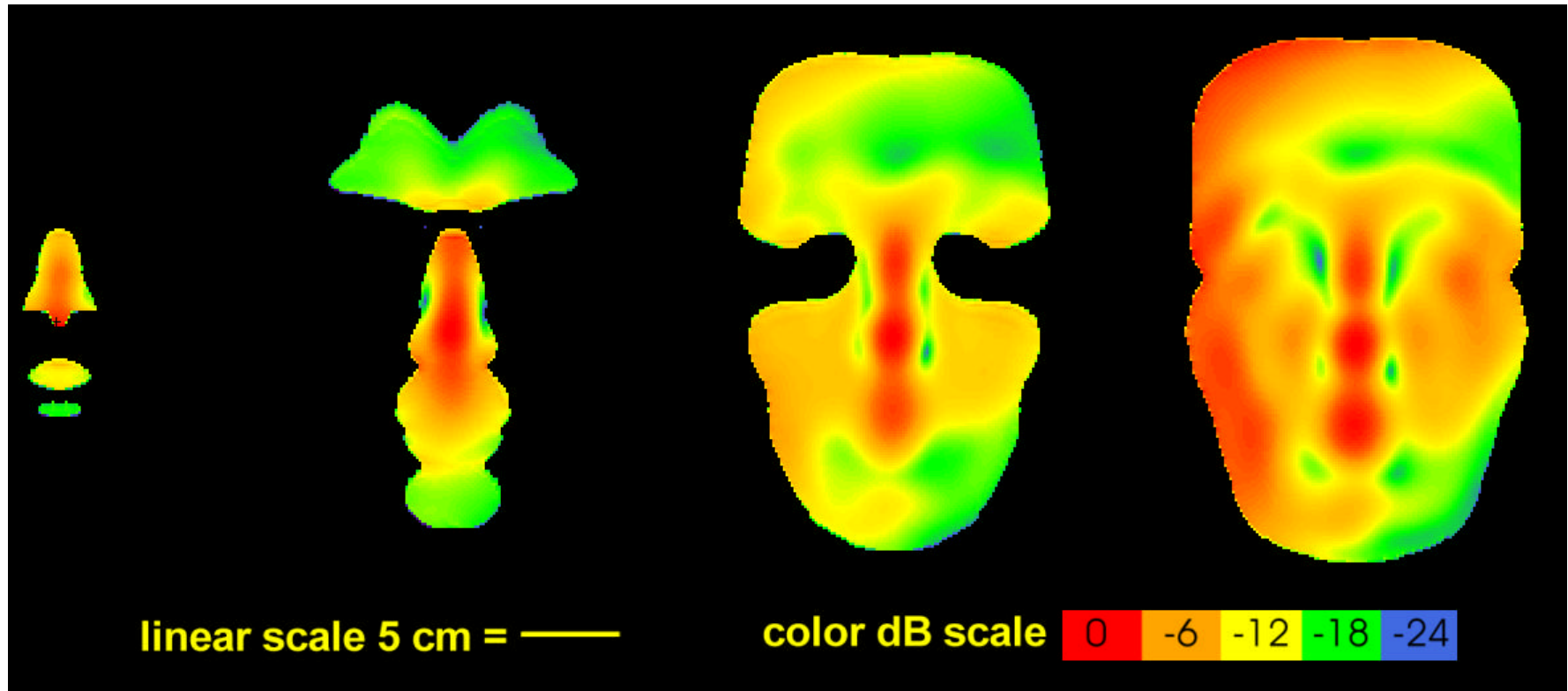


scan G, slice 170
0 dB = 0.286 W/kg

scan H, slice 210
0 dB = 0.0614 W/kg

scan I, slice 255
0 dB = 0.0784 W/kg

Figure 6.11. FDTD derived x-y plane SAR distributions (G-I) in Kuster model head exposed to AT&T RU Antenna with tip of nose in contact with radome and centered over lower right patch.



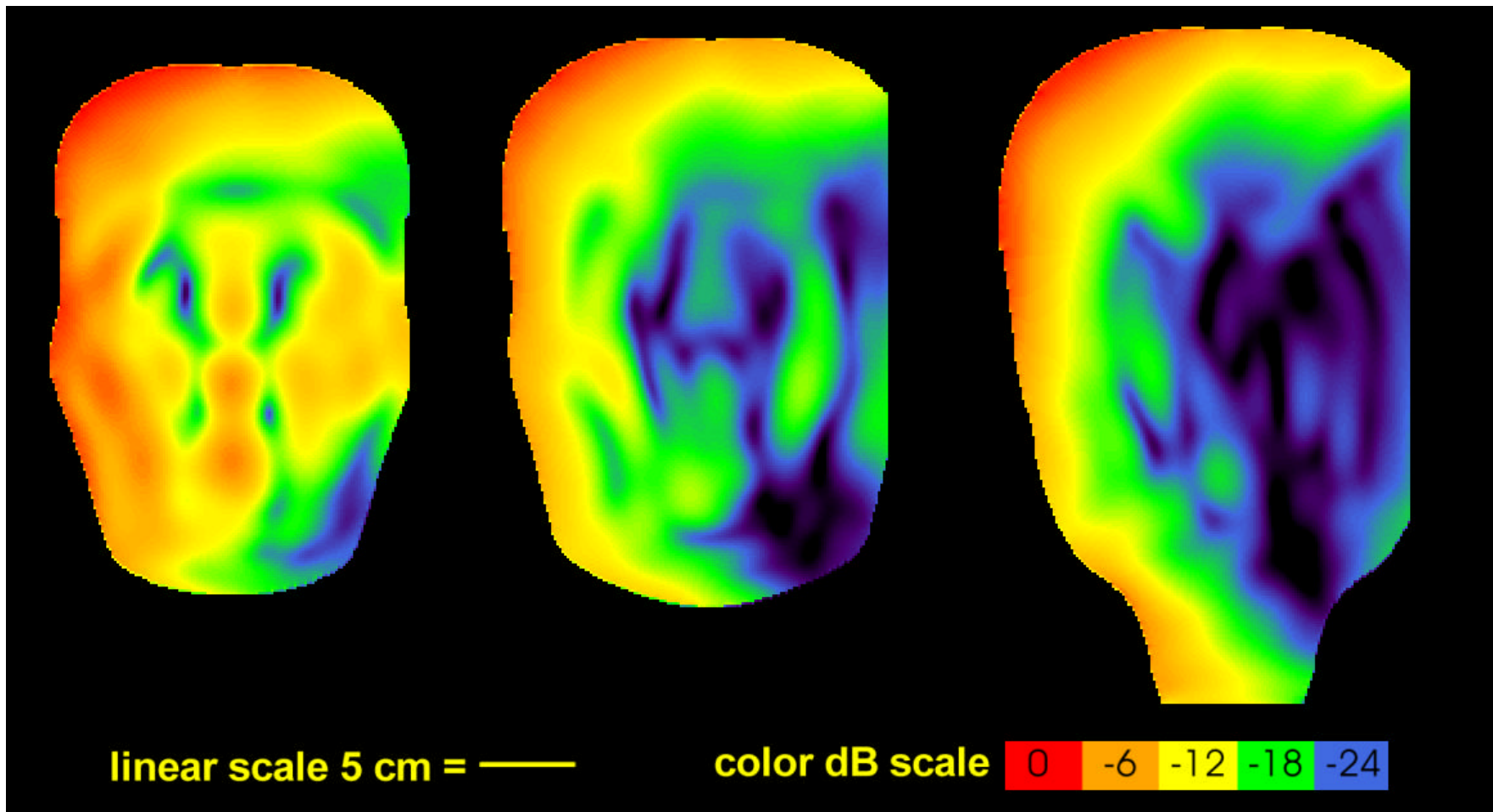
scan L,
 slice 63
 0 dB =
 3.49 W/kg

scan M, slice 70
 0 dB = 0.977 W/kg

scan N, slice 80
 0 dB = 0.320 W/kg

scan O, slice 90
 0 dB = 0.0829 W/kg

Figure 6.12. FDTD derived x-y plane SAR distributions (L-O) in Kuster model head exposed to AT&T RU Antenna with tip of nose in contact with radome and centered over lower right patch (black + denotes position of maximum SAR for entire model).

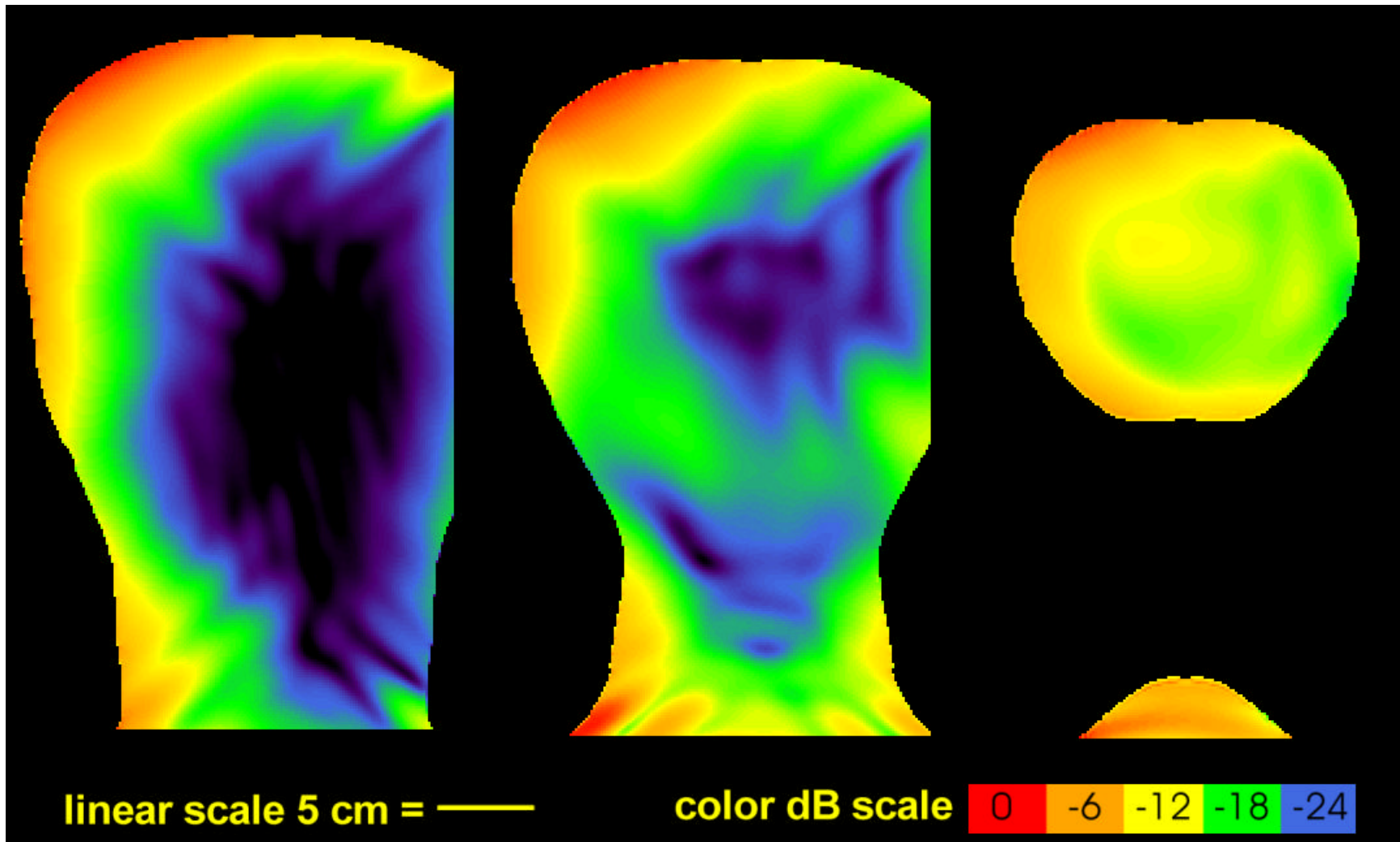


scan P, slice 100
0 dB = 0.0714 W/kg

scan Q, slice 120
0 dB = 0.0982 W/kg

scan R, slice 140
0 dB = 0.0723 W/kg

Figure 6.13. FDTD derived y-z plane SAR distributions (P-R) in Kuster model head exposed to AT&T RU Antenna with tip of nose in contact with radome and centered over lower right patch.

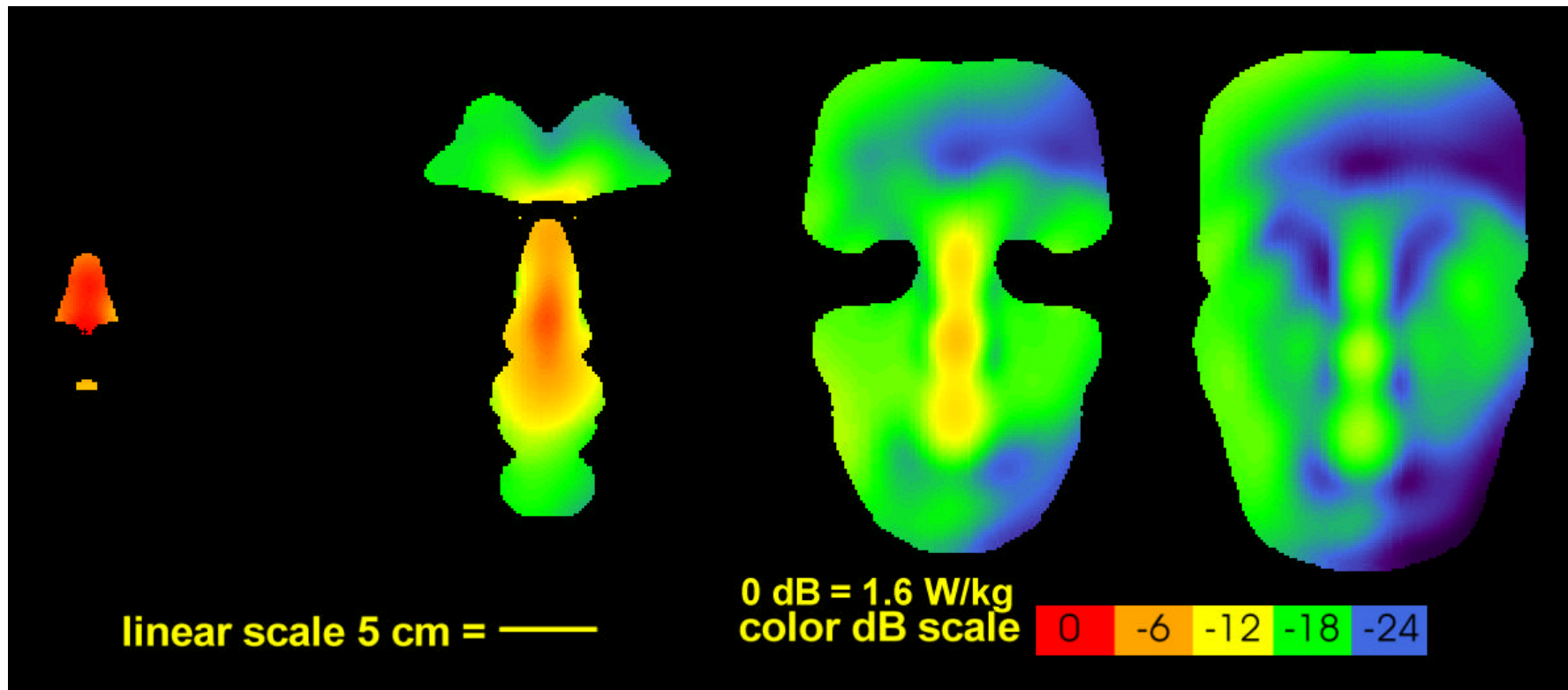


scan S, slice 180
0 dB = 0.0531 W/kg

scan T, slice 220
0 dB = 0.0296 W/kg

scan U, slice 250
0 dB = 0.0163 W/kg

Figure 6.14. FDTD derived y-z plane SAR distributions (S-R) in Kuster model head exposed to AT&T RU Antenna with tip of nose in contact with radome and centered over lower right patch.



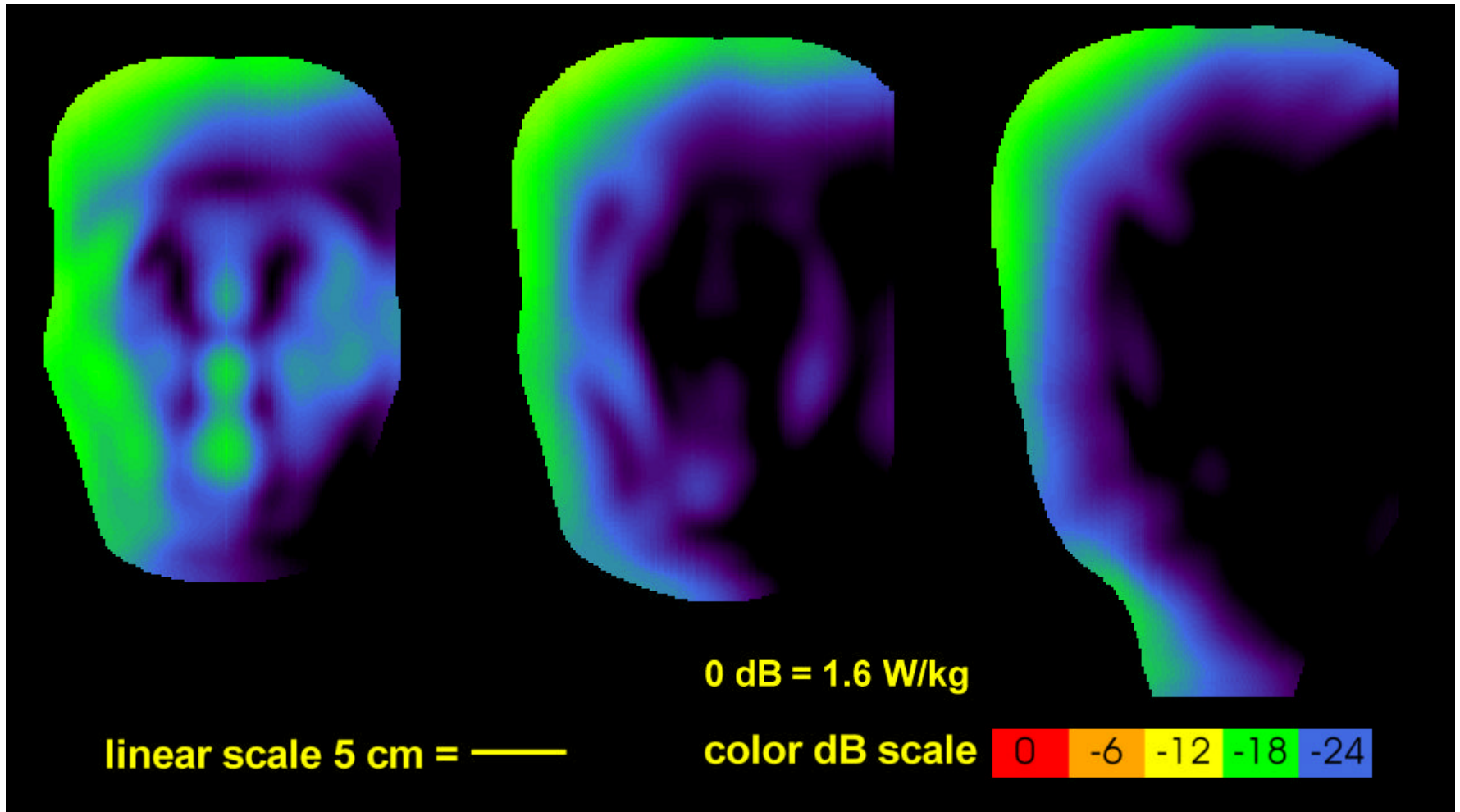
scan K,
 slice 63
 Max. =
 1.53 W/kg

scan M, slice 70
 Max. = 0.763 W/kg

scan N, slice 80
 Max. = 0.258 W/kg

scan O, slice 90
 Max. = 0.0701 W/kg

Figure 6.15. FDTD derived x-y plane 1 gram average SAR distributions (K-O) in Kuster model head exposed to AT&T RU Antenna with tip of nose in contact with radome and centered over lower right patch compared to FCC MPL (black + denotes position of maximum SAR for entire model).

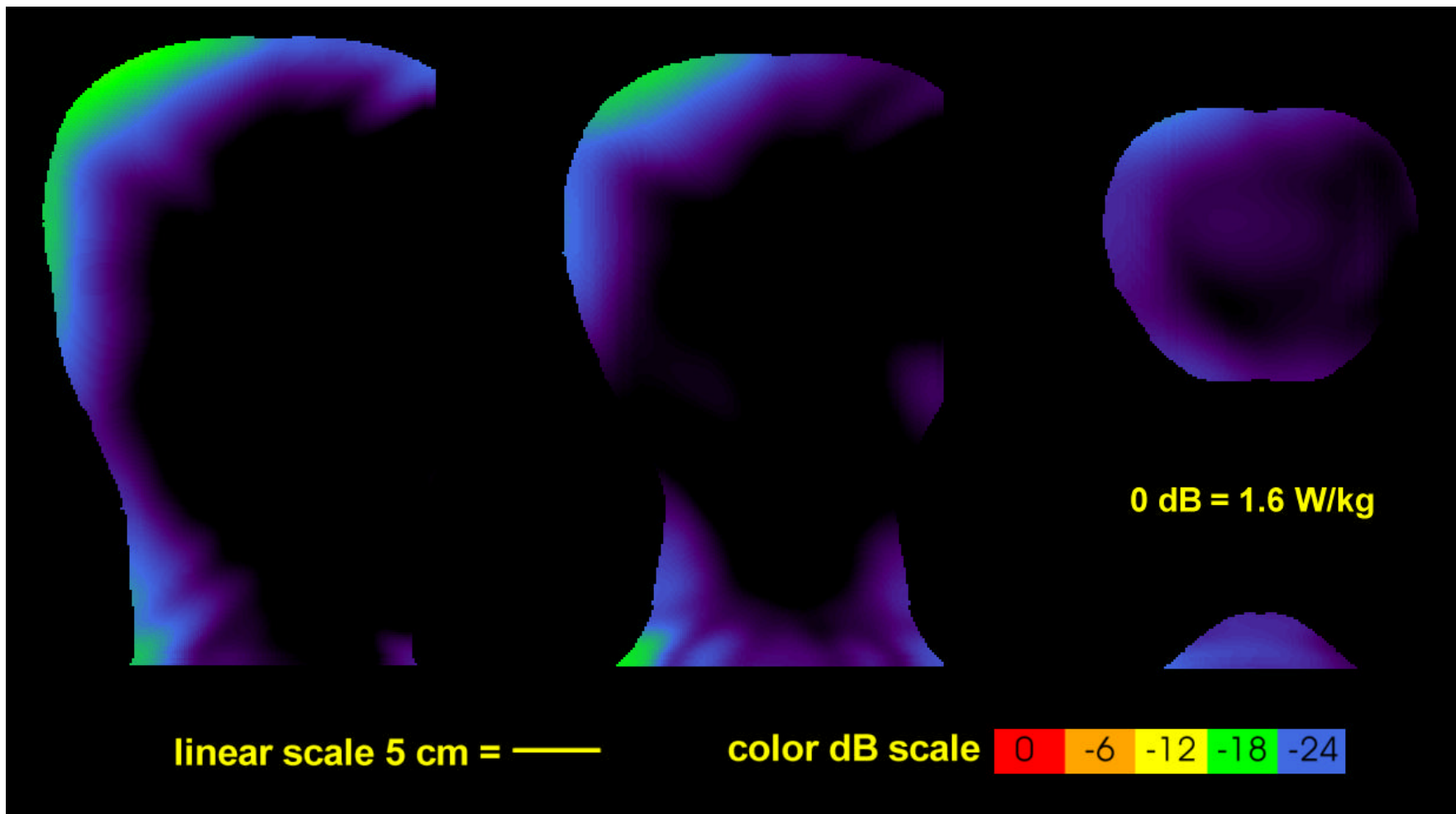


scan P, slice 100
Max. = 0.0519 W/kg

scan Q, slice 120
Max. = 0.0569 W/kg

scan R, slice 140
Max. = 0.0488 W/kg

Figure 6.16. FDTD derived y-z plane 1 gram average SAR distributions (P-R) in Kuster model head exposed to AT&T RU Antenna with tip of nose in contact with radome and centered over lower right patch.



scan S, slice 180
Max. = 0.0519 W/kg

scan T, slice 220
Max. = 0.0569 W/kg

scan U, slice 250
Max. = 0.0488 W/kg

Figure 6.17. FDTD derived y-z plane 1 gram average SAR distributions (S-U) in Kuster model head exposed to AT&T RU Antenna with tip of nose in contact with radome and centered over lower right patch compared to FCC MPL.

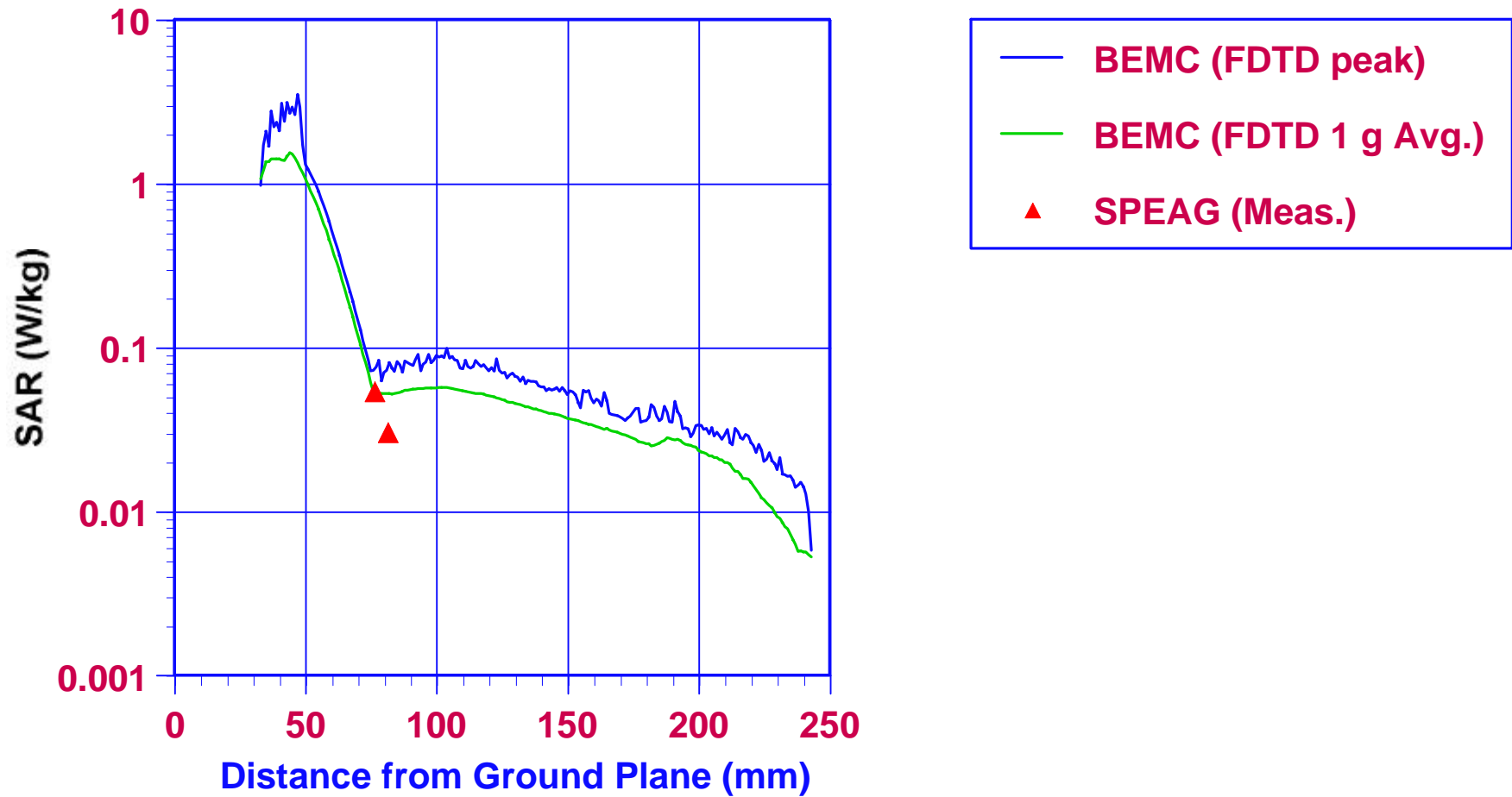


Figure 6.18. Comparison of FDTD maximum derived values of peak and 1 gram average SAR by BEMC in each yz plane slice of the Kuster head model as a function of distance x from ground plane with face of Kuster phantom head model exposed to AT&T RU antenna with tip of nose in contact with radome (31 cm from ground plane) and centered over lower right patch (red symbols indicate SPEAG measured values taken 76-mm and 81-mm from the ground plane, respectively).

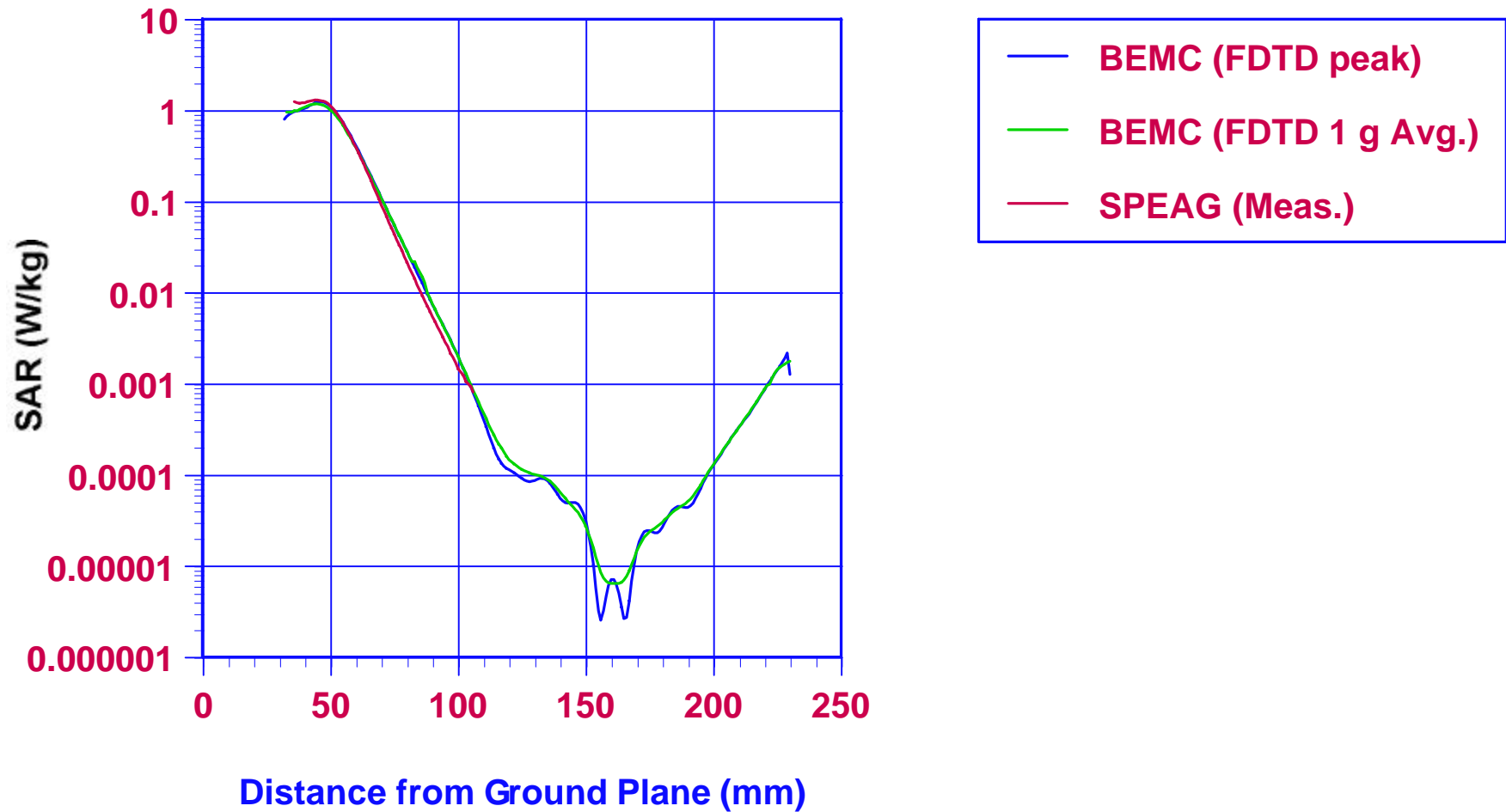


Figure 6.19. Comparison of FDTD derived values of SAR by BEMC and measured values by SPEAG with face of Kuster phantom head model exposed to AT&T RU antenna with tip of nose in contact with radome (31 cm from ground plane) and centered over lower right patch (values plotted along line through tip of nose and perpendicular to ground plane).

7 FDTD Calculation of SAR in REMCOM Head and Shoulders Inhomogeneous Model

FDTD calculations were made of the peak and 1-gram average of the SARs in the REMCOM inhomogeneous head model (described in section 3.3) exposed to the AT&T RU antenna. The head was exposed with the face toward the antenna with the nose in direct contact with the radome at 9-mm below the geometric center of the 4-patch array. Graphical SAR data files and plots calculated throughout the entire head model was scaled to correspond to an input power of 79.62 mW to the antenna.

Table 7.1 summarizes the calculated results of both the peak and average SARs calculated for each 1-mm thick slice in the xy plane as well as for the entire exposed head model. The format of the table is the same as that used in Tables 6.1 and 6.3. It may be noted from the table that the maximum SAR of 0.439 W/kg for the entire head model is in the 213th slice (file attremh.xy213.sar) at x=73 mm and y=163 mm and the average SAR for the 24614 cells for that slice is 0.002678 W/kg. It can also be seen at the bottom of the table that the SAR as averaged over the 5694630 cells of the entire head is 0.003965 W/kg. The 0.4388 W/kg maximum peak SAR for the inhomogeneous head is more than twice the value found for the homogeneous head model for the same exposure conditions. The higher SAR will later be shown to be due to an artifact resulting from a sharp corner of an air void within the nasal tissue resulting from the cubical shape of the FDTD cells. Sharp corners made by the cubical FDTD cells can cause a “staircasing” effect that results in a much higher than average peak SAR in the small 1-mm cubical volume because of its effect in intensifying the field when at the edge of a medium with a much lower permittivity such as air. This would not occur in real tissue and if the SAR is averaged over several adjacent FDTD cells the SAR should be about the same as for tissue at a more realistic smooth interface.

Table 7.2 illustrates the results of the 1-gram averaging of the FDTD output data, which can be related to the FCC MPL. It may be noted from the table that the highest 1-gram average SAR of 0.06860 W/kg occurs in the slice at z=113 mm, x=94 mm and y=149 mm. This is 13.7 dB below FCC MPL of 1.6 W/kg.. Using the same procedure as outlined in the previous section for the homogeneous head, the total absorbed power is calculated to be 22.494 mW which is 28.3% of the antenna input power and the whole-body averaged SAR for an adult man with a head similar to that of the REMCOM phantom head would be somewhere between 0.001377 and 0.003965 W/kg or from 20 to 58 times less than that allowed by the FCC MPL of 0.08 W/kg.

Table 7.1. Slice and Whole Head Model Peak and average SAR (averaged over slice) for Kuster Head and Shoulders Model Exposed to AT&T RU Antenna with Nose in Contact with Radome 9 mm Below Middle of Patch Array and (slice file number is distance in mm from FDTD space rectangular coordinates origin in z direction).

Name of Slice Data File	Peak SAR x and y coordinates	Peak SAR (W/kg)	Avg. SAR (W/kg)	Voxels in tissue
attremh.xy78.sar	145 160	0.6046E-01	0.4927E-02	27429
attremh.xy79.sar	145 160	0.6005E-01	0.4924E-02	27433
attremh.xy80.sar	145 160	0.5778E-01	0.4962E-02	27433
attremh.xy81.sar	145 160	0.5457E-01	0.4872E-02	27159
attremh.xy82.sar	145 160	0.5098E-01	0.4797E-02	27160
attremh.xy83.sar	130 119	0.8517E-01	0.4866E-02	27159
attremh.xy84.sar	132 117	0.5704E-01	0.4904E-02	26858
attremh.xy85.sar	132 117	0.5738E-01	0.4770E-02	26899
attremh.xy86.sar	127 139	0.7120E-01	0.4851E-02	26897
attremh.xy87.sar	130 116	0.9118E-01	0.4831E-02	26526
attremh.xy88.sar	129 117	0.6445E-01	0.5602E-02	27494
attremh.xy89.sar	115 174	0.9941E-01	0.5634E-02	27491
attremh.xy90.sar	111 132	0.6250E-01	0.5112E-02	27051
attremh.xy91.sar	123 180	0.8779E-01	0.4998E-02	27266
attremh.xy92.sar	109 144	0.1007E+00	0.5002E-02	27261
attremh.xy93.sar	111 126	0.6573E-01	0.4739E-02	26353
attremh.xy94.sar	109 141	0.5874E-01	0.4524E-02	26481
attremh.xy95.sar	112 121	0.1023E+00	0.4556E-02	26475
attremh.xy96.sar	93 159	0.6959E-01	0.4627E-02	25775
attremh.xy97.sar	93 159	0.6399E-01	0.4500E-02	25816
attremh.xy98.sar	91 162	0.1231E+00	0.4580E-02	25808
attremh.xy99.sar	90 158	0.9349E-01	0.4721E-02	25131
attremh.xy100.sar	88 156	0.7803E-01	0.4707E-02	25302
attremh.xy101.sar	91 165	0.1409E+00	0.4875E-02	25295
attremh.xy102.sar	90 135	0.9982E-01	0.4812E-02	24551
attremh.xy103.sar	90 135	0.8192E-01	0.4672E-02	24639
attremh.xy104.sar	88 134	0.1366E+00	0.4881E-02	24633
attremh.xy105.sar	91 132	0.1050E+00	0.5057E-02	24116
attremh.xy106.sar	91 132	0.9441E-01	0.4945E-02	24185
attremh.xy107.sar	89 168	0.1221E+00	0.5285E-02	24177
attremh.xy108.sar	94 151	0.1121E+00	0.5369E-02	23502
attremh.xy109.sar	94 151	0.1230E+00	0.5311E-02	23576
attremh.xy110.sar	94 151	0.1514E+00	0.5540E-02	23568
attremh.xy111.sar	94 148	0.1282E+00	0.5670E-02	23167
attremh.xy112.sar	94 149	0.1333E+00	0.5567E-02	23131
attremh.xy113.sar	106 109	0.1784E+00	0.5707E-02	23125
attremh.xy114.sar	94 146	0.1653E+00	0.5769E-02	22920
attremh.xy115.sar	94 146	0.1589E+00	0.5634E-02	22878
attremh.xy116.sar	94 146	0.1503E+00	0.5703E-02	22872
attremh.xy117.sar	94 149	0.1183E+00	0.5656E-02	22705
attremh.xy118.sar	94 149	0.1079E+00	0.5458E-02	22709
attremh.xy119.sar	91 121	0.1220E+00	0.5482E-02	22707
attremh.xy120.sar	95 144	0.1658E+00	0.5484E-02	22667
attremh.xy121.sar	96 144	0.1265E+00	0.5289E-02	22510
attremh.xy122.sar	91 121	0.1165E+00	0.5234E-02	22509
attremh.xy123.sar	103 111	0.1187E+00	0.5159E-02	22569
attremh.xy124.sar	103 111	0.9509E-01	0.4899E-02	22482
attremh.xy125.sar	103 107	0.1099E+00	0.4872E-02	22482
attremh.xy126.sar	94 116	0.9258E-01	0.4755E-02	22657

Name of Slice Data File	Peak SAR x and y coordinates	Peak SAR (W/kg)	Avg. SAR (W/kg)	Voxels in tissue
attremh.xy127.sar	94 116	0.8019E-01	0.4554E-02	22544
attremh.xy128.sar	94 115	0.1164E+00	0.4618E-02	22535
attremh.xy129.sar	77 153	0.1085E+00	0.4661E-02	22749
attremh.xy130.sar	77 144	0.7445E-01	0.4486E-02	22759
attremh.xy131.sar	76 152	0.1185E+00	0.4619E-02	22758
attremh.xy132.sar	75 150	0.8018E-01	0.4609E-02	23106
attremh.xy133.sar	76 156	0.6846E-01	0.4441E-02	23135
attremh.xy134.sar	73 150	0.9320E-01	0.4577E-02	23134
attremh.xy135.sar	82 125	0.7117E-01	0.4670E-02	23459
attremh.xy136.sar	80 127	0.6880E-01	0.4524E-02	23488
attremh.xy137.sar	82 174	0.9878E-01	0.4654E-02	23488
attremh.xy138.sar	77 130	0.8026E-01	0.4671E-02	23777
attremh.xy139.sar	77 130	0.6782E-01	0.4499E-02	23800
attremh.xy140.sar	76 130	0.9087E-01	0.4593E-02	23800
attremh.xy141.sar	92 186	0.6975E-01	0.4543E-02	24035
attremh.xy142.sar	91 150	0.7059E-01	0.4357E-02	24054
attremh.xy143.sar	97 103	0.9351E-01	0.4430E-02	24053
attremh.xy144.sar	98 112	0.6484E-01	0.4453E-02	24284
attremh.xy145.sar	89 109	0.7041E-01	0.4298E-02	24304
attremh.xy146.sar	91 189	0.8541E-01	0.4382E-02	24302
attremh.xy147.sar	89 109	0.1145E+00	0.4343E-02	24429
attremh.xy148.sar	89 109	0.8723E-01	0.4193E-02	24446
attremh.xy149.sar	88 109	0.1322E+00	0.4244E-02	24446
attremh.xy150.sar	91 108	0.9837E-01	0.4254E-02	24630
attremh.xy151.sar	91 108	0.7453E-01	0.4041E-02	24650
attremh.xy152.sar	97 100	0.8003E-01	0.4058E-02	24650
attremh.xy153.sar	94 105	0.7591E-01	0.4009E-02	24887
attremh.xy154.sar	86 109	0.6363E-01	0.3835E-02	24893
attremh.xy155.sar	86 110	0.7504E-01	0.3843E-02	24892
attremh.xy156.sar	91 104	0.7999E-01	0.3799E-02	25066
attremh.xy157.sar	89 106	0.6857E-01	0.3637E-02	25070
attremh.xy158.sar	89 106	0.7797E-01	0.3618E-02	25069
attremh.xy159.sar	91 108	0.6871E-01	0.3607E-02	25159
attremh.xy160.sar	88 108	0.6055E-01	0.3398E-02	25165
attremh.xy161.sar	89 106	0.7118E-01	0.3364E-02	25164
attremh.xy162.sar	91 105	0.6330E-01	0.3309E-02	25418
attremh.xy163.sar	94 102	0.6196E-01	0.3059E-02	25461
attremh.xy164.sar	92 103	0.6939E-01	0.2988E-02	25460
attremh.xy165.sar	94 101	0.7114E-01	0.2916E-02	25666
attremh.xy166.sar	94 102	0.6467E-01	0.2712E-02	25682
attremh.xy167.sar	97 98	0.8049E-01	0.2673E-02	25681
attremh.xy168.sar	95 102	0.5006E-01	0.2632E-02	25702
attremh.xy169.sar	95 102	0.4757E-01	0.2424E-02	25675
attremh.xy170.sar	85 112	0.5381E-01	0.2404E-02	25675
attremh.xy171.sar	98 99	0.6932E-01	0.2377E-02	25719
attremh.xy172.sar	98 99	0.5786E-01	0.2215E-02	25725
attremh.xy173.sar	98 99	0.5477E-01	0.2221E-02	25724
attremh.xy174.sar	92 101	0.7182E-01	0.2188E-02	25728
attremh.xy175.sar	92 100	0.5687E-01	0.2089E-02	25573
attremh.xy176.sar	94 97	0.8080E-01	0.2119E-02	25573
attremh.xy177.sar	97 99	0.6565E-01	0.2110E-02	25731
attremh.xy178.sar	93 102	0.5895E-01	0.2010E-02	25539
attremh.xy179.sar	93 102	0.6154E-01	0.2044E-02	25539
attremh.xy180.sar	93 104	0.4735E-01	0.2093E-02	25613
attremh.xy181.sar	93 104	0.4913E-01	0.2057E-02	25440

Name of Slice Data File	Peak SAR x and y coordinates	Peak SAR (W/kg)	Avg. SAR (W/kg)	Voxels in tissue
attremh.xy182.sar	67 154	0.6716E-01	0.2133E-02	25440
attremh.xy183.sar	70 156	0.1494E+00	0.2291E-02	25634
attremh.xy184.sar	67 156	0.7427E-01	0.2287E-02	24090
attremh.xy185.sar	67 150	0.8171E-01	0.2345E-02	24090
attremh.xy186.sar	67 150	0.1550E+00	0.2465E-02	24449
attremh.xy187.sar	64 149	0.5850E-01	0.2390E-02	24059
attremh.xy188.sar	64 149	0.6541E-01	0.2472E-02	24058
attremh.xy189.sar	64 148	0.1097E+00	0.2716E-02	24462
attremh.xy190.sar	64 151	0.7726E-01	0.2721E-02	24320
attremh.xy191.sar	64 151	0.9479E-01	0.2818E-02	24319
attremh.xy192.sar	64 151	0.1506E+00	0.3008E-02	24624
attremh.xy193.sar	73 142	0.8553E-01	0.2870E-02	24466
attremh.xy194.sar	64 151	0.9383E-01	0.2908E-02	24465
attremh.xy195.sar	64 157	0.1603E+00	0.3018E-02	24506
attremh.xy196.sar	64 159	0.1183E+00	0.2914E-02	24230
attremh.xy197.sar	64 154	0.1944E+00	0.2993E-02	24227
attremh.xy198.sar	112 194	0.1744E+00	0.3071E-02	24295
attremh.xy199.sar	64 157	0.1270E+00	0.2869E-02	23981
attremh.xy200.sar	64 157	0.1545E+00	0.2922E-02	23980
attremh.xy201.sar	64 158	0.1458E+00	0.3025E-02	24143
attremh.xy202.sar	64 160	0.9716E-01	0.2851E-02	23957
attremh.xy203.sar	67 160	0.2710E+00	0.2905E-02	23955
attremh.xy204.sar	67 160	0.4007E+00	0.2982E-02	24126
attremh.xy205.sar	67 160	0.2478E+00	0.2749E-02	24005
attremh.xy206.sar	67 160	0.2303E+00	0.2775E-02	24003
attremh.xy207.sar	67 160	0.2375E+00	0.2860E-02	24157
attremh.xy208.sar	67 160	0.1934E+00	0.2664E-02	24026
attremh.xy209.sar	67 160	0.1682E+00	0.2729E-02	24024
attremh.xy210.sar	76 166	0.2182E+00	0.2677E-02	24278
attremh.xy211.sar	76 166	0.1183E+00	0.2519E-02	24168
attremh.xy212.sar	73 163	0.2349E+00	0.2576E-02	24166
attremh.xy213.sar	73 163	0.4388E+00	0.2678E-02	24614
attremh.xy214.sar	73 163	0.2609E+00	0.2522E-02	24520
attremh.xy215.sar	73 163	0.1947E+00	0.2607E-02	24518
attremh.xy216.sar	73 163	0.1056E+00	0.2699E-02	24864
attremh.xy217.sar	72 163	0.7994E-01	0.2502E-02	24849
attremh.xy218.sar	64 156	0.8309E-01	0.2602E-02	24846
attremh.xy219.sar	69 153	0.1014E+00	0.2594E-02	24915
attremh.xy220.sar	76 163	0.9387E-01	0.2535E-02	24881
attremh.xy221.sar	70 150	0.1760E+00	0.2743E-02	24878
attremh.xy222.sar	76 163	0.1240E+00	0.2794E-02	24804
attremh.xy223.sar	76 163	0.1184E+00	0.2736E-02	24809
attremh.xy224.sar	89 109	0.1217E+00	0.3014E-02	24807
attremh.xy225.sar	89 109	0.1279E+00	0.2958E-02	24854
attremh.xy226.sar	71 153	0.8779E-01	0.2995E-02	24762
attremh.xy227.sar	70 155	0.1353E+00	0.3218E-02	24758
attremh.xy228.sar	79 163	0.1207E+00	0.3234E-02	24952
attremh.xy229.sar	79 163	0.1021E+00	0.3206E-02	24898
attremh.xy230.sar	73 161	0.1204E+00	0.3369E-02	24891
attremh.xy231.sar	75 160	0.1045E+00	0.3420E-02	25024
attremh.xy232.sar	73 155	0.8910E-01	0.3434E-02	25120
attremh.xy233.sar	73 158	0.1252E+00	0.3552E-02	25118
attremh.xy234.sar	75 157	0.8837E-01	0.3511E-02	25827
attremh.xy235.sar	74 154	0.7752E-01	0.3428E-02	25889
attremh.xy236.sar	74 154	0.7234E-01	0.3468E-02	25885

Name of Slice Data File	Peak SAR x and y coordinates	Peak SAR (W/kg)	Avg. SAR (W/kg)	Voxels in tissue
attremh.xy237.sar	91 112	0.7635E-01	0.3574E-02	25892
attremh.xy238.sar	91 112	0.6744E-01	0.3381E-02	25953
attremh.xy239.sar	91 101	0.7398E-01	0.3358E-02	25950
attremh.xy240.sar	98 192	0.7307E-01	0.3383E-02	26036
attremh.xy241.sar	83 111	0.5796E-01	0.3187E-02	26107
attremh.xy242.sar	82 113	0.1024E+00	0.3260E-02	26101
attremh.xy243.sar	87 111	0.7455E-01	0.3543E-02	26134
attremh.xy244.sar	84 113	0.6814E-01	0.3324E-02	26141
attremh.xy245.sar	79 117	0.8879E-01	0.3397E-02	26134
attremh.xy246.sar	87 108	0.1128E+00	0.3732E-02	26115
attremh.xy247.sar	87 108	0.1163E+00	0.3705E-02	26092
attremh.xy248.sar	87 106	0.1311E+00	0.3966E-02	26085
attremh.xy249.sar	88 105	0.8927E-01	0.3823E-02	25864
attremh.xy250.sar	84 113	0.7196E-01	0.3918E-02	25926
attremh.xy251.sar	86 198	0.1084E+00	0.4154E-02	25922
attremh.xy252.sar	102 96	0.7116E-01	0.4335E-02	25903
attremh.xy253.sar	102 96	0.7465E-01	0.4388E-02	25892
attremh.xy254.sar	91 201	0.1337E+00	0.4606E-02	25887
attremh.xy255.sar	84 114	0.7532E-01	0.4625E-02	25719
attremh.xy256.sar	84 114	0.8177E-01	0.4620E-02	25696
attremh.xy257.sar	79 117	0.9899E-01	0.4793E-02	25689
attremh.xy258.sar	84 114	0.8915E-01	0.4759E-02	25426
attremh.xy259.sar	87 111	0.9978E-01	0.4664E-02	25376
attremh.xy260.sar	85 109	0.1693E+00	0.4854E-02	25369
attremh.xy261.sar	89 108	0.1070E+00	0.4702E-02	24997
attremh.xy262.sar	81 119	0.8491E-01	0.4567E-02	24988
attremh.xy263.sar	94 103	0.1737E+00	0.4873E-02	24986
attremh.xy264.sar	81 120	0.9433E-01	0.4618E-02	24559
attremh.xy265.sar	92 108	0.9760E-01	0.4399E-02	24550
attremh.xy266.sar	97 103	0.2337E+00	0.4825E-02	24541
attremh.xy267.sar	90 111	0.1212E+00	0.4408E-02	23892
attremh.xy268.sar	94 108	0.9190E-01	0.4222E-02	23889
attremh.xy269.sar	82 121	0.2173E+00	0.4569E-02	23887
attremh.xy270.sar	88 115	0.1151E+00	0.4382E-02	23474
attremh.xy271.sar	97 108	0.9796E-01	0.4285E-02	23465
attremh.xy272.sar	94 109	0.2169E+00	0.4919E-02	23454
attremh.xy273.sar	97 107	0.1166E+00	0.4485E-02	22677
attremh.xy274.sar	95 111	0.8470E-01	0.4317E-02	22662
attremh.xy275.sar	88 122	0.1642E+00	0.4620E-02	22653
attremh.xy276.sar	87 125	0.9287E-01	0.4498E-02	22053
attremh.xy277.sar	97 111	0.8454E-01	0.4449E-02	22053
attremh.xy278.sar	94 115	0.2135E+00	0.4967E-02	22047
attremh.xy279.sar	97 113	0.1096E+00	0.4674E-02	21375
attremh.xy280.sar	91 124	0.7845E-01	0.4469E-02	21399
attremh.xy281.sar	91 127	0.1611E+00	0.4737E-02	21391
attremh.xy282.sar	91 127	0.8621E-01	0.4573E-02	20898
attremh.xy283.sar	97 117	0.7285E-01	0.4443E-02	20898
attremh.xy284.sar	97 118	0.1669E+00	0.4899E-02	20888
attremh.xy285.sar	99 117	0.9367E-01	0.4604E-02	20117
attremh.xy286.sar	101 189	0.7062E-01	0.4394E-02	20102
attremh.xy287.sar	101 189	0.1881E+00	0.4807E-02	20089
attremh.xy288.sar	100 186	0.8589E-01	0.4440E-02	19382
attremh.xy289.sar	103 116	0.6681E-01	0.4217E-02	19382
attremh.xy290.sar	103 115	0.1389E+00	0.4518E-02	19370
attremh.xy291.sar	104 117	0.7133E-01	0.4397E-02	18456

Name of Slice Data File	Peak SAR x and y coordinates	Peak SAR (W/kg)	Avg. SAR (W/kg)	Voxels in tissue
attremh.xy292.sar	103 120	0.6634E-01	0.4220E-02	18438
attremh.xy293.sar	103 121	0.1555E+00	0.4667E-02	18426
attremh.xy294.sar	103 121	0.7971E-01	0.4365E-02	17460
attremh.xy295.sar	104 122	0.5715E-01	0.4163E-02	17460
attremh.xy296.sar	106 118	0.1276E+00	0.4655E-02	17448
attremh.xy297.sar	106 120	0.6878E-01	0.4329E-02	16467
attremh.xy298.sar	104 180	0.5771E-01	0.4126E-02	16467
attremh.xy299.sar	106 183	0.1417E+00	0.4631E-02	16454
attremh.xy300.sar	108 125	0.6428E-01	0.4418E-02	15279
attremh.xy301.sar	106 178	0.5507E-01	0.4212E-02	15279
attremh.xy302.sar	112 183	0.1305E+00	0.4725E-02	15267
attremh.xy303.sar	108 176	0.6747E-01	0.4414E-02	14031
attremh.xy304.sar	108 176	0.5251E-01	0.4233E-02	14016
attremh.xy305.sar	109 177	0.1102E+00	0.4776E-02	14005
attremh.xy306.sar	108 137	0.5282E-01	0.4456E-02	12744
attremh.xy307.sar	115 126	0.4514E-01	0.4201E-02	12744
attremh.xy308.sar	112 174	0.1134E+00	0.4686E-02	12734
attremh.xy309.sar	117 126	0.5392E-01	0.4420E-02	11535
attremh.xy310.sar	112 160	0.4138E-01	0.4175E-02	11535
attremh.xy311.sar	112 158	0.1076E+00	0.4691E-02	11526
attremh.xy312.sar	112 158	0.5235E-01	0.4278E-02	10392
attremh.xy313.sar	115 162	0.4302E-01	0.4053E-02	10392
attremh.xy314.sar	115 165	0.1055E+00	0.4549E-02	10383
attremh.xy315.sar	115 160	0.5614E-01	0.4350E-02	9225
attremh.xy316.sar	116 160	0.4641E-01	0.4170E-02	9183
attremh.xy317.sar	118 155	0.9156E-01	0.4646E-02	9174
attremh.xy318.sar	117 157	0.5399E-01	0.4843E-02	8076
attremh.xy319.sar	126 137	0.3500E-01	0.4656E-02	8033
attremh.xy320.sar	127 166	0.8044E-01	0.5063E-02	8025
attremh.xy321.sar	124 162	0.7411E-01	0.5422E-02	6974
attremh.xy322.sar	129 160	0.4952E-01	0.5263E-02	6672
attremh.xy323.sar	133 148	0.6559E-01	0.5690E-02	6665
attremh.xy324.sar	135 155	0.4342E-01	0.5266E-02	5390
attremh.xy325.sar	135 155	0.4275E-01	0.4968E-02	5340
attremh.xy326.sar	139 162	0.8678E-01	0.5399E-02	5333
attremh.xy327.sar	141 161	0.3934E-01	0.4915E-02	4304
attremh.xy328.sar	141 153	0.3676E-01	0.4577E-02	4284
attremh.xy329.sar	142 155	0.6211E-01	0.4995E-02	4275
attremh.xy330.sar	147 166	0.3465E-01	0.5189E-02	3421
attremh.xy331.sar	148 166	0.2834E-01	0.4889E-02	3375
attremh.xy332.sar	148 149	0.6271E-01	0.5266E-02	3371
attremh.xy333.sar	154 171	0.4191E-01	0.7375E-02	2744
attremh.xy334.sar	150 157	0.2229E-01	0.6796E-02	2568
attremh.xy335.sar	160 168	0.3726E-01	0.6364E-02	2565
attremh.xy336.sar	157 165	0.4654E-01	0.9129E-02	2134
attremh.xy337.sar	165 155	0.2953E-01	0.8983E-02	1652
attremh.xy338.sar	166 156	0.3636E-01	0.7737E-02	1650
attremh.xy339.sar	187 163	0.1245E-01	0.5375E-02	908
attremh.xy340.sar	180 139	0.9655E-02	0.4515E-02	646
attremh.xy341.sar	187 148	0.1834E-01	0.3175E-02	641
attremh.xy342.sar	187 148	0.5390E-02	0.1689E-02	58

Location and values for peak and average SAR for total volume of exposed tissue

attremh.xy213.sar	73 163	0.4388E+00	0.3965E-02	5694630
-------------------	--------	------------	------------	---------

Table 7.2. Slice and Whole Head Model Peak and average (averaged over slice) 1 Gram Average SAR for REMCOM Head and Shoulders Model Exposed to AT&T RU Antenna with Nose in Contact with Radome 9 mm Below Middle of Patch Array and (slice file number is distance in mm from FDTD space rectangular coordinates origin in z direction).

Name of Slice Data File	Peak SAR x and y coordinates	Peak SAR (W/kg)	Avg. SAR (W/kg)	Voxels in tissue
attremh.xy78.lgsa	144 164	0.2517E-01	0.4914E-02	27429
attremh.xy79.lgsa	144 164	0.2517E-01	0.4943E-02	27433
attremh.xy80.lgsa	143 164	0.2618E-01	0.4884E-02	27433
attremh.xy81.lgsa	144 164	0.2699E-01	0.4853E-02	27159
attremh.xy82.lgsa	132 116	0.2717E-01	0.4854E-02	27160
attremh.xy83.lgsa	131 119	0.2782E-01	0.4810E-02	27159
attremh.xy84.lgsa	129 119	0.2876E-01	0.4794E-02	26858
attremh.xy85.lgsa	130 119	0.2918E-01	0.4762E-02	26899
attremh.xy86.lgsa	131 117	0.2938E-01	0.4690E-02	26897
attremh.xy87.lgsa	130 119	0.2959E-01	0.4680E-02	26526
attremh.xy88.lgsa	107 139	0.3353E-01	0.5291E-02	27494
attremh.xy89.lgsa	105 140	0.3364E-01	0.5136E-02	27491
attremh.xy90.lgsa	106 140	0.3404E-01	0.5139E-02	27051
attremh.xy91.lgsa	108 141	0.3432E-01	0.5118E-02	27266
attremh.xy92.lgsa	108 141	0.3432E-01	0.4934E-02	27261
attremh.xy93.lgsa	108 141	0.3428E-01	0.4932E-02	26353
attremh.xy94.lgsa	108 141	0.3397E-01	0.4800E-02	26481
attremh.xy95.lgsa	114 138	0.3513E-01	0.4608E-02	26475
attremh.xy96.lgsa	95 163	0.3674E-01	0.4699E-02	25775
attremh.xy97.lgsa	92 163	0.3957E-01	0.4665E-02	25816
attremh.xy98.lgsa	92 163	0.4171E-01	0.4506E-02	25808
attremh.xy99.lgsa	90 163	0.4435E-01	0.4691E-02	25131
attremh.xy100.lgs	89 163	0.4631E-01	0.4743E-02	25302
attremh.xy101.lgs	89 137	0.4896E-01	0.4621E-02	25295
attremh.xy102.lgs	87 137	0.5281E-01	0.4946E-02	24551
attremh.xy103.lgs	86 137	0.5482E-01	0.4941E-02	24639
attremh.xy104.lgs	89 132	0.5434E-01	0.4853E-02	24633
attremh.xy105.lgs	87 132	0.5687E-01	0.5221E-02	24116
attremh.xy106.lgs	86 132	0.5820E-01	0.5230E-02	24185
attremh.xy107.lgs	86 131	0.5893E-01	0.5169E-02	24177
attremh.xy108.lgs	87 128	0.5984E-01	0.5347E-02	23502
attremh.xy109.lgs	87 128	0.6076E-01	0.5377E-02	23576
attremh.xy110.lgs	93 148	0.6317E-01	0.5339E-02	23568
attremh.xy111.lgs	94 149	0.6582E-01	0.5672E-02	23167
attremh.xy112.lgs	94 149	0.6787E-01	0.5657E-02	23131
attremh.xy113.lgs	94 149	0.6860E-01	0.5594E-02	23125
attremh.xy114.lgs	94 149	0.6801E-01	0.5766E-02	22920
attremh.xy115.lgs	94 149	0.6645E-01	0.5716E-02	22878
attremh.xy116.lgs	94 148	0.6489E-01	0.5624E-02	22872
attremh.xy117.lgs	94 148	0.6243E-01	0.5730E-02	22705
attremh.xy118.lgs	94 148	0.5937E-01	0.5636E-02	22709
attremh.xy119.lgs	101 111	0.5828E-01	0.5513E-02	22707
attremh.xy120.lgs	101 112	0.5802E-01	0.5448E-02	22667
attremh.xy121.lgs	101 112	0.5764E-01	0.5349E-02	22510
attremh.xy122.lgs	102 112	0.5629E-01	0.5194E-02	22509
attremh.xy123.lgs	100 113	0.5619E-01	0.5169E-02	22569
attremh.xy124.lgs	101 112	0.5662E-01	0.5045E-02	22482
attremh.xy125.lgs	100 113	0.5597E-01	0.4890E-02	22482

Name of Slice Data File	Peak SAR x and y coordinates	Peak SAR (W/kg)	Avg. SAR (W/kg)	Voxels in tissue
attremh.xy126.lgs	101 112	0.5529E-01	0.4847E-02	22657
attremh.xy127.lgs	99 111	0.5456E-01	0.4747E-02	22544
attremh.xy128.lgs	99 113	0.5267E-01	0.4590E-02	22535
attremh.xy129.lgs	98 113	0.5116E-01	0.4691E-02	22749
attremh.xy130.lgs	96 114	0.4958E-01	0.4622E-02	22759
attremh.xy131.lgs	95 113	0.4839E-01	0.4501E-02	22758
attremh.xy132.lgs	95 111	0.4893E-01	0.4715E-02	23106
attremh.xy133.lgs	80 131	0.4849E-01	0.4674E-02	23135
attremh.xy134.lgs	81 130	0.4886E-01	0.4570E-02	23134
attremh.xy135.lgs	79 132	0.4869E-01	0.4691E-02	23459
attremh.xy136.lgs	79 131	0.4817E-01	0.4634E-02	23488
attremh.xy137.lgs	95 113	0.4748E-01	0.4529E-02	23488
attremh.xy138.lgs	95 114	0.4869E-01	0.4681E-02	23777
attremh.xy139.lgs	95 112	0.4894E-01	0.4624E-02	23800
attremh.xy140.lgs	96 111	0.4946E-01	0.4534E-02	23800
attremh.xy141.lgs	95 112	0.5027E-01	0.4646E-02	24035
attremh.xy142.lgs	96 113	0.5087E-01	0.4579E-02	24054
attremh.xy143.lgs	92 109	0.5151E-01	0.4489E-02	24053
attremh.xy144.lgs	94 111	0.5148E-01	0.4517E-02	24284
attremh.xy145.lgs	94 110	0.5197E-01	0.4444E-02	24304
attremh.xy146.lgs	94 111	0.5176E-01	0.4363E-02	24302
attremh.xy147.lgs	94 111	0.5148E-01	0.4318E-02	24429
attremh.xy148.lgs	93 110	0.5119E-01	0.4267E-02	24446
attremh.xy149.lgs	92 109	0.5111E-01	0.4185E-02	24446
attremh.xy150.lgs	91 108	0.5111E-01	0.4210E-02	24630
attremh.xy151.lgs	90 109	0.5064E-01	0.4143E-02	24650
attremh.xy152.lgs	91 109	0.5051E-01	0.4050E-02	24650
attremh.xy153.lgs	91 109	0.4967E-01	0.4037E-02	24887
attremh.xy154.lgs	90 107	0.4837E-01	0.3947E-02	24893
attremh.xy155.lgs	89 109	0.4694E-01	0.3847E-02	24892
attremh.xy156.lgs	90 109	0.4530E-01	0.3813E-02	25066
attremh.xy157.lgs	90 107	0.4460E-01	0.3717E-02	25070
attremh.xy158.lgs	90 109	0.4398E-01	0.3611E-02	25069
attremh.xy159.lgs	90 106	0.4359E-01	0.3570E-02	25159
attremh.xy160.lgs	90 104	0.4446E-01	0.3466E-02	25165
attremh.xy161.lgs	90 104	0.4400E-01	0.3354E-02	25164
attremh.xy162.lgs	92 105	0.4188E-01	0.3285E-02	25418
attremh.xy163.lgs	92 106	0.4079E-01	0.3170E-02	25461
attremh.xy164.lgs	92 106	0.3963E-01	0.3053E-02	25460
attremh.xy165.lgs	92 106	0.3854E-01	0.2938E-02	25666
attremh.xy166.lgs	92 106	0.3831E-01	0.2831E-02	25682
attremh.xy167.lgs	92 106	0.3823E-01	0.2722E-02	25681
attremh.xy168.lgs	93 102	0.3791E-01	0.2647E-02	25702
attremh.xy169.lgs	93 101	0.3851E-01	0.2563E-02	25675
attremh.xy170.lgs	93 101	0.3812E-01	0.2477E-02	25675
attremh.xy171.lgs	93 101	0.3663E-01	0.2390E-02	25719
attremh.xy172.lgs	93 104	0.3602E-01	0.2327E-02	25725
attremh.xy173.lgs	93 104	0.3440E-01	0.2263E-02	25724
attremh.xy174.lgs	93 101	0.3425E-01	0.2186E-02	25728
attremh.xy175.lgs	92 101	0.3366E-01	0.2164E-02	25573
attremh.xy176.lgs	92 101	0.3347E-01	0.2130E-02	25573
attremh.xy177.lgs	91 101	0.3537E-01	0.2122E-02	25731
attremh.xy178.lgs	91 101	0.3504E-01	0.2115E-02	25539
attremh.xy179.lgs	91 101	0.3422E-01	0.2111E-02	25539
attremh.xy180.lgs	92 99	0.3428E-01	0.2107E-02	25613

Name of Slice Data File	Peak SAR x and y coordinates	Peak SAR (W/kg)	Avg. SAR (W/kg)	Voxels in tissue
attremh.xy181.lgs	92 99	0.3376E-01	0.2126E-02	25440
attremh.xy182.lgs	90 101	0.3355E-01	0.2139E-02	25440
attremh.xy183.lgs	90 101	0.3344E-01	0.2184E-02	25634
attremh.xy184.lgs	92 99	0.3375E-01	0.2311E-02	24090
attremh.xy185.lgs	92 99	0.3466E-01	0.2350E-02	24090
attremh.xy186.lgs	92 99	0.3536E-01	0.2451E-02	24449
attremh.xy187.lgs	92 99	0.3609E-01	0.2504E-02	24059
attremh.xy188.lgs	92 99	0.3674E-01	0.2540E-02	24058
attremh.xy189.lgs	68 154	0.3779E-01	0.2638E-02	24462
attremh.xy190.lgs	67 155	0.4000E-01	0.2739E-02	24320
attremh.xy191.lgs	67 155	0.4355E-01	0.2778E-02	24319
attremh.xy192.lgs	67 155	0.4628E-01	0.2898E-02	24624
attremh.xy193.lgs	65 155	0.4927E-01	0.2885E-02	24466
attremh.xy194.lgs	65 155	0.5242E-01	0.2924E-02	24465
attremh.xy195.lgs	65 155	0.5510E-01	0.2919E-02	24506
attremh.xy196.lgs	65 155	0.5815E-01	0.2924E-02	24230
attremh.xy197.lgs	65 155	0.6022E-01	0.2951E-02	24227
attremh.xy198.lgs	67 155	0.6487E-01	0.2980E-02	24295
attremh.xy199.lgs	67 155	0.6686E-01	0.2947E-02	23981
attremh.xy200.lgs	68 156	0.6748E-01	0.2964E-02	23980
attremh.xy201.lgs	67 157	0.6842E-01	0.2897E-02	24143
attremh.xy202.lgs	68 157	0.6821E-01	0.2868E-02	23957
attremh.xy203.lgs	68 157	0.6758E-01	0.2876E-02	23955
attremh.xy204.lgs	68 158	0.6686E-01	0.2883E-02	24126
attremh.xy205.lgs	68 159	0.6570E-01	0.2869E-02	24005
attremh.xy206.lgs	68 158	0.6381E-01	0.2866E-02	24003
attremh.xy207.lgs	68 159	0.6337E-01	0.2756E-02	24157
attremh.xy208.lgs	69 161	0.6217E-01	0.2733E-02	24026
attremh.xy209.lgs	70 161	0.6163E-01	0.2725E-02	24024
attremh.xy210.lgs	70 161	0.5885E-01	0.2677E-02	24278
attremh.xy211.lgs	71 162	0.5719E-01	0.2643E-02	24168
attremh.xy212.lgs	73 162	0.5540E-01	0.2642E-02	24166
attremh.xy213.lgs	72 163	0.5347E-01	0.2607E-02	24614
attremh.xy214.lgs	74 163	0.5368E-01	0.2616E-02	24520
attremh.xy215.lgs	73 163	0.5287E-01	0.2612E-02	24518
attremh.xy216.lgs	74 163	0.5294E-01	0.2645E-02	24864
attremh.xy217.lgs	75 163	0.5063E-01	0.2688E-02	24849
attremh.xy218.lgs	74 163	0.4958E-01	0.2721E-02	24846
attremh.xy219.lgs	74 162	0.4662E-01	0.2663E-02	24915
attremh.xy220.lgs	74 164	0.4514E-01	0.2725E-02	24881
attremh.xy221.lgs	74 163	0.4365E-01	0.2783E-02	24878
attremh.xy222.lgs	69 154	0.4350E-01	0.2767E-02	24804
attremh.xy223.lgs	71 152	0.4584E-01	0.2836E-02	24809
attremh.xy224.lgs	71 153	0.4731E-01	0.2922E-02	24807
attremh.xy225.lgs	71 154	0.4848E-01	0.2907E-02	24854
attremh.xy226.lgs	70 154	0.5038E-01	0.3072E-02	24762
attremh.xy227.lgs	71 154	0.5167E-01	0.3160E-02	24758
attremh.xy228.lgs	71 155	0.5201E-01	0.3231E-02	24952
attremh.xy229.lgs	71 157	0.5302E-01	0.3291E-02	24898
attremh.xy230.lgs	72 156	0.5121E-01	0.3340E-02	24891
attremh.xy231.lgs	72 157	0.5229E-01	0.3338E-02	25024
attremh.xy232.lgs	72 157	0.5040E-01	0.3395E-02	25120
attremh.xy233.lgs	72 157	0.5026E-01	0.3414E-02	25118
attremh.xy234.lgs	72 157	0.4943E-01	0.3435E-02	25827
attremh.xy235.lgs	72 157	0.4778E-01	0.3448E-02	25889

Name of Slice Data File	Peak SAR x and y coordinates	Peak SAR (W/kg)	Avg. SAR (W/kg)	Voxels in tissue
attremh.xy236.lgs	72 157	0.4601E-01	0.3416E-02	25885
attremh.xy237.lgs	85 110	0.4444E-01	0.3470E-02	25892
attremh.xy238.lgs	86 112	0.4400E-01	0.3427E-02	25953
attremh.xy239.lgs	86 111	0.4345E-01	0.3381E-02	25950
attremh.xy240.lgs	86 109	0.4243E-01	0.3424E-02	26036
attremh.xy241.lgs	85 110	0.4205E-01	0.3395E-02	26107
attremh.xy242.lgs	86 109	0.4118E-01	0.3382E-02	26101
attremh.xy243.lgs	86 109	0.4158E-01	0.3458E-02	26134
attremh.xy244.lgs	83 110	0.4219E-01	0.3501E-02	26141
attremh.xy245.lgs	82 113	0.4276E-01	0.3524E-02	26134
attremh.xy246.lgs	81 110	0.4449E-01	0.3681E-02	26115
attremh.xy247.lgs	82 110	0.4487E-01	0.3763E-02	26092
attremh.xy248.lgs	82 110	0.4540E-01	0.3844E-02	26085
attremh.xy249.lgs	83 112	0.4416E-01	0.3884E-02	25864
attremh.xy250.lgs	80 115	0.4505E-01	0.4013E-02	25926
attremh.xy251.lgs	80 115	0.4526E-01	0.4127E-02	25922
attremh.xy252.lgs	80 115	0.4557E-01	0.4222E-02	25903
attremh.xy253.lgs	80 115	0.4639E-01	0.4324E-02	25892
attremh.xy254.lgs	78 116	0.4605E-01	0.4436E-02	25887
attremh.xy255.lgs	78 116	0.4652E-01	0.4505E-02	25719
attremh.xy256.lgs	78 116	0.4707E-01	0.4612E-02	25696
attremh.xy257.lgs	78 116	0.4808E-01	0.4705E-02	25689
attremh.xy258.lgs	80 116	0.4740E-01	0.4674E-02	25426
attremh.xy259.lgs	80 118	0.4716E-01	0.4748E-02	25376
attremh.xy260.lgs	81 113	0.4822E-01	0.4795E-02	25369
attremh.xy261.lgs	81 116	0.4792E-01	0.4656E-02	24997
attremh.xy262.lgs	82 116	0.4958E-01	0.4710E-02	24988
attremh.xy263.lgs	83 113	0.5059E-01	0.4740E-02	24986
attremh.xy264.lgs	86 114	0.5069E-01	0.4486E-02	24559
attremh.xy265.lgs	83 116	0.5160E-01	0.4535E-02	24550
attremh.xy266.lgs	84 113	0.5364E-01	0.4578E-02	24541
attremh.xy267.lgs	86 113	0.5166E-01	0.4315E-02	23892
attremh.xy268.lgs	95 107	0.5244E-01	0.4419E-02	23889
attremh.xy269.lgs	92 108	0.5284E-01	0.4497E-02	23887
attremh.xy270.lgs	89 113	0.5197E-01	0.4282E-02	23474
attremh.xy271.lgs	91 113	0.5281E-01	0.4383E-02	23465
attremh.xy272.lgs	89 114	0.5389E-01	0.4485E-02	23454
attremh.xy273.lgs	93 113	0.5187E-01	0.4193E-02	22677
attremh.xy274.lgs	92 113	0.5177E-01	0.4344E-02	22662
attremh.xy275.lgs	92 113	0.5367E-01	0.4474E-02	22653
attremh.xy276.lgs	96 112	0.5004E-01	0.4370E-02	22053
attremh.xy277.lgs	96 110	0.4953E-01	0.4491E-02	22053
attremh.xy278.lgs	92 116	0.5092E-01	0.4588E-02	22047
attremh.xy279.lgs	92 119	0.4574E-01	0.4354E-02	21375
attremh.xy280.lgs	96 116	0.4589E-01	0.4485E-02	21399
attremh.xy281.lgs	90 123	0.4559E-01	0.4589E-02	21391
attremh.xy282.lgs	96 116	0.4398E-01	0.4432E-02	20898
attremh.xy283.lgs	92 122	0.4420E-01	0.4542E-02	20898
attremh.xy284.lgs	98 114	0.4418E-01	0.4620E-02	20888
attremh.xy285.lgs	96 122	0.4051E-01	0.4352E-02	20117
attremh.xy286.lgs	98 116	0.4117E-01	0.4434E-02	20102
attremh.xy287.lgs	98 117	0.4130E-01	0.4510E-02	20089
attremh.xy288.lgs	99 120	0.3863E-01	0.4234E-02	19382
attremh.xy289.lgs	99 119	0.3931E-01	0.4329E-02	19382
attremh.xy290.lgs	99 120	0.3985E-01	0.4399E-02	19370

Name of Slice Data File	Peak SAR x and y coordinates	Peak SAR (W/kg)	Avg. SAR (W/kg)	Voxels in tissue
attremh.xy291.lgs	101 119	0.3720E-01	0.4241E-02	18456
attremh.xy292.lgs	101 119	0.3804E-01	0.4346E-02	18438
attremh.xy293.lgs	101 121	0.3750E-01	0.4425E-02	18426
attremh.xy294.lgs	104 119	0.3501E-01	0.4173E-02	17460
attremh.xy295.lgs	104 122	0.3496E-01	0.4292E-02	17460
attremh.xy296.lgs	104 120	0.3505E-01	0.4392E-02	17448
attremh.xy297.lgs	105 124	0.3229E-01	0.4122E-02	16467
attremh.xy298.lgs	105 122	0.3197E-01	0.4254E-02	16467
attremh.xy299.lgs	104 125	0.3257E-01	0.4363E-02	16454
attremh.xy300.lgs	107 122	0.2979E-01	0.4135E-02	15279
attremh.xy301.lgs	107 122	0.2977E-01	0.4289E-02	15279
attremh.xy302.lgs	107 125	0.2907E-01	0.4408E-02	15267
attremh.xy303.lgs	111 125	0.2721E-01	0.4131E-02	14031
attremh.xy304.lgs	110 125	0.2715E-01	0.4281E-02	14016
attremh.xy305.lgs	112 125	0.2726E-01	0.4398E-02	14005
attremh.xy306.lgs	114 126	0.2504E-01	0.4124E-02	12744
attremh.xy307.lgs	114 127	0.2471E-01	0.4266E-02	12744
attremh.xy308.lgs	114 125	0.2474E-01	0.4376E-02	12734
attremh.xy309.lgs	110 172	0.2267E-01	0.4141E-02	11535
attremh.xy310.lgs	110 172	0.2262E-01	0.4273E-02	11535
attremh.xy311.lgs	110 166	0.2269E-01	0.4377E-02	11526
attremh.xy312.lgs	113 163	0.2319E-01	0.4050E-02	10392
attremh.xy313.lgs	114 163	0.2394E-01	0.4184E-02	10392
attremh.xy314.lgs	113 161	0.2415E-01	0.4338E-02	10383
attremh.xy315.lgs	116 162	0.2352E-01	0.4130E-02	9225
attremh.xy316.lgs	114 159	0.2397E-01	0.4318E-02	9183
attremh.xy317.lgs	115 158	0.2382E-01	0.4531E-02	9174
attremh.xy318.lgs	116 158	0.2224E-01	0.4411E-02	8076
attremh.xy319.lgs	116 158	0.2193E-01	0.4668E-02	8033
attremh.xy320.lgs	116 158	0.2084E-01	0.4886E-02	8025
attremh.xy321.lgs	118 162	0.2024E-01	0.4733E-02	6974
attremh.xy322.lgs	126 160	0.1981E-01	0.4963E-02	6672
attremh.xy323.lgs	124 161	0.2101E-01	0.5186E-02	6665
attremh.xy324.lgs	125 158	0.2148E-01	0.4694E-02	5390
attremh.xy325.lgs	131 158	0.2010E-01	0.4793E-02	5340
attremh.xy326.lgs	131 158	0.2144E-01	0.5024E-02	5333
attremh.xy327.lgs	137 157	0.1732E-01	0.4426E-02	4304
attremh.xy328.lgs	137 157	0.1807E-01	0.4641E-02	4284
attremh.xy329.lgs	137 157	0.2002E-01	0.5032E-02	4275
attremh.xy330.lgs	143 163	0.1578E-01	0.4756E-02	3421
attremh.xy331.lgs	143 163	0.1664E-01	0.5099E-02	3375
attremh.xy332.lgs	143 161	0.1695E-01	0.5646E-02	3371
attremh.xy333.lgs	146 157	0.1456E-01	0.5579E-02	2744
attremh.xy334.lgs	146 157	0.1476E-01	0.6104E-02	2568
attremh.xy335.lgs	146 157	0.1476E-01	0.6389E-02	2565
attremh.xy336.lgs	150 157	0.1272E-01	0.6403E-02	2134
attremh.xy337.lgs	152 167	0.1218E-01	0.6640E-02	1652
attremh.xy338.lgs	153 160	0.1215E-01	0.6972E-02	1650
attremh.xy339.lgs	152 167	0.1179E-01	0.6499E-02	908
attremh.xy340.lgs	167 157	0.1132E-01	0.7071E-02	646
attremh.xy341.lgs	167 157	0.1211E-01	0.7356E-02	641
attremh.xy342.lgs	186 148	0.6359E-02	0.5131E-02	58

Location and values for peak and average SAR for total volume of Exposed Tissue

attremh.xy113.sar	94 149	0.6860E-01	0.3950E-02	5694630
-------------------	--------	------------	------------	---------

Figure 3.6 illustrates the orientation of the REMCOM head model with respect to the antenna in the sagittal or xz plane at $y = 154$ mm from the origin of the rectangular coordinate system at the lower-front-left corner of the fdtd mesh. The horizontal black lines, A through K denotes the horizontal xy planes where the SAR data was plotted and printed. However, SAR data were calculated for all of the 264, 1-mm thick horizontal xy slices as well as for the vertical slices denoted by L through N in the sagittal xz plane of the simulated head tissue illustrated in Figure 3.7.

Figure 7.1 illustrates the SAR distribution in xz planes through the head corresponding to the vertical slices L (through the center of the left row of antenna patches), M (through the center of the array of patches) and N (through the right row of patches) defined in Figure 3.7. Note that the maximum SAR in the head slice color plots varies from 0.177 to 0.190 W/kg very close to the maximum 0.172 W/kg observed on the equivalent plots of the homogeneous head model.

Figures 7.2 and 7.3 respectively illustrate the SAR distribution in the horizontal xy planes at slices labeled as A through E and F through K as denoted in Figure 3.6. The peak SAR for the entire head model, 0.439 W/kg occurs in the scan through the slice denoted as scan G or slice 213 in Figure 7.2. The white arrow points to the FDTD location of the FDTD cell experiencing the highest SAR. Figure 7.4 compares the color plot (left) of the peak SAR containing the highest value to the color plot (right) of the 1-gram average SAR for the same location. With the 1 gram averaging the maximum SAR at the position of the same cell is 0.0535 W/kg which is 14.8 dB below the FCC MPL.

Figures 7.5 and 7.6 illustrate the respective color plots of the SAR distribution in the xy planes denoted by A through E and F through K as identified in Figure 3.6. As for the case of the homogeneous head, the legend for these plots is set to allow the color red to represent all SARs at or greater than the value 1.6 W/kg allowed by the FCC MPL and the maximum value of the SAR for each plot is shown in the text below the plots. The maximum 1-gram average for the entire head model, 0.06860 W/kg occurs through the slice denoted as D in Figure 7.5 at the location of the black plus sign. The dynamic range of the 1-gram average distribution based on $0 \text{ dB} = 0.0686$ is shown in Figure 7.6.